

---

Theses and Dissertations

---

Summer 2015

# Community based air quality monitoring near proppant sand facilities

Ryan James Grant  
*University of Iowa*

Copyright 2015 Ryan James Grant

This thesis is available at Iowa Research Online: <http://ir.uiowa.edu/etd/1846>

---

## Recommended Citation

Grant, Ryan James. "Community based air quality monitoring near proppant sand facilities." MS (Master of Science) thesis, University of Iowa, 2015.  
<http://ir.uiowa.edu/etd/1846>.

---

Follow this and additional works at: <http://ir.uiowa.edu/etd>

 Part of the [Biomedical Engineering and Bioengineering Commons](#)

**COMMUNITY BASED AIR QUALITY MONITORING  
NEAR PROPPANT SAND FACILITIES**

by

Ryan James Grant

A thesis submitted in partial fulfillment  
of the requirements for the Master of Science  
degree in Biomedical Engineering in the  
Graduate College of  
The University of Iowa

August 2015

Thesis Supervisor: Associate Professor Thomas Peters

Copyright by  
RYAN JAMES GRANT  
2015  
All Rights Reserved

Graduate College  
The University of Iowa  
Iowa City, Iowa

CERTIFICATE OF APPROVAL

---

MASTER'S THESIS

---

This is to certify that the Master's thesis of

Ryan James Grant

has been approved by the Examining Committee for  
the thesis requirement for the Master of Science degree  
in Biomedical Engineering at the August 2015 graduation.

Thesis Committee:

---

Thomas Peters, Thesis Supervisor

---

Nicole M. Grosland

---

Peter S. Thorne

To: my little brother Logan  
May 8, 2000 - December 9, 2014

## ACKNOWLEDGEMENTS

I have had great support and guidance throughout my graduate work. Thomas Peters has been a great research advisor and has been a huge help in guiding me through this process. The wonderful frac sand team has been helpful in setting up sampling locations and providing valuable feedback. I would like to thank Nicole Grosland and Peter Thorne for being a part of my defense committee. I am appreciative of my lab group for providing constructive feedback, helping out coding MATLAB, and lending a helping hand when it was needed.

My family and friends have been extremely supportive during my graduate work. My parents David and Annette Grant who have continuously encouraged me to keep working hard and reminding me there is an end even when I could not see it. I would like to thank my friends and Deirdre Encke for helping me unwind after difficult days at the lab, or after the long road trips to Wisconsin.

None of this would not have been possible without great research funding. This research was funded by NIEHS/NIH P30 ES005605.

## ABSTRACT

Silica sand is used in the hydraulic fracturing process as a proppant—a material that holds open fissures in a rock formation to allow oil and gas to escape. Due to the increased demand for proppant sand, numerous sand mining and processing facilities have been constructed in the vicinity of small communities. Silica sand contains crystalline silica, which can cause chronic health problems such as silicosis. This study monitored airborne particulate matter at residences within 800 m from the property line of facilities with active mining, processing, and/or transport. Real-time particulate air monitoring with automated acquisition of explanatory variables: sound and motion to detect transportation; and wind speed and direction to attribute measured PM concentrations to specific sources. The highest daily mean concentrations were  $37.3 \mu\text{g}/\text{m}^3$  for  $\text{PM}_{10}$  and  $14.5 \mu\text{g}/\text{m}^3$  for  $\text{PM}_{2.5}$ , both of which are well below the EPA National Ambient Air Quality Standards. Using conditional probability plots of PM relative to wind direction elevated short-term (20 second) elevated concentrations were more likely to occur when the wind was blowing from the sand facility. These elevated concentrations occurred infrequently, ranging from 0% to 3% of the sampling time. This study did not measure crystalline silica specifically, but low PM concentrations were observed so crystalline silica is expected to be low. Since PM concentrations were low near the facilities, it can be concluded that these facilities do not increase airborne particulate matter to hazardous concentrations that could cause chronic health conditions.

## PUBLIC ABSTRACT

Silica sand is used in the hydraulic fracturing process as a proppant—a material that holds open fissures in a rock formation to allow oil and gas to escape. Due to the increased demand for proppant sand, numerous sand mining and processing facilities have been constructed in the vicinity of small communities. Silica sand contains crystalline silica, which can cause long term health problems such as silicosis. This study monitored dust at residences within 800 m from the facilities property line, with active mining, processing, and/or transport. Real-time dust monitoring paired with: sound and motion to detect transportation; and wind speed and direction to link measured dust concentrations to specific sources. The highest 24-hour average dust concentrations were well below the regulatory air quality standards. Using wind direction data it was observed that elevated short-term dust concentrations were more likely to occur when the wind was blowing from the sand facility. These elevated concentrations occurred infrequently, ranging from 0% to 3% of the time. This study did not measure crystalline silica specifically, but low dust concentrations were observed so crystalline silica is expected to also be low. Since dust concentrations were low near the facilities, it can be concluded that these facilities do not increase dust to hazardous levels that could cause long term health problems.



## TABLE OF CONTENTS

LIST OF TABLES .....	vii
LIST OF FIGURES .....	viii
CHAPTER I: INTRODUCTION.....	1
Overview.....	1
Sand Mining.....	2
Air Quality Concerns .....	4
Regulations .....	6
Exposure Techniques .....	7
Community impact.....	9
Shortcomings of Literature .....	10
Objective.....	11
CHAPTER II: COMMUNITY BASED AIR QUALITY MONITORING	
NEAR PROPPANT SAND FACILITIES .....	12
Introduction.....	12
Methods.....	16
Results.....	19
Discussion .....	21
Limitations .....	26
Conclusions.....	27
CHAPTER III: CONCLUSIONS .....	42
APPENDIX A: FIRMWARE FOR DATA LOGGER .....	45
APPENDIX B: MATLAB CODE .....	57
APPENDIX C: SITE DESCRIPTION AND SUMMARIES OF COLLECTED DATA.....	90
REFERENCES .....	127

## LIST OF TABLES

Table II - 1: Overview of Site Information.....	28
Table II - 2: Summary of Daily Averages for PM <sub>10</sub> and PM <sub>2.5</sub> .....	29
Table II - 3: Breakpoint Values and Percentile Mass Concentrations $\mu\text{g}/\text{m}^3$ by PM Metric and Site .....	30
Table II - 4: Summary of Final Models by PM Metric and Site.....	31
Table C - 1: Regression Analysis for PM>Breakpoint Concentration at Site 1 .....	94
Table C - 2: Regression Analysis for PM>Breakpoint Concentration at Site 2 .....	100
Table C - 3: Regression Analysis for PM>Breakpoint Concentration at Site 3 .....	106
Table C - 4: Regression Analysis for PM>Breakpoint Concentration at Site 4 .....	112
Table C - 5: Regression Analysis for PM>Breakpoint Concentration at Site 5 .....	118
Table C - 6: Regression Analysis for PM>Breakpoint Concentration at Site 6 .....	124

## LIST OF FIGURES

Figure II - 1: Monitoring setup at Site 5 .....	32
Figure II - 2: Trailer with monitoring equipment deployed at each sampling site .....	33
Figure II - 3: Probability plot of 20-sec PM <sub>10-2.5</sub> by site for all data (a) and for data only >95 <sup>th</sup> percentile (b).....	34
Figure II - 4: Probability plot of 20-sec PM <sub>2.5</sub> by site for all data (a) and for data only >95 <sup>th</sup> percentile (b).....	35
Figure II - 5: Site 1 PM <sub>10-2.5</sub> conditional probability plots showing values over a breakpoint concentration of 26.7 µg/m <sup>3</sup> (a) and 150 µg/m <sup>3</sup> (b) .....	36
Figure II - 6: Site 2 conditional probability plots, PM <sub>10-2.5</sub> threshold 40.8 µg/m <sup>3</sup> (a) threshold 150 µg/m <sup>3</sup> (b), and PM <sub>2.5</sub> threshold 22 µg/m <sup>3</sup> (c) threshold 35 µg/m <sup>3</sup> (d) .....	37
Figure II - 7: Site 3 Conditional Probability Plot for PM <sub>2.5</sub> threshold of 22 µg/m <sup>3</sup> .....	38
Figure II - 8: Site 4 conditional probability plots for PM <sub>10-2.5</sub> threshold of 22 µg/m <sup>3</sup> (a) and threshold 150 µg/m <sup>3</sup> (b) .....	39
Figure II - 9: Site 5 conditional probability plots, PM <sub>10-2.5</sub> threshold 45 µg/m <sup>3</sup> (a) threshold 150 µg/m <sup>3</sup> (b), and PM <sub>2.5</sub> threshold 35.6 µg/m <sup>3</sup> (c) threshold 35 µg/m <sup>3</sup> (d) .....	40
Figure II - 10: Site 6 conditional probability plots, PM <sub>10-2.5</sub> threshold 40.5 µg/m <sup>3</sup> .....	41
Figure C - 1: Map Image of Site 1 Relative to the Facility.....	91
Figure C - 2: PM <sub>10-2.5</sub> µg/m <sup>3</sup> Break point (indicated by arrow) = 26.7 µg/m <sup>3</sup> at a percentile = 97.9% .....	92
Figure C - 3: PM <sub>2.5</sub> µg/m <sup>3</sup> Break point (indicated by arrow) = 18.7 µg/m <sup>3</sup> at a percentile = 99.72 .....	92
Figure C - 4: Probability Plots of PM>Breakpoint Concentration for Site 1 .....	93
Figure C - 5: Conditional Probability Plots for Site 1 .....	95
Figure C - 6: Wind Rose for Site 1 .....	96
Figure C - 7: Map Image of Site 2 Relative to the Facility.....	97
Figure C - 8: PM <sub>10-2.5</sub> µg/m <sup>3</sup> Break point (indicated by arrow) = 40.8 µg/m <sup>3</sup> at a percentile = 97.6 .....	98
Figure C - 9: PM <sub>2.5</sub> µg/m <sup>3</sup> Break point (indicated by arrow) = 22 µg/m <sup>3</sup> at a percentile = 99.3 .....	98
Figure C - 10: Probability Plots of PM>Breakpoint Concentration for Site 2 .....	99
Figure C - 11: Conditional Probability Plots for Site 2 .....	101

Figure C - 12: Wind Rose for Site 2 .....	102
Figure C - 13: Map Image of Site 3 Relative to the Facility.....	103
Figure C - 14: PM <sub>10-2.5</sub> µg/m <sup>3</sup> Break point (indicated by arrow) = 22.5 µg/m <sup>3</sup> at a percentile = 99.7 .....	104
Figure C - 15: PM <sub>2.5</sub> µg/m <sup>3</sup> Break point (indicated by arrow) = 19.7 µg/m <sup>3</sup> at a percentile = 99.53 .....	104
Figure C - 16: Probability Plots of PM>Breakpoint Concentration for Site 3 .....	105
Figure C - 17: Conditional Probability Plots for Site 3 .....	107
Figure C - 18: Wind Rose for Site 3 .....	108
Figure C - 19: Map Image of Site 4 Relative to the Facility.....	109
Figure C - 20: PM <sub>10-2.5</sub> µg/m <sup>3</sup> Break point (indicated by arrow) = 22.9 µg/m <sup>3</sup> at a percentile = 97.6.....	110
Figure C - 21: PM <sub>2.5</sub> µg/m <sup>3</sup> Break point (indicated by arrow) = 23.1 µg/m <sup>3</sup> at a percentile = 99.8.....	110
Figure C - 22: Probability Plots of PM>Breakpoint Concentration for Site 4 .....	111
Figure C - 23: Conditional Probability Plots for Site 4 .....	113
Figure C - 24: Wind Rose for Site 4 .....	114
Figure C - 25: Map Image of Site 5 Relative to the Facility.....	115
Figure C - 26: PM <sub>10-2.5</sub> µg/m <sup>3</sup> Break point (indicated by arrow) = 45 µg/m <sup>3</sup> at a percentile = 97.4.....	116
Figure C - 27: PM <sub>2.5</sub> µg/m <sup>3</sup> Break point (indicated by arrow) = 35.6 µg/m <sup>3</sup> at a percentile = 99.1 .....	116
Figure C - 28: Probability Plots of PM>Breakpoint Concentration for Site 5 .....	117
Figure C - 29: Conditional Probability Plots for Site 1 .....	119
Figure C - 30: Wind Rose for Site 5 .....	120
Figure C - 31: Map Image of Site 1 Relative to the Facility.....	121
Figure C - 32: PM <sub>10-2.5</sub> µg/m <sup>3</sup> Break point (indicated by arrow) = 40.5 µg/m <sup>3</sup> at a percentile = 97.6.....	122
Figure C - 33: PM <sub>2.5</sub> µg/m <sup>3</sup> Break point (indicated by arrow) = 19.8 µg/m <sup>3</sup> at a percentile = 99.6.....	122
Figure C - 34: Probability Plots of PM>Breakpoint Concentration for Site 6 .....	123
Figure C - 35: Conditional Probability Plots for Site 6 .....	125
Figure C - 36: Wind Rose for Site 6 .....	126

## CHAPTER I: INTRODUCTION

### Overview

Hydraulic fracturing is a method of extracting natural gas and oil by cracking open shale rock formations located deep within the Earth's crust (Wisconsin Department of Natural Resources DNR, 2012b). A fluid mixture containing a proppant is used to keep the cracks open (Esswein et al., 2013). Common materials used as proppants are glass, sand, and ceramics (Hellmann et al., 2014). Silica sand is a favorable material due to its spherical shape, high strength properties, and the fact that it is relatively inexpensive.

Silica sand with optimal proppant properties is found in the West-Central region of Wisconsin making this state the leading industrial sand producer in 2013 (Dolley, 2014). In 1999, crystalline silica was classified as a Group 1 carcinogen due to its toxic nature (IARC, 1999). The primary health effect of exposure to crystalline silica is chronic silicosis (SCOEL, 2003). Most exposure to crystalline silica is work related; therefore, silicosis is considered an occupational disease. There are approximately 1 to 3 million workers exposed to crystalline silica, and in 2004, 166 deaths were silicosis related (Linch et al., 1998; NIOSH, 2008).

Wisconsin has environmental regulations, such as Wis. Adm Code NR 415 (DNR, 2012a), that aim to reduce the impact of mining processes on air quality. Wis. Adm Code NR 415 addresses Particulate Matter (PM) emissions from industrial sand facilities. The Environmental Protection Agency (EPA) has established National Ambient Air Quality Standards (NAAQS), for general dust PM of less than 10  $\mu\text{m}$  and 2.5  $\mu\text{m}$  in diameter ( $\text{PM}_{10}$  and  $\text{PM}_{2.5}$ ) (EPA, 2012).

Communities where sand facilities are located have numerous concerns, including how the sand facilities might affect their local economies, infrastructure, and most importantly, the health of their citizens (Pearson, 2013). Despite several studies showing occupational exposures

to dust and crystalline silica of concern at fracturing sites, little information is available on the impacts of sand mining activities on community exposures. The principle aim of this study was to determine how much of the community's exposure to ambient dust is attributable to the activities of sand facilities.

### **Sand Mining**

Hydraulic fracturing (fracking), a method of extracting natural resources from formations in the Earth's crust, has been around for 60 years (DNR, 2012b). In the past decade, the number of fracking wells has increased with rapid advances in drilling and related technologies that make fracking substantially less complicated and more economical. The fracking process starts with drilling horizontal channels in the shale rock formation and then blasting to open up cracks along the channel. Once blasted, a fluid mixture containing water, chemicals, and a material called proppant is pumped into the drilled channel and forced into the cracks created by the blasting process. The proppant holds the cracks open, allowing oil and gas to flow into the channel (Esswein et al., 2013). There are many different types of materials that are used as proppant, including glass, sand, and engineered ceramics (Hellmann et al., 2014). Some silica sand (silicon dioxide) has ideal physical (spherical shape and high compressive strength) and chemical properties needed for a proppant and is cheap compared to the engineered ceramics (DNR, 2012b; Hellmann et al., 2014).

A silica sand particularly desirable for use in fracking can be found in sandstones of the Cambrian age (DNR, 2012b; Pettijohn, Potter, & Siever, 1987), which occur in the west-central region of Wisconsin. The increasing need for silica sand in recent years has escalated due to the proliferation of fracturing. In the United States, the sand mining industry, as a whole, is a \$2.6 billion dollar industry, and during 2013, 62% of the industrial sand mines were supporting

hydraulic fracturing processes, with Wisconsin leading production (Dolley, 2014). In July 2011 Wisconsin had 16 active mines and processing facilities, whereas by May 2014, the state has 63 active mines and 45 active processing facilities ("Locations of Industrial Sand Mines and Processing Plants in Wisconsin," 2014; Smathers, 2011).

There are four major procedures necessary to obtain silica sand suitable for hydraulic fracturing: mining, processing, transportation, and reclamation. Mining starts with the removal of overburden, or large bluffs of foliage, undesired topsoil, and rock layers, which exposes the sandstone formation (Survey, 2013b). The exposed sandstone is then blasted into large pieces that are further broken down into sand in a crushing unit. Any material not suitable for fracking is sold for various purposes (glass industry, sand blasting, and construction) or saved for reclamation of the excavated land. The usable sand is either moved to the processing part of the facility or transported by truck or train to an offsite processing plant (Survey, 2013b). In processing, the mined sand is washed and sieved to remove unwanted components (fine sand and clay particles) and then dried and stockpiled until loading (DNR, 2012b; Survey, 2013b). Transportation of materials happens at every stage of the mining processes. The principle methods of material transportation are conveyer belts, dump trucks, trains, and barges (DNR, 2012b). For short distances, conveyors and trucks are used, whereas trains and barges are typically used for long distance shipping. The final step in the mining process is reclamation, which is the covering of the mine with unused rock and topsoil. Reclamation can result in land usable for agriculture or recreational purposes (Pearson, 2013). However, reclamation does not restore the land to its previous state.

## Air Quality Concerns

Mining, processing, and transport of sand generates increased airborne dust concentrations (Watson et al., 2012). Dust is part of a larger mixture that is called particulate matter (PM) (EPA, 2013). PM is classified by particle size, where particles smaller than 10  $\mu\text{m}$  are classified as  $\text{PM}_{10}$ , and particles smaller than 2.5  $\mu\text{m}$  are classified as fine particles ( $\text{PM}_{2.5}$ ) (EPA, 2013). In terms of pulmonary health, an increased risk of developing a health problem occurs when particles are inhaled to terminal bronchioles and alveoli (Kirkhorn & Garry, 2000). Particles that can reach deep lung tissue are part of the respirable dust fraction, and according to ACGIH (2014) TLVs and BEIs, respirable dust has a median diameter of 4.0  $\mu\text{m}$  or smaller ( $\text{PM}_4$ ). Some states such as California and Minnesota use  $\text{PM}_4$  to regulate ambient crystalline silica concentrations.

Whereas inhalation exposure to dust in general can create health problems, exposures to crystalline silica, like that found in proppant sand, elevates the possibility of more severe problems (Parks et al., 1999). The two forms of silica that are important are amorphous and crystalline silica, and the most common form of crystalline silica is quartz (OSHA, 2010). Crystalline silica has a tetrahedron chemical structure. When the silica molecule is fractured, its surface contains highly reactive oxygen sites increasing its toxicity (Fubini et al., 1995; Minerals, 1992). Crystalline silica particles smaller than 5  $\mu\text{g}/\text{m}^3$  inhaled as dust are most toxic (Parks et al., 1999).

The International Agency for Research on Cancer has classified crystalline silica as a Group 1 carcinogen (IARC, 1999). Exposure to crystalline silica increases the risk of developing silicosis (Parks et al., 1999). According to SCOEL (2003) exposure to crystalline silica does not directly cause lung cancer, but development of silicosis does increase the probability of developing the disease. There are three types of silicosis: acute, accelerated, and chronic



silicosis. It takes ten or more years of low-level exposure to crystalline silica to develop chronic silicosis, and this form is generally related to the type of exposure from sand facilities (Center for Disease Control and Prevention, CDC, 2004). According to (NIOSH, 1978) when workers were exposed to greater than 20 particles per cubic foot, negative health effects were present, and workers exposed to less than 9 particles per cubic foot had no indications negative health effects.

Silicosis occurs when crystalline silica reaches the deep lung tissue, where gas exchange takes place. Alveolar macrophages attack the silica particles, and due to the shape and insoluble nature of silica the macrophages are unable to remove the particles from the lung tissue (Mossman & Churg, 1998). The reaction between the silica particles and macrophages induces an inflammation and scarring of the lung tissue which is irreversible (Mossman & Churg, 1998). There have been many toxicological studies on this subject, such as that conducted by Muhle et al. (1989). Of one hundred rats exposed to 1 mg/m<sup>3</sup> of respirable crystalline over 24 months, 6 hr/day, 5 days/week, they found 18 rats contained tumors after 24 weeks of exposure, and 99 rats had varying degrees of fibrosis after 24 months. In extreme cases, silica particles can spread to other organ systems (DNR, 2011).

Silicosis is considered an occupational disease. Therefore, most of the epidemiological research and statistics are based on occupational health information (OSHA, 2010). According to a study done by Linch et al. (1998) the number of workers exposed to crystalline silica ranges from 1 to 3 million. An article published in the CDC Morbidity and Mortality Weekly Report (MMWR) (2005) discussed silica-related deaths reported to NIOSH's National Occupational Respiratory Mortality System (NORMS) between 1968 and 2002. The report found that in this time period, 16,305 deaths were considered to be either caused by or related to silicosis. From 1970 to 1974 there were 4,263 reported silicosis-related deaths compared to 809 during 2000-

2004 (166 of which occurred in 2004) (NIOSH, 2008). The decrease in the number of fatalities correlates with the decline in the number of exposed workers as well as the addition of Permissible Exposure Limits (PEL) and Recommended Exposure Limits (REL) to silica in 1974 (CDC, 2005).

### **Regulations**

In Wisconsin, dust is regulated by the Wisconsin DNR as PM emissions under Chapter Natural Resources (NR) 415, Wis. Adm. Code (DNR, 2012a). Section NR 415.075 is specific for PM emissions from industrial sand mines and states that sand mines must take precautions to prevent PM from becoming airborne. The regulation requires mines to participate in a PM ambient air monitoring program established by the U.S. EPA. NR 415.075(2) and NR 415.075(4) only apply to mines that include a “production of more than 2,000 tons per month on a rolling 12 month average” (“NR 415 Control of Particulate Emissions,” 2003). Wisconsin Adm. Code NR 415.076 is specific to emissions from sand and gravel plants. Portable plants are exempt from this code if they have a capacity of less than 150 tons per hour, and fixed plants are exempt if capacity is less than 25 tons per hour. The law states that all sand plants must take “precautions to prevent particulate matter from becoming airborne” (“NR 415 Control of Particulate Emissions,” 2003).

Both NR 415.075 and NR 415.076 require facilities to prevent fugitive dust, and NR 415.04 specifically addresses all fugitive dust requirements (“NR 415 Control of Particulate Emissions,” 2003). The DNR (2012c) encourages sand mining and processing facilities to use a provided template, which includes control recommendations for potential sources. The template states that “the standard for fugitive dust emission quantification is by visual observation.” So, if dust is visible, then action must be taken.

There are occupational regulatory limits for crystalline silica that apply to sand facilities. OSHA's Annotated Table Z-3 Mineral Dust (OSHA, 2013) shows OSHA PEL for respirable crystalline silica is of  $10 \text{ mg/m}^3 / (\% \text{SiO}_2 + 2)$  (OSHA, 2006), and ACGIH Threshold Limit Values (TLV) of  $0.025 \text{ mg/m}^3$  (respirable). Both limits are for an 8-hour Time Weighted Average (TWA). Comparatively, the NIOSH Recommended Exposure Limits (REL) for respirable crystalline silica is  $0.05 \text{ mg/m}^3$  for a 10-hour TWA.

Currently, there are no federal air quality standards specifically for crystalline silica concentrations in the ambient air (DNR, 2011). Under the Clean Air Act, the US EPA is required to set National Ambient Air Quality Standards (NAAQS) (EPA, 2012). The NAAQS includes general dust standards for  $\text{PM}_{10}$  and  $\text{PM}_{2.5}$  in ambient air. The standard for  $\text{PM}_{10}$  is  $150 \text{ } \mu\text{g/m}^3$  and  $35 \text{ } \mu\text{g/m}^3$  for  $\text{PM}_{2.5}$ , both of which are 24-hour averages for the 98<sup>th</sup> percentile averaged over a 3-year period. While there are no federal air quality standard for crystalline silica, some states have implemented limits of their own. For instance, California has a inhalation reference exposure level of  $3 \text{ } \mu\text{g/m}^3$  for respirable crystalline silica (OEHHA, 2005), and Minnesota has adopted a long-term exposure limit for respirable crystalline silica of  $3 \text{ } \mu\text{g/m}^3$  (EQB, 2013).

### **Exposure Techniques**

Direct reading instruments (DRIs) allow instant logging of PM concentrations at specific recorded time intervals. Time-resolved PM data from DRIs allow a wide versatility of applications when paired with other forms of data. For example, Klepeis et al. (2013) combined a low-cost DRI photometer with a visual display to alert household residents of high levels of tobacco smoke. The firmware used in this study recorded data from the photometer, and when levels exceeded threshold values, different alarms would activate. The objective of this study was to observe the effect of visual feedback on the behavioral patterns of smokers. Steinle et al.

(2015) paired a low-cost particle counter with GPS to categorize high personal exposures to six discrete locations.

Filter-based sampling is a method that allows composition measurements of dust, which is an advantage when quantifying exposure to respirable crystalline silica. The method uses a sampling unit containing a filter cassette on which dust is collected. After the sampling period, the cassette is weighed and analyzed to determine the specific compositions in the dust. X-ray diffraction is commonly used to determine the concentration of crystalline silica on a filter. Garcia et al. (2014) paired an aerosol photometer DRI to measure respirable dust with filter-based sampling for crystalline silica content on a construction site. They found that the time-weighted averages for the DRI were higher than the filter-based samplers. However, the respirable time-weighted averages were not significantly different between the two methods. Both methods showed that crystalline silica exceeded occupational exposure limits.

Occupational exposures to crystalline silica have been studied using both personal and job site sampling. Esswein et al. (2013) measured personal, respirable crystalline silica exposures at hydraulic fracturing sites. Of 111 samples that covered different jobs within the hydraulic fracturing site, 93 were above the ACGIH TLV, 76 were above the NIOSH REL, and 57 were above the OSHA PEL. Ehrlich et al. (2013) found that all of the area samples collected on-site at sand processing facilities near the processing operations exceeded the German respirable crystalline silica emission limit of  $1 \text{ mg/m}^3$ . Radnoff et al. (2014) found that 94% of works personal exposures in sand processing facilities exceeded the Alberta OEL and 81% exceeded the NIOSH REL for respirable crystalline silica.

Meteorological data paired with filter-based methods can be used to determine how wind speed and direction affect concentrations of dust. Richards et al. (2009) modified an EPA  $\text{PM}_{10}$

sampler with a cyclone sampler to provide a 50% cut point of 4  $\mu\text{m}$ . They also paired local meteorological data to determine silica concentrations within processing facilities to validate whether or not the dust plume remained stationary relative to the source and to calculate ambient air flow during sampling. They sampled at two locations and the highest upwind daily average was 1.3  $\mu\text{g}/\text{m}^3$  for the first location and 2.8  $\mu\text{g}/\text{m}^3$  for the second location, and the highest downwind average was 1.1  $\mu\text{g}/\text{m}^3$  for the first location, and 0.9  $\mu\text{g}/\text{m}^3$  for the second location. Shiraki & Holmen (2002) used meteorological data paired with filter-based methods to determine upwind and downwind exposures from a sand and gravel processing facility. Using one upwind and four downwind samplers they determined how wind direction and proximity affects the emissions of the facility. The meteorological data allowed them to determine wind direction for their setup. They found that all of the downwind filters had higher crystalline silica concentrations compared to samples collected upwind, and as the distance between the sampler and the facility increased, the filter concentration decreased.

### **Community impact**

A non-health related concern with sand mining is the impact it has on nearby communities in terms of government, economics, and infrastructure. According to Pearson (2013), in Wisconsin only the DNR and local government have any regulatory power over air quality, land use, and conditions of operations. The small communities where new facilities are being built have out-of-date or inadequate zoning ordinances, making it difficult to keep facilities out of the community (Pearson, 2013; Seely, 2011). Conflicts of interest arise when there is involvement of local official who have proposed opening facilities on their property (Kennedy, 2012).

There has been much concern over the economic impacts of new sand mines or processing facilities. According to DNR (2012b), an average mine will create 10 new jobs, and a

processing facility could create 50-80 new jobs. A new processing plant can cost up to \$20-\$40 million dollars in equipment and infrastructure, some of which will go to local building and equipment distributors (DNR, 2012b). Locally-owned and operated companies are more beneficial to local economic growth, compared to what are often non-local owners and operators of the incoming mining facilities (Deller & Schreiber, 2012). If a company or laborer resides outside of the local area then profits and economic benefits will leave the local area, as well (Pearson, 2013).

A concern that many community members have is the impact that sand facilities will have on area infrastructure and landscape. Increased dump truck traffic on local roadways can lead to premature wear on the infrastructure, and increased maintenance costs can detract from any economic benefits introduced by the mining operations (Pearson, 2013). Community members have some concerns about how sand mining will destroy their picturesque landscape, which is a vital component of the communities' tourism industry. A debate over the ability to dramatically change a "shared landscape" has been brought up in many public forum discussions (Bridge, 2004; Pearson, 2013).

### **Shortcomings of Literature**

The number of sand mining, processing, and transport facilities in the Midwest, particularly in Wisconsin, have risen dramatically in the past several years to support the booming hydraulic fracturing industry. Occupational exposures to respirable crystalline silica have been found in sand mining and processing facilities that have exceeded guidelines and regulatory limits. Regulatory limits are in place to reduce the risk of workers developing health problems due to high levels of exposures to harmful airborne substances. In contrast, little is known about community exposures from fugitive dust sources from sand facilities, and many community members are concerned with the impact these facilities will have on air quality.

Community-based sampling is needed to determine the impact that industrial fugitive dust sources have on local community air quality. Such studies would help determine if the increased mining activity in Wisconsin has caused an increase in ambient dust concentrations.

### **Objective**

The objective of this study was to perform community-based air quality monitoring near sand mining, processing, and transportation facilities in Wisconsin and Minnesota. The goal was to observe ambient dust concentrations at community members' homes located near sand facilities. Specific aims of this study were:

1. Determine if PM observed at residences near different sand mining, processing, and transportation facilities exceed EPA NAAQS for PM<sub>10</sub> and PM<sub>2.5</sub>.
2. Determine if elevated PM can be attributed to sand facilities using paired data from a DRI with meteorological data, sound levels, and images of passing objects.

## CHAPTER II: COMMUNITY BASED AIR QUALITY MONITORING NEAR PROPPANT SAND FACILITIES

### **Introduction**

Hydraulic fracturing (fracking) is a 60-year-old method of extracting natural resources by vertically drilling into strata containing natural gas or oil in the Earth's crust. Recent advances in the technology enabled by horizontal drilling have made fracking more economical, resulting in its proliferation throughout the US (DNR, 2012b). In modern fracking, ~1,600-m horizontal channels are drilled radially from a 3,500-m depth vertical shaft (Osborn et al., 2011). Blasting in the horizontal channel opens cracks in the shale rock formation. A slurry of water, proppant, and other proprietary chemicals are pumped into the cracks. Oil and/or gas in the shale pushes the water and chemicals out of the cracks leaving the proppant in place to hold open the cracks and increase the longevity of a horizontal channel.

Crystalline silica sand is commonly used as proppant because it is inexpensive, spherical, and has a high compressive strength (DNR, 2012b). Consequently, the demand for sand has increased with the expansion of fracking. The particular sand used for fracking is mainly found in specific sandstones located in the west-central region of Wisconsin (DNR, 2012b). The specific sandstones in Wisconsin that contain silica sand are Jordan and St. Peter formations. Sand mining is a 2.6 billion dollar industry, with Wisconsin leading the nation in production at 62% of the national total (Dolley, 2014). In the past few years, there has been a dramatic increase in the number of facilities in this region. In July 2011 there was a combined total of 16 active mines and processing facilities, which has increased to 63 active sand mines and 45 processing facilities as of May 2014 ("Locations of Industrial Sand Mines and Processing Plants in Wisconsin," 2014; Smathers, 2011).



There are three major components to industrial sand mining (mining, processing, and transportation). Mining consists of removing topsoil and extracting the underlying sandstone formation containing the silica sand (Survey, 2013a). Processing takes the sandstone from the mines and sorts, washes, and dries the sands to prepare it for use by the fracking facility (DNR, 2012b). According to DNR (2012b) the transportation of material from one facility to another can include transportation by conveyor, truck, train, or barge. These processes all generate fugitive dust, increased airborne dust concentrations (Watson et al., 2012).

Communities near sand facilities have expressed urgent concern that fugitive emissions of dust from sand facilities may be a health hazard. Airborne particulate matter is a known health hazard to humans (Davidson et al., 2005; Valavanidis et al., 2008). The different pollutants contained in ambient dust can be harmful when exposed to concentrations that are above the National Ambient Air Quality Standards (NAAQS) general dust values (Davidson et al., 2005; Harrison & Yin, 2000). Dust blowing off the sand facilities may also contain crystalline silica, which when in the respirable size fraction (PM<sub>4</sub>) can penetrate into the deep portions of the lung (ACGIH, 2014; Kirkhorn & Garry, 2000; Parks et al., 1999). Since the sand is being blasted and crushed, some of the particles could be freshly fractured, which can change surface chemistry increasing crystalline silica's toxicity (Fubini et al., 1995; Minerals, 1992). The International Agency for Research on Cancer (IARC) classified crystalline silica as a group 1 carcinogen (IARC, 1999). Exposure to low-level crystalline silica can lead to the development of chronic silicosis (CDC, 2004; Parks et al., 1999; SCOEL, 2003).

Fugitive emissions are regulated by the United States Environmental Protection Agency (EPA) through NAAQS (EPA, 2013): particulate matter (PM) smaller than 10 µm (PM<sub>10</sub>) and smaller than 2.5 µm, or fine particles (PM<sub>2.5</sub>). PM<sub>10</sub> includes fine and coarse particles, for which

coarse particles are defined as particles with a diameter between 2.5  $\mu\text{m}$  and 10  $\mu\text{m}$   $\text{PM}_{10-2.5}$ . The NAAQS for a 24-hr averaging period is 150  $\mu\text{g}/\text{m}^3$  for  $\text{PM}_{10}$  and 35  $\mu\text{g}/\text{m}^3$  for  $\text{PM}_{2.5}$ , both defined as the 98<sup>th</sup> percentile of PM over a 3-year time period (EPA, 2012). There is no federal regulation for ambient crystalline silica concentrations. However, states have adopted state-specific crystalline silica guidelines, such as California's Office of Environmental Health Hazard Assessment (OEHHA) inhalation reference exposure level of 3  $\mu\text{g}/\text{m}^3$  (EQB, 2013; OEHHA, 2005) and Minnesota's Environmental Quality Board (EQB) long-term exposure limit of 3  $\mu\text{g}/\text{m}^3$ .

Personal exposures to crystalline silica commonly exceed occupational exposure limits in the hydraulic fracking and sand mining profession. Radnoff et al. (2014) observed geometric mean respirable quartz exposures of 115  $\mu\text{g}/\text{m}^3$  among hydraulic fracturing workers and 90  $\mu\text{g}/\text{m}^3$  among sand mining and processing workers. Esswein et al. (2013) collected a total of 111 personal breathing zone samples at multiple hydraulic fracturing facilities, and found 93 samples above the ACGIH TLV, 76 samples above the NIOSH REL, and 57 samples above OSHA PEL. Ehrlich et al. (2013) studied respirable crystalline silica emissions from several industrial operations in Germany and found that silica sand processing plants exceeded the emissions limit value (ELV) of 1  $\text{mg}/\text{m}^3$ . According to the German respirable crystalline silica measurement programs, complying with the ELV reduces ambient air health risk for people living near the facility.

Although these studies show elevated exposures to crystalline silica are common in sand mining, little information is available on PM and crystalline silica exposures of residents living in close proximity to sand facilities. Relating emissions from an industrial source, such as a sand facility, to PM concentrations is difficult and results from literature are unclear. Shiraki &

Holmen (2002) used meteorological data to determine the dust contribution from a sand and gravel facility, using samplers situated upwind and downwind of the facility. They found that the average downwind mass concentrations ( $192 \mu\text{g}/\text{m}^3$ ) were much higher than average upwind mass concentrations ( $35.2 \mu\text{g}/\text{m}^3$ ). Yu et al. (2004) used wind speed and direction applied in a nonparametric regression to identify sources of emission within an airport. Likewise, Richards et al. (2009) sampled at two locations (upwind and downwind) and used wind speed and direction data to estimate the contribution of crystalline silica in ambient air from three sand and gravel processing plants in California. They observed that sand facilities did not contribute substantially to ambient crystalline silica concentrations with upwind daily average crystalline silica concentrations ( $1.3 \mu\text{g}/\text{m}^3$  for the first location and  $2.8 \mu\text{g}/\text{m}^3$  for the second location) sometimes exceeding downwind concentrations ( $1.1 \mu\text{g}/\text{m}^3$  for the first location and  $0.9 \mu\text{g}/\text{m}^3$  for the second location). Richards et al. (2009) stated the reason the upwind concentrations were larger than the downwind concentrations due to an unpaved road near the upwind samplers.

The goal of this work was to determine the impact of sand mining activities specifically in Wisconsin on community PM concentrations. Real-time PM monitoring was conducted with automatic acquisition of potential explanatory variables: sound and motion to detect transportation; and wind speed and direction to attribute measured concentrations to specific sources. The analysis presented in this chapter is based on data collected from six sites with various combinations of sand facilities including mining, processing, and transportation operations. The effect of the nearby facilities on community air quality was determined using the explanatory variables.

## Methods

### *Monitoring Sites*

Air monitoring was conducted at six sites as presented in Table II - 1. These sites were selected using county zoning websites and community organizations based on the following criteria: location within 2,500 feet of the property line of a sand facility having mining, processing, and/or transport operations; predominantly downwind from the facility; ability to provide onsite power; and owner permission. There were 29 sites that fit the selection criteria, and six sites were selected from those. Limited sites were selected based on availability of the resident and due to the short duration of the study. Three sites were near mines with onsite processing, two were near train trans-load/transportation facilities, and one was near a processing-only facility. Each site had unique characteristics that could affect community PM concentrations. Site 1 was located at a residence surrounded by the property lines of the sand facility, containing mining, processing, and truck transportation. Site 2, a train loading facility, and Site 6, a processing facility, were located in the same city and had large identifiable open mounds of sand. At Site 3, monitoring was conducted 10 m away from a rail line with known sand transport. There are ~50 trains that pass by at a speed of ~72 Km/hr per day. Sites 4 and 5 were located near facilities with a combination of mining, processing, and transporting operations. Site 4 had identifiable separation between each type of operation within the facility.

The typical arrangement of the air monitoring site relative to the sand facility is shown in Figure II – 1. At each site the monitoring equipment was set up as follows: as far away from trees as possible; near a power source; and with a clear sightline to the nearest facility. The sampling time at each site varied from one week to four weeks. The overall sampling time frame (June 2014 - November 2014) aligned with the mining season. During the sampling time frame, typical summer and early fall weather conditions were observed.

### *Equipment*

Monitoring equipment was positioned in a trailer (Wells Cargo Mini Wagon, Wells Cargo Inc., Elkhart, IN) as shown in Figure II - 2. An optical particle counter (OPC, Environmental Dust Monitor, Model EDM164, GRIMM Aerosols Technik, Ainring, Germany), positioned inside the trailer, was used to measure  $PM_{10}$  and  $PM_{2.5}$ . A sampling head mounted 15 cm above the roof of the trailer was used to convey ambient aerosol to the OPC. External sensors mounted on a pole and attached to the side of the trailer were used to measure wind speed, wind direction, sound level, and motion. Wind speed and wind direction were measured with an ultrasonic anemometer (Model 85000, R.M. Young Company, Traverse, MI) mounted 3.7 m from the ground. Motion was detected and images were obtained with a weatherproof camera (613, Serial JPEG Camera with NTSC Video and IR LEDs, Adafruit Industries, New York City, NY). A small microphone (SEN-12642, SparkFun Sound Detector, SparkFun Electronics, Boulder, CO) was used to measure sound.

A microcontroller (Arduino Mega 2560 Rev 3, Adafruit, NY) with a data logging shield (Data Logging Shield, Adafruit, NY) running custom firmware (Appendix A) was used to collect  $PM_{10}$  and  $PM_{2.5}$  from the OPC every 6 seconds and external sensor data every second. These measurements were averaged and logged to an SD card every 20 seconds. The camera was used to record images when motion was detected and sound was above a preset threshold. The sound level threshold was set using a potentiometer, and set to a percentage of the total output voltage of the microphone. The potentiometer threshold was set to 10%, which was low enough to capture a passing train.

Inadvertently, the averaging of wind direction data prior to logging did not account for the cyclic nature of wind direction, and 20-sec periods that contained 1-sec values greater than  $0^\circ$  and  $360^\circ$  were averaged incorrectly. A second issue is that the anemometer was always mounted

with the instrument north aligned with true south. As a consequence, wind direction values from the south ( $180^\circ \pm \sim 10^\circ$ ) may have been inadvertently recorded incorrectly. The impact of these errors on the overall project are expected to be minimal because the wind directions of interest (those from the sand facility) were not within the affect region ( $180^\circ \pm \sim 10^\circ$ ).

### *Analysis*

MATLAB (8.3.0.532 R2014a, MathWorks, Natick, MA) was used to calculate  $PM_{10-2.5}$  (calculated by subtracting  $PM_{2.5}$  from  $PM_{10}$ ), categorize explanatory variables, and remove unreadable records due to short power outages at Site 3 for less than 30 minutes (MATLAB code provided in Appendix B). For each site, mean daily (from 12:00 am to 11:59 pm) concentrations were calculated as the arithmetic mean of 20-sec data. Statistical software (Minitab 17, Minitab Inc., State College, PA) was used to generate probability plots of 20-sec  $PM_{2.5}$  and  $PM_{10-2.5}$  (Figure II-3 and Appendix C). A bimodal distribution of concentrations were observed on probability plots for all sites. Thus, a breakpoint concentration, defined as the maximum curvature (represented with an arrow in Figure II - 3), was determined to separate the two modes. Conditional probability plots of PM data versus wind direction data were then generated for PM data above the breakpoint concentration and for above the EPA NAAQS following Kim & Hopke (2004).

Site-specific explanatory variables (wind direction, wind speed, and sound level) were categorized into generalized descriptive categories. For example, wind direction for the site in Figure II - 1 was categorized as 'over the facility' if wind was blowing from between  $315^\circ$  to  $13^\circ$ , and 'not over the facility' if wind was from  $14^\circ$  to  $314^\circ$ . Wind speed was categorized as high ( $> 3$  m/s) or low ( $\leq 3$  m/s), which was based on the average wind speed of 3 m/s. Sound was categorized similarly with high values above 2% and low values below 2% of maximum voltage

from the sound detector. The threshold value was set to 2.7%, except at Site 3 due to the proximity and loudness of the train.

For each site and 20-sec PM values higher than the breakpoint value, two linear regression models were constructed with the log of PM ( $PM_{10-2.5}$  or  $PM_{2.5}$ ) as the dependent variable and categorical variables as the independent variables. Backward elimination was used to eliminate variables that were not significant in the model. Variables were removed if they were not statistically significant at a 5% level of significance.

## Results

Daily average PM and highest PM by site are compared to EPA NAAQS in Table II - 2. Average PM concentrations were well below the NAAQS for  $PM_{2.5}$  and  $PM_{10}$ . The highest daily average  $PM_{2.5}$  was  $14.5 \mu\text{g}/\text{m}^3$  observed at Site 2, and  $PM_{10}$  was  $38 \mu\text{g}/\text{m}^3$  observed at Site 5.

Probability plots of 20-sec data by site are shown in Figure II – 3 for  $PM_{10-2.5}$  and in Figure II – 4 for  $PM_{2.5}$ . The breakpoint concentrations and concentrations associated with 5<sup>th</sup>, 16<sup>th</sup>, 50<sup>th</sup>, 84<sup>th</sup>, and 95<sup>th</sup> percentiles are shown in Table II – 3 for all sites. An example of the probability curves for  $PM_{10-2.5}$  are provided in Figure II – 3 with the breakpoint concentration for Site 3 identified with a red arrow. Breakpoint concentrations represent the division between two modes in the probability plot, with one mode associated with low concentrations and the other associated with higher concentrations. The breakpoint concentrations were associated with the ~97<sup>th</sup> percentile for  $PM_{10-2.5}$  and the ~99<sup>th</sup> percentile for  $PM_{2.5}$ . The highest 20-sec OPC concentrations were observed at Site 5 ( $1211 \mu\text{g}/\text{m}^3$  for  $PM_{10-2.5}$ ; and  $912 \mu\text{g}/\text{m}^3$  for  $PM_{2.5}$ ). All site-specific information and plots are provided in Appendix C.

Linear regression analyses for the elevated concentrations ( $PM > \text{breakpoint concentration}$ ) are summarized in Table II - 4. In general, the regression models explained some

of the variability in  $PM_{10-2.5}$  ( $R^2 < 4.7\%$ ) and  $PM_{2.5}$  ( $R^2 < 23.9\%$ ). For each site, residuals were tested for normality, and all failed except for  $PM_{2.5}$  at Site 1 (p-value = 0.33) and Site 4 (p-value = 0.41). For  $PM_{10-2.5}$ , none of the explanatory variables were statistically significant in the model for Site 1 and Site 3. For the other sites, wind speed was the only variable statistically significant, explaining 0.18% to 4.7% of the variability in  $PM_{10-2.5}$ . For Sites 4, 5, and 6,  $PM_{10-2.5}$  was lower (0.30 to 0.57 times) when the wind speeds were higher than 3 m/s, and for Site 2,  $PM_{10-2.5}$  was slightly higher (0.06 times) when the wind was higher than 3 m/s.

For  $PM_{2.5}$ , no variables were statistically significant in the regression model for Site 1. For the remaining sites, the models explained 0.74% to 23.9% of the variability in  $PM_{2.5}$ . Wind speed was significant for most of the sites, although the influence of wind speed was not consistent across sites.  $PM_{2.5}$  was higher for high wind speeds at one site (Site 2, 0.22 times higher times higher), whereas it was lower for high winds at others (Site 5, 0.19 times lower; Site 6, 0.32 times lower). The regression model for Site 4 explained the most variability in  $PM_{2.5}$  ( $R^2 = 24\%$ ). The only variable that was significant for Site 4 was sound level, which had a coefficient of 0.56. Wind direction was not significant in the regression models for  $PM_{2.5}$ .

Conditional probability plots of elevated PM concentrations by wind direction are provided in Figure II – 5 to Figure II – 10. These plots help to determine if elevated PM concentrations are associated with different operations at the sand facilities or unrelated sources. The center of the conditional probability plot represents the trailer, and the radial axis represents wind direction with the top representing north. The concentric circles on these plots represent probability values with increasing probability of PM concentration above the threshold with the radial distance from the center. Site specific breakpoint concentrations and the EPA NAAQS values were used as threshold values for  $PM_{10}$  and  $PM_{2.5}$  conditional probability plots. The wind



directions marked on the plots are consistent with the wind directions related to the facility property lines.

Sites containing different operations (mining, processing, and transportation) were Site 1, Site 4, and Site 5. As shown in Figure II - 5 the probability of having a reading above the breakpoint concentration and NAAQS for  $PM_{10-2.5}$  at Site 1 was greater when the wind is blowing over the sand mine. Site 4 had three distinct sections in the facility as shown in Figure II - 8. The mine itself contains the highest probability of a  $PM_{10-2.5}$  data point above the breakpoint concentration and NAAQS, while other facilities have a lower probability. Elevated  $PM_{10-2.5}$  readings at Site 5 were observed south of the sampling site from an unrelated source, as seen in Figure II - 9a and 9b. The high probability peaks for  $PM_{2.5}$  at site 5 were primarily from the same direction as the facility (Figure II - 9c and 9d).

Site 2, Site 3, and Site 6 were all located near facilities that only contained specialized operations such as trans-loading or processing. At Site 2, the highest probability of a data point being above breakpoint and  $PM_{2.5}$  NAAQS concentrations occurred when the wind was blowing between  $330^\circ$  to  $350^\circ$  (As shown in Figures II - 6a, 6c, and 6d). In Figure II - 6b the highest probability of having a data point above the NAAQS limit was from a source unrelated to the sand facility. As shown in Figure II - 7, at Site 3, there was a higher probability of concentrations above the  $PM_{2.5}$  breakpoint ( $22 \mu\text{g}/\text{m}^3$ ) when the wind was blowing over the rail line. The facility near Site 6 did not dramatically affect the probability of a high reading for  $PM_{10-2.5}$  when the wind was attributed to the facility.

## Discussion

Daily mean  $PM_{10}$  and  $PM_{2.5}$  measured at residences near sand facilities were substantially lower than NAAQSs. The highest daily average  $PM_{10}$  was  $38 \mu\text{g}/\text{m}^3$  (Table II-2), which is 25%

of the  $150 \mu\text{g}/\text{m}^3$  NAAQS daily average limit. Similarly, the maximum daily average  $\text{PM}_{2.5}$  was  $14.5 \mu\text{g}/\text{m}^3$ , which is less than half of the  $35 \mu\text{g}/\text{m}^3$  NAAQS limit.

Similar results have been obtained recently by Wisconsin's DNR and Minnesota's Pollution Control Agency. The Wisconsin DNR requires sand facilities with production of  $> 907$  kg per month to monitor PM using EPA-approved, filter-based methods near the facility ("NR 415 Control of Particulate Emissions," 2003). Of the  $\sim 150$  samples taken near sand facilities by the Wisconsin DNR, none have been above the  $\text{PM}_{10}$  NAAQS. One of the DNR sampling sites located near Site 5 showed an average value of  $18 \mu\text{g}/\text{m}^3$  for  $\text{PM}_{10}$  compared to a  $\text{PM}_{10}$ -averaged concentration of  $20 \mu\text{g}/\text{m}^3$  for Site 5. The highest  $\text{PM}_{10}$  measurement observed by the DNR monitor at that site was  $40 \mu\text{g}/\text{m}^3$ .

Minnesota's Pollution Control Agency performed similar air quality monitoring near sand facilities (Ellickson & Hedman, 2014a, 2014b). They monitor three different locations within Minnesota, with one location near Site 2 and Site 6. The location near Sites 2 and 6 had a single 24-hour average above the NAAQS limit for  $\text{PM}_{2.5}$  within the past year. However, the other monitoring locations have not recorded a concentration greater than the NAAQS values.

Measurements of respirable crystalline silica have been found to be low near sand facilities. Minnesota's Pollution Control Agency also monitored respirable crystalline silica at all three monitoring locations. Few samples were above the limit of detection for crystalline silica, but samples that exceeded the limit of detection were all lower than the  $3 \mu\text{g}/\text{m}^3$  limit set by the state of Minnesota. Richards et al. (2009) sampled for crystalline silica at three sand and gravel processing plants located in California. Upwind and downwind sampling locations were used, and the highest downwind  $\text{PM}_4$  crystalline silica concentration reported was  $1.1 \mu\text{g}/\text{m}^3$ . This concentration does not exceed the California inhalation reference exposure level of  $3 \mu\text{g}/\text{m}^3$ .

Although daily average concentrations were low, elevated readings in  $PM_{10-2.5}$  and  $PM_{2.5}$  were attributed to sand facilities. In the regression models (Table II – 4), wind speed was found significant for most sites. In most cases, elevated wind speed was associated with lower  $PM_{10-2.5}$  and  $PM_{2.5}$ . However, Site 2 had the opposite affect where high wind speeds increased the PM concentrations. This observation may be due to the close proximity of the monitoring location to the main activity of the facility (i.e., sand loading with a diesel front-end loader). The sound level variable all had similar effect with higher PM concentrations observed with higher sound levels. The increase in PM concentration when the sound is high is an expected result, because higher sound levels typically occur when there is activity near the sampling trailer. Site 5 and Site 6 were both located near roadways with dump truck traffic so increases in concentration when sound level is high could be due to that traffic. Wind speed could affect the sound level due to the wind noise on the microphone. There was a foam cover on the microphone to prevent wind noise elevating sound levels. The regression models suggests that wind noise did not affect sound level readings due to the variables having an opposite effect.

Conditional probability plots suggest that elevated concentrations are associated with operations at the sand facilities with multiple operations (Site 1, 4, and 5). For Site 1, the spikes in the conditional probability plot from the west were consistent with observed transportation activity at the facility (Figure II – 5). For Site 4, operations were limited to blasting and removing overburden, which is consistent the highest concentrations being when the wind was blowing over the mine (Figure II – 8, wind directions between  $10^{\circ}$  -  $169^{\circ}$ ). For Site 5, higher  $PM_{2.5}$  was observed when wind was blowing from the facility (Figure II – 9c and 9d), although the opposite was true for  $PM_{10-2.5}$  (Figure II – 9a and b). Higher  $PM_{10-2.5}$  from the south may be related to dairy operations on the property used for monitoring.

Elevated concentrations also seem to be associated with sand facilities having only a single operation (Sites 2, 3, and 6). Site 2 was located near a trans-load facility and significant spikes were in the probability of PM<sub>2.5</sub> and PM<sub>10-2.5</sub> were observed between 330° and 350° (Figure II – 6), which was consistent with the location where incoming trucks discharge sand and a front-end loader loads sand on to trains (350°). Elevated PM<sub>2.5</sub> is likely attributed to diesel exhaust from the dump trucks and bucket loaders, whereas elevated PM<sub>10-2.5</sub> is likely from the sand discharge. For Site 3, higher probabilities of elevated PM<sub>2.5</sub> concentrations were likely associated with diesel train engines (Figure II – 7). For Site 6, in contrast, the association of higher probabilities of elevated concentrations with wind blowing over the facility was less strong. This site was located in an urban environment with many trees situated between the sampling site and facility, which may have caused swirling eddies in wind that complicated our interpretation.

Shiraki & Holmen (2002) investigated the influence of wind direction on PM concentrations around gravel facilities. They sampled upwind of the facility to get a background measurement, and had four downwind samplers to observe the differences due to proximity from the source and the upwind sampler. They found that the downwind samplers had higher silica than the upwind sampler, and the amount of dust collected decreased with increasing distance. This literature agrees with the results presented in the current study because the conditional probability plots for most sites do contain a higher probability when the wind is blowing from the sand facility as opposed to from an unrelated source. The higher breakpoint concentrations observed for Sites 2 and 6 agree with Shiraki & Holmen (2002) conclusion that proximity to the source plays a significant role in concentration. Both sites were close to the facility due to an urban environment where the facility property lines border the residential areas.

Wind speed and direction are common descriptive variables used to determine where a source of pollution is located. The study by Yu et al. (2004) used wind speed and direction to determine where sources of aircraft emissions are located within large airports. Using the concentrations paired with wind data they were able to determine the general areas with high emission rates. Similar to this study, Minnesota's Pollution Control Agency used conditional probability plots of wind speed and direction versus PM concentration to determine how much dust the facility is contributing to the ambient air.

The results from this study suggest that the PM from sand facilities does not increase the risk of developing chronic health effects among residents living in nearby communities. Daily averages were well below the NAAQS for PM<sub>10</sub> and PM<sub>2.5</sub>. Concentrations above the breakpoint concentration (Figure II – 3) occur infrequently and for short duration. As part of other ongoing work by our team, respirable samples contain approximately 2% of crystalline silica by mass near sand facilities in this region of Wisconsin. Two percent of the highest PM<sub>10</sub> average observed in this study (2% of 38  $\mu\text{g}/\text{m}^3 = 0.76 \mu\text{g}/\text{m}^3$ ) is well below the California and Minnesota exposure limits of 3  $\mu\text{g}/\text{m}^3$ . Richards et al. (2009) found the amount of respirable crystalline silica from three sand and gravel processing facilities to range from 0.3  $\mu\text{g}/\text{m}^3$  to 2.8  $\mu\text{g}/\text{m}^3$ , which is also below the 3  $\mu\text{g}/\text{m}^3$  state limits. Likewise the concentration of respirable crystalline silica found at the Minnesota sampling locations is below the 3  $\mu\text{g}/\text{m}^3$  limit, and in most cases below the limit of detection (Ellickson & Hedman, 2014a, 2014b).

The equipment used in this study paired with the data analysis techniques was successful in identifying determinants of concentrations. Pairing wind speed and direction with PM concentrations and using data to generate conditional probability plots of wind direction versus PM concentrations proved important in relating elevated PM concentration with sand facilities.

The use of motion detection and sound level played an essential part in determining when a train was passing by, allowing passing trains to be compared directly to corresponding PM concentrations. A similar methodology could be used for other types of sampling, with minimal sensor modification and a different setup to capture a broad range of events. While using and linking multiple sensors to capture a broad range of determinates is novel, the use of meteorological data is an accepted method of identifying a source of exposure. Shiraki & Holmen (2002) successfully used wind direction to determine that higher concentrations were detected downwind of a gravel processing facility. Wind speed and direction were successfully used by Yu et al. (2004) in a nonparametric regression to identify emission sources from regions within an airport. The method used in this study is from Kim & Hopke (2004) where meteorological data was used in conditional probability plots to aid in identifying the source of PM. Finally, this methodology could be used to validate dispersion models by placing equipment at different locations to see if the result reflects the model's prediction.

### **Limitations**

Dichotomized regression variables may be too simple to create an accurate regression model. Wind speed is a variable where simple dichotomization does not accurately represent the data. Factors such as temperature, humidity, and pressure combine with wind speed to affect the PM dispersion. The number of potential locations that could be used in this study was somewhat limited as there were specific criteria for site selection. With this limitation, sampling proximity to most of the facilities was not optimal. However, since most sites were the closest available residential site, it does represent the surrounding community exposures to these sand facilities fairly well. Monitoring was conducted once at each site, although ranging from a week to four weeks of continuous monitoring. Facility operations were not logged and may have changed

during the monitoring period. In future studies, multiple monitoring locations around a facility with multiple sampling occurrences and logging of facility operations should be considered.

This study also only monitored PM, rather than crystalline silica, near sand facilities. Filter-based sampling methods should be conducted near the sampling site to determine if respirable crystalline silica is above  $3 \mu\text{g}/\text{m}^3$ . While crystalline silica was not specifically measured in this study, the PM concentrations observed were low, so crystalline silica concentrations are expected to be low as well.

### **Conclusions**

Daily PM<sub>10</sub> and PM<sub>2.5</sub> observed at residences within 800 m from the property line of facilities with active mining, processing, and/or transport were well below the EPA NAAQSs. Elevated, short-term (20 second) concentrations were determined more likely to occur when the wind was blowing from the sand facility, although these elevated concentrations occurred infrequently, ranging from 0% to 3% of the sampling time. This study did not measure crystalline silica specifically, but low average PM concentrations were observed so crystalline silica is expected to be low. Since PM concentrations were low near the facilities, it can be concluded that these facilities do not increase airborne particulate matter to hazardous concentrations that could cause chronic health conditions, such as silicosis.

Table II - 1: Overview of Site Information

Site #	Description of Facility Operations	Distance Between Sampling Site and Center of Facility (Meters)	Sampling Period (2014)	Site Observations
1	Mining; Processing; Truck Transportation;	454	Aug 8 – Aug 15	Rural, Most facility activity to the west, Closest farm was to the Southwest
2	Trans-load with: Truck Transportation In; Bucket Loading Train Transportation Out;	188	Sept9 – Oct 9	Urban, Privacy wall between sampler and facility, Sand Dumped to the north of sampler at 350°
3	Passing Rail Transportation;	9.8	Jun 24 – Jul 7	Urban, Sampler location was in-between river and highly traveled road, ~50 trains per day
4	Mining; Conveyor; Processing; Train Transportation Out;	Mining = 518 Conveyor = 747 Processing = 1463	Jul 31 – Aug 8	Rural, Gravel driveway to the south of the sampler, Facility property line close but mining activities farther away
5	Mining; Processing; Train Transportation Out;	1469	Jul 7 – Jul 31	Rural, Sand Driveway next to the sampler, Located on a dairy farm
6	Truck In; Processing;	384	Oct 9 – Nov 4	Urban, Location secluded within trees



Table II - 2: Summary of Daily Averages for PM<sub>10</sub> and PM<sub>2.5</sub>

Site #	PM <sub>10</sub>			PM <sub>2.5</sub>		
	Mean (µg/m <sup>3</sup> )	Standard Deviation (µg/m <sup>3</sup> )	Highest 24-hr Average (µg/m <sup>3</sup> )	Mean (µg/m <sup>3</sup> )	Standard Deviation (µg/m <sup>3</sup> )	Highest 24-hr Average (µg/m <sup>3</sup> )
1	14.7	3.9	19.2	7.7	2.8	11.4
2	17.8	8.4	37.3	7	3.6	14.5
3	11.1	4.4	18.6	6.8	3.1	13.5
4	18.4	2.9	23.2	10	1.8	13.6
5	19.8	9.1	38	7.8	3.2	13.3
6	16.8	9.0	37	6.5	3	11.8

Table II - 3: Breakpoint Values and Percentile Mass Concentrations  $\mu\text{g}/\text{m}^3$  by PM Metric and Site

Site	Break Value		Mass Concentration Assigned With Given Percentile ( $\mu\text{g}/\text{m}^3$ )				
	Mass Concentration ( $\mu\text{g}/\text{m}^3$ )	Percentile	5 <sup>th</sup>	16 <sup>th</sup>	50 <sup>th</sup>	84 <sup>th</sup>	95 <sup>th</sup>
a. PM <sub>10-2.5</sub>							
1	26.7	97.9	0.5	1.6	5.2	10.8	17.9
2	40.9	97.6	0.8	2.4	7.8	15.5	27.8
3	22.5	99.8	0.6	1.5	3.5	6.5	10.3
4	22.9	97.6	0.9	2.2	6.2	11.1	15.8
5	45.0	97.4	0.7	2.0	5.7	13.7	30.6
6	40.5	97.6	0.4	1.2	4.1	12.3	29.4
b. PM <sub>2.5</sub>							
1	18.7	99.7	2.6	4.1	6.9	11.9	15.6
2	22.0	99.4	1.9	3.0	6.7	13.1	17.1
3	19.7	99.5	1.3	2.6	6.1	10.8	15.3
4	23.1	99.9	5.7	6.5	9.9	13.6	15.2
5	35.6	99.0	1.7	2.9	6.4	11.2	17.0
6	19.8	99.6	1.4	2.4	6.0	10.5	13.0

Table II - 4: Summary of Final Models by PM Metric and Site.

Site #	Regression Variables			R <sup>2</sup>
	Sound Level	Wind Speed	Wind Direction	
a. PM <sub>10-2.5</sub>				
1	--	--	--	--
2	--	High +0.06	--	0.18
3	--	--	--	--
4	--	High -0.31	Processing -0.10 Conveyer -0.40 Mine +0.24	4.7 %
5	High +0.12	High -0.30	--	2.5 %
6	High +0.31	High -0.57	Mine -0.10	3.1 %
b. PM <sub>2.5</sub>				
1	--	--	--	--
2	--	High +0.22	--	9.5 %
3	--	--	--	--
4	High +0.56	--	--	23.9 %
5	--	High -0.19	--	2.2 %
6	High +0.76	High -0.32	--	12.3 %

-- Variable is not statistically significant at a 5% level of significant

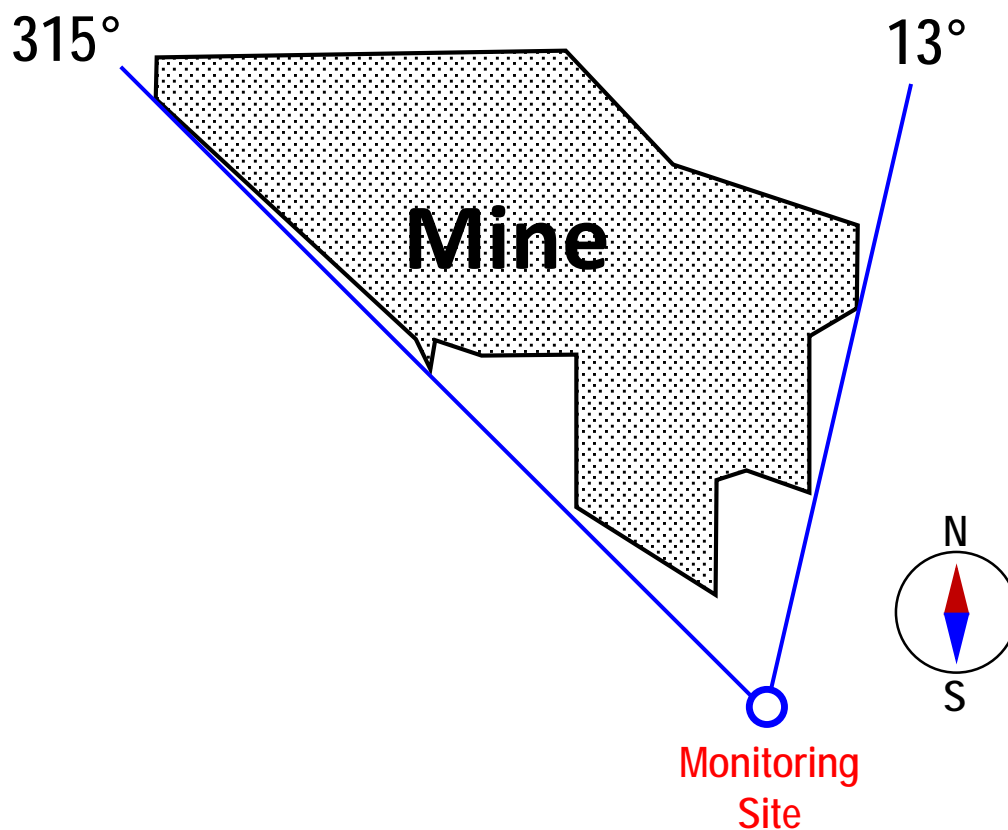


Figure II - 1: Monitoring setup at Site 5. The circle in the center identified as “Monitoring Site” represents the position of the trailer. Concentrations were attributed to the facility when wind was blowing from 315° to 13°. These wind directions were based on facility property lines as found on county mapping websites and the trailer position.

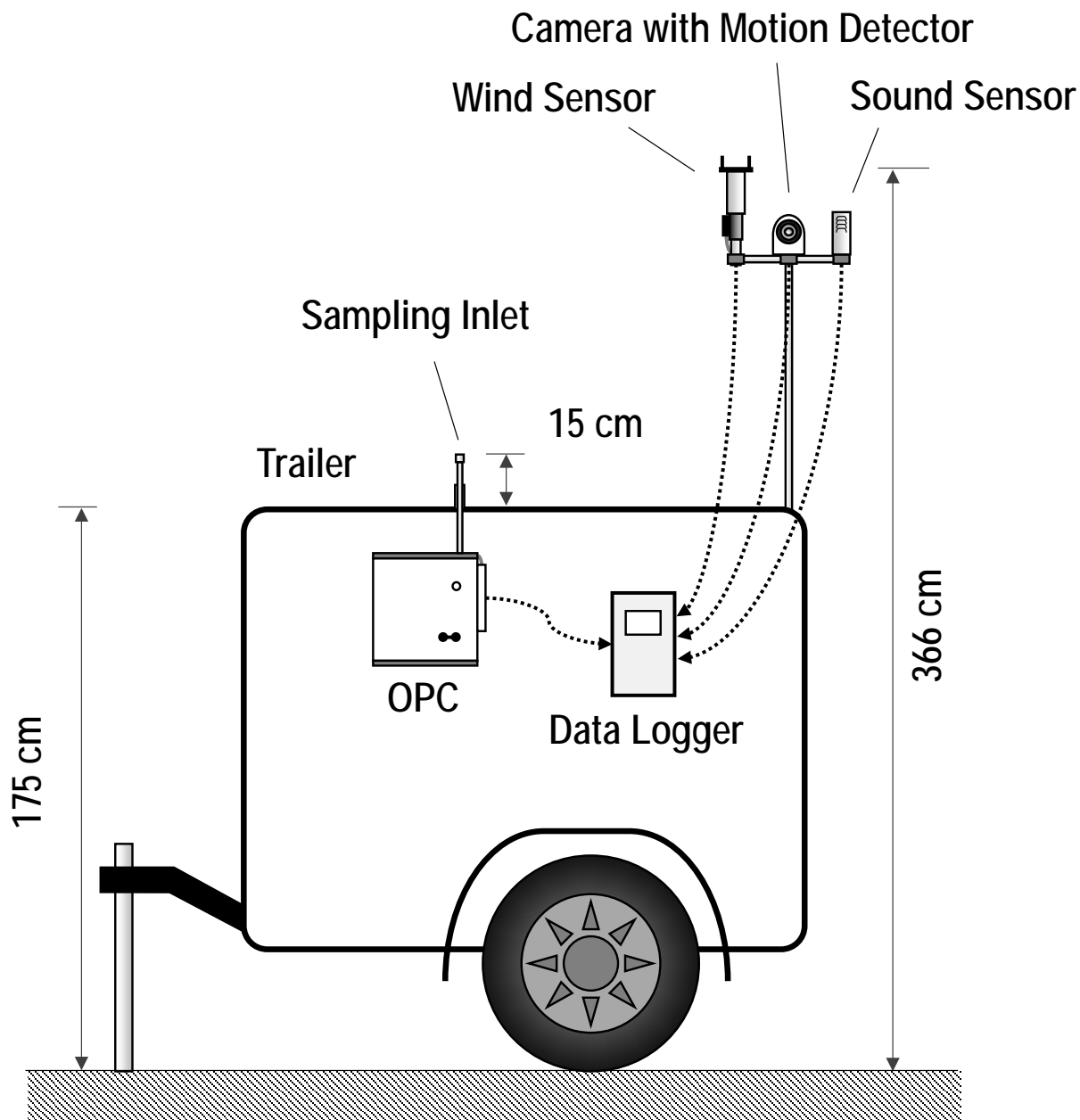


Figure II - 2: Trailer with monitoring equipment deployed at each sampling site. The OPC, wind sensor, camera, and sound sensor sent data to the data logger, which logged values every 20 seconds. The wind sensor, camera, and sound sensor were attached to a pole to reduce any obstructions from the trailer body.

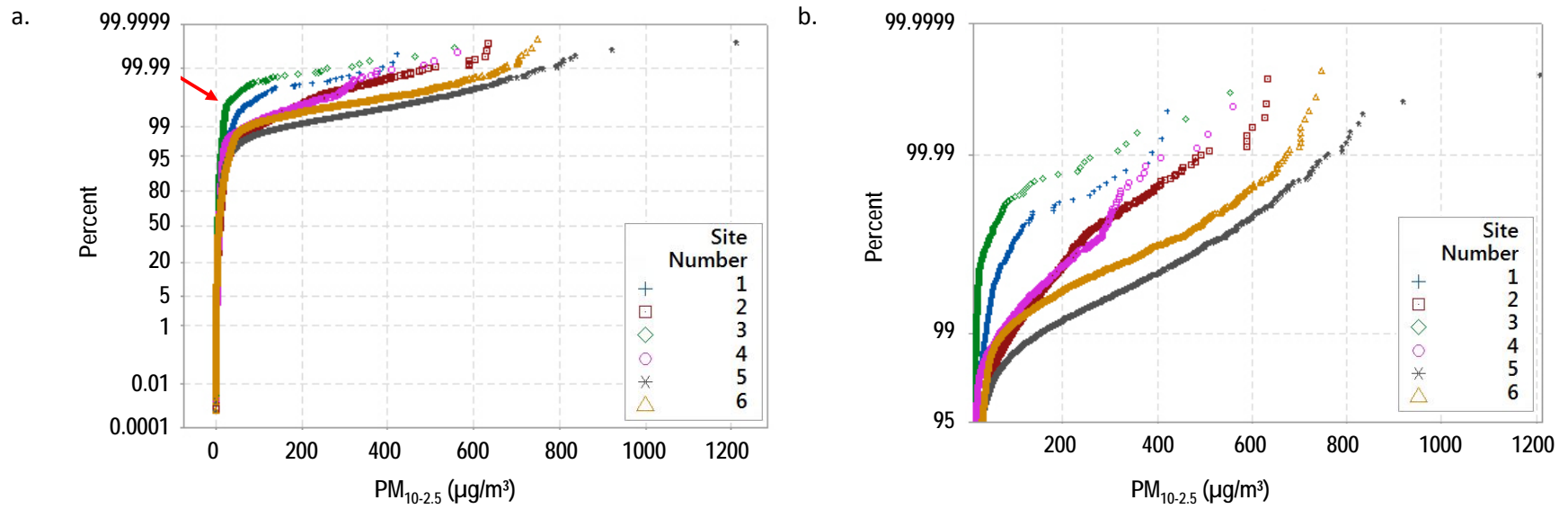
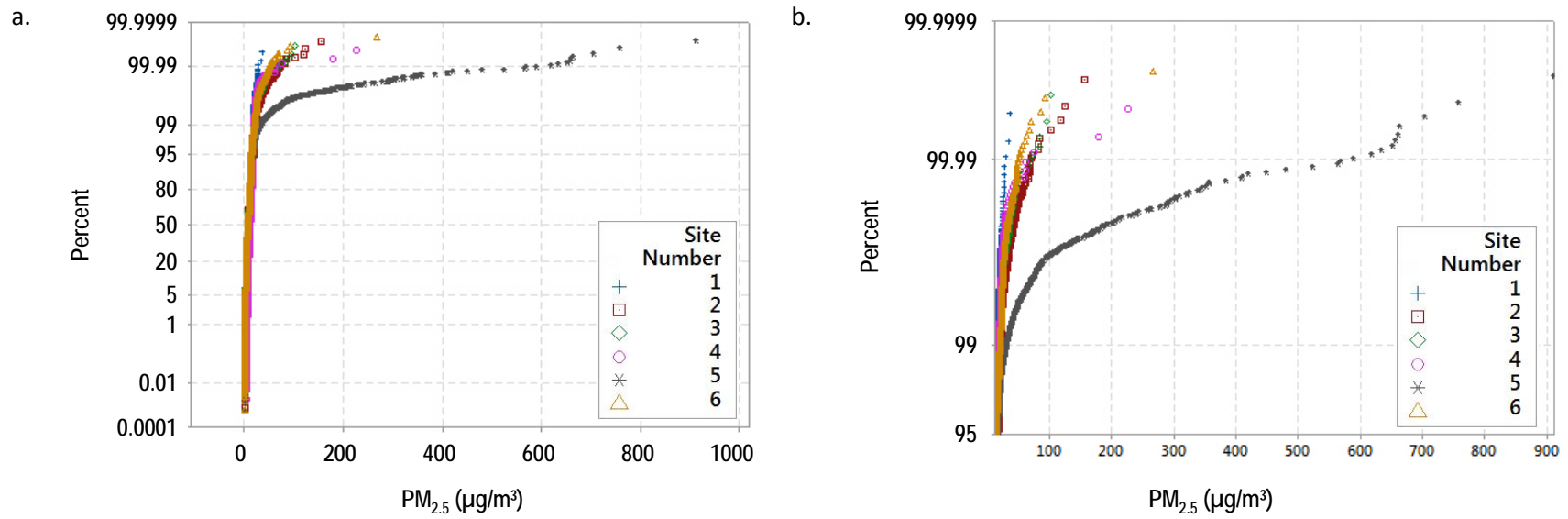


Figure II - 3: Probability plot of 20-sec PM<sub>10-2.5</sub> by site for all data (a) and for data only >95<sup>th</sup> percentile (b).



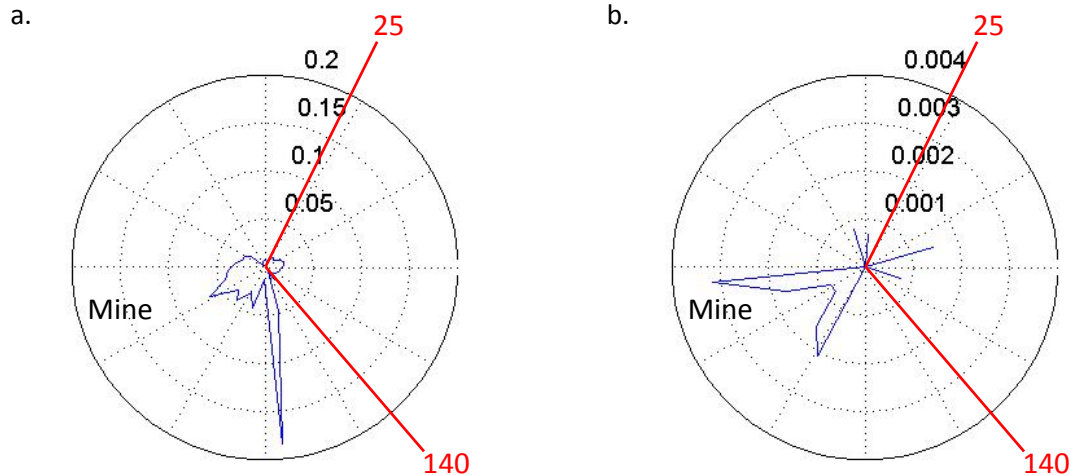


Figure II - 5: Site 1 PM<sub>10-2.5</sub> conditional probability plots showing values over a breakpoint concentration of 26.7 µg/m<sup>3</sup> (a) and 150 µg/m<sup>3</sup> (b). The center of the conditional probability plot represents the trailer at the sampling site. The radial axis represents wind direction where the top of the graph is north and bottom represents south. The concentric circles on the plots represent probability values, as the distance from the center increases the probability of a PM concentration above the threshold increases. Site specific breakpoint concentrations and the EPA NAAQS values were used as threshold values for PM<sub>10</sub> and PM<sub>2.5</sub> conditional probability plots. The wind directions marked on the plots are consistent with the wind directions related to the facility property lines. Wind directions between 140° to 25° represent wind directions that are attributed to the facility.



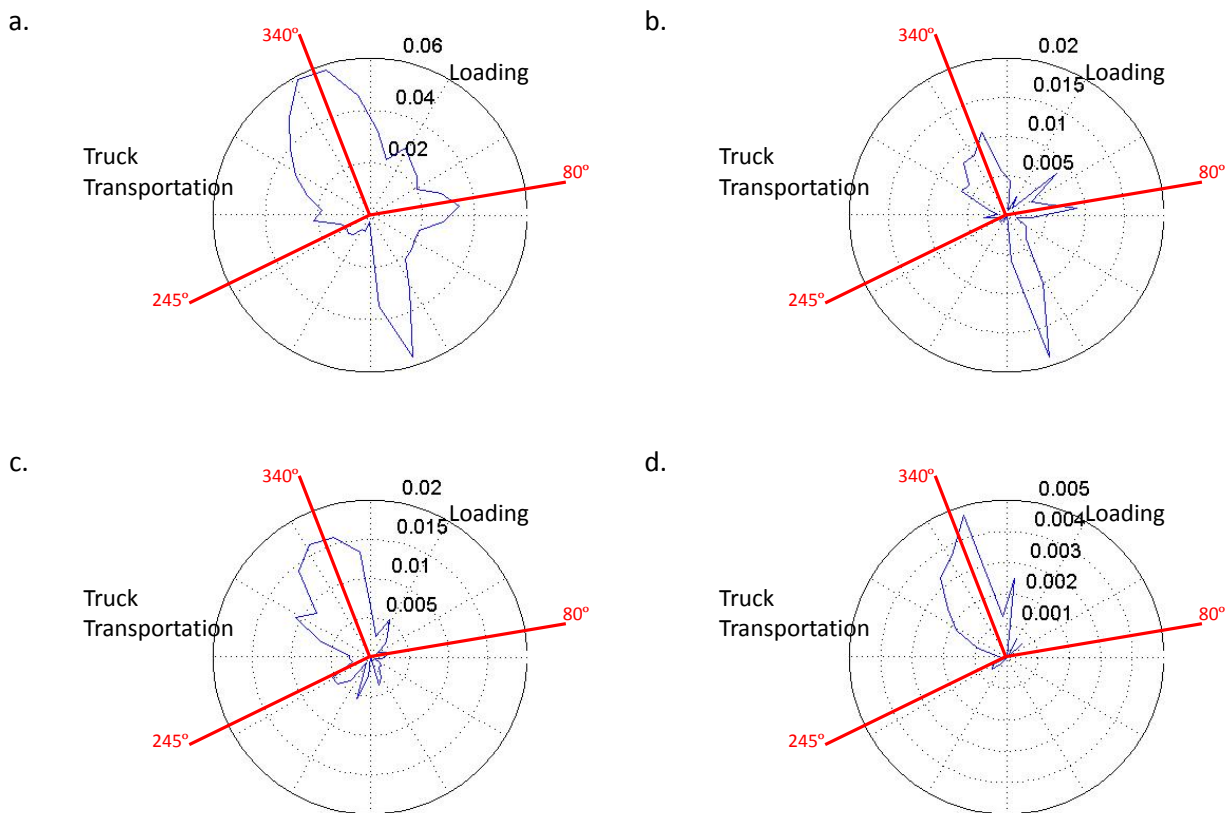


Figure II - 6: Site 2 conditional probability plots, PM<sub>10-2.5</sub> threshold 40.8  $\mu\text{g}/\text{m}^3$  (a) threshold 150  $\mu\text{g}/\text{m}^3$  (b), and PM<sub>2.5</sub> threshold 22  $\mu\text{g}/\text{m}^3$  (c) threshold 35  $\mu\text{g}/\text{m}^3$  (d). The center point represents the location of sampling trailer. Wind blowing between 245° to 340° is coming from truck transportation into the facility and wind blowing between 340° to 80° is coming from the loading portion of facility operations.

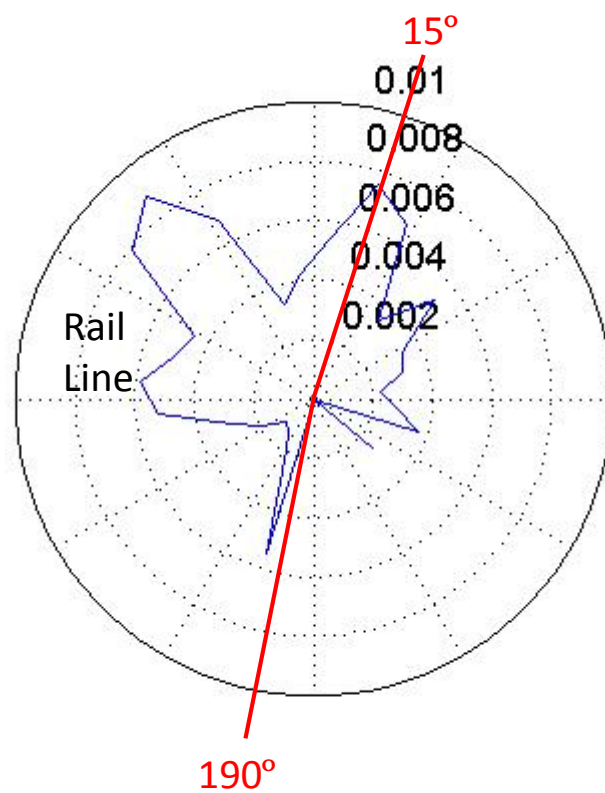


Figure II - 7: Site 3 Conditional Probability Plot for  $PM_{2.5}$  threshold of  $22 \mu\text{g}/\text{m}^3$ . Wind blowing between  $190^\circ$  to  $15^\circ$  is defined as blowing over the rail line.

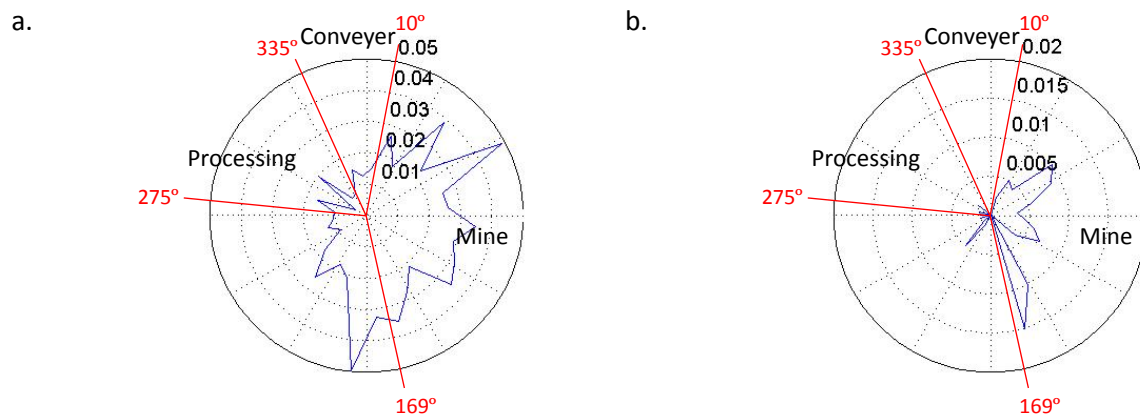


Figure II - 8: Site 4 conditional probability plots for  $PM_{10-2.5}$  threshold of  $22 \mu\text{g}/\text{m}^3$  (a) and threshold  $150 \mu\text{g}/\text{m}^3$  (b). The center point represents the location of sampling trailer and degree markings represent wind directions that are attributed to the different facility processes.

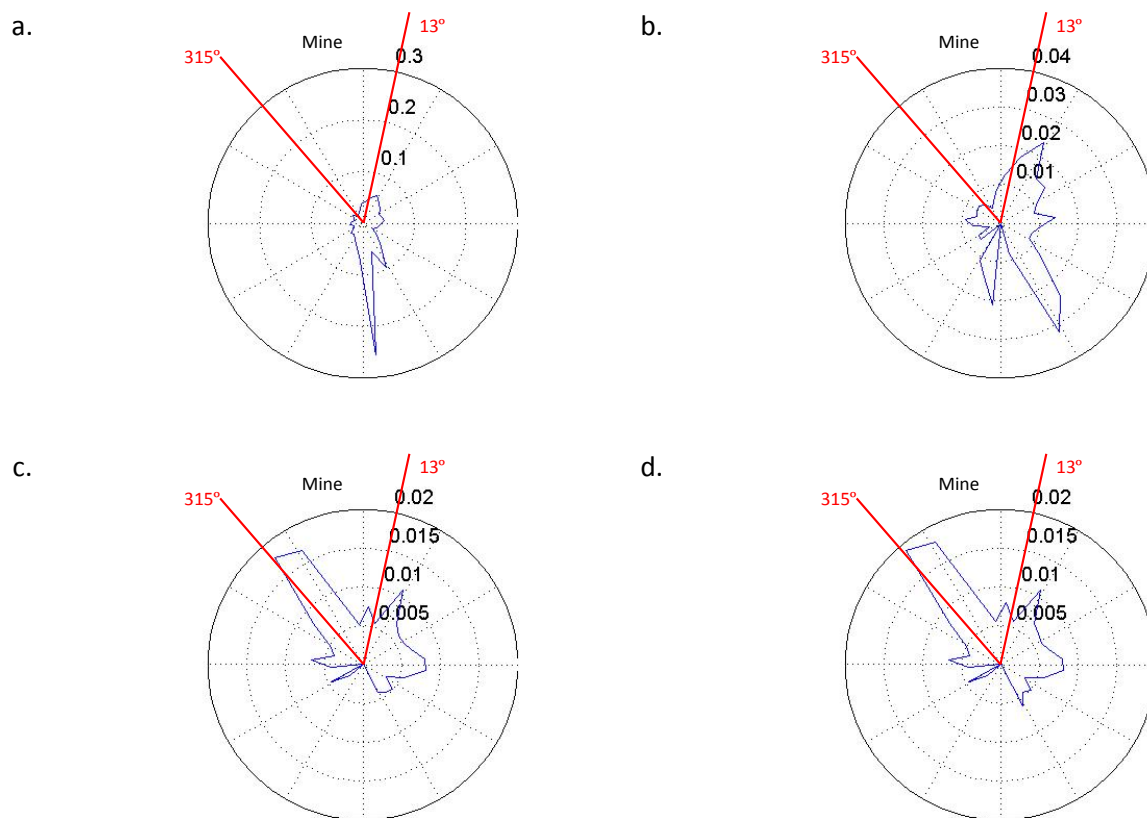


Figure II - 9: Site 5 conditional probability plots,  $PM_{10-2.5}$  threshold  $45 \mu\text{g}/\text{m}^3$  (a) threshold  $150 \mu\text{g}/\text{m}^3$  (b), and  $PM_{2.5}$  threshold  $35.6 \mu\text{g}/\text{m}^3$  (c) threshold  $35 \mu\text{g}/\text{m}^3$  (d). The center point represents the location of sampling trailer, and wind blowing between  $315^\circ$  to  $13^\circ$  is coming from the loading portion facility operations.

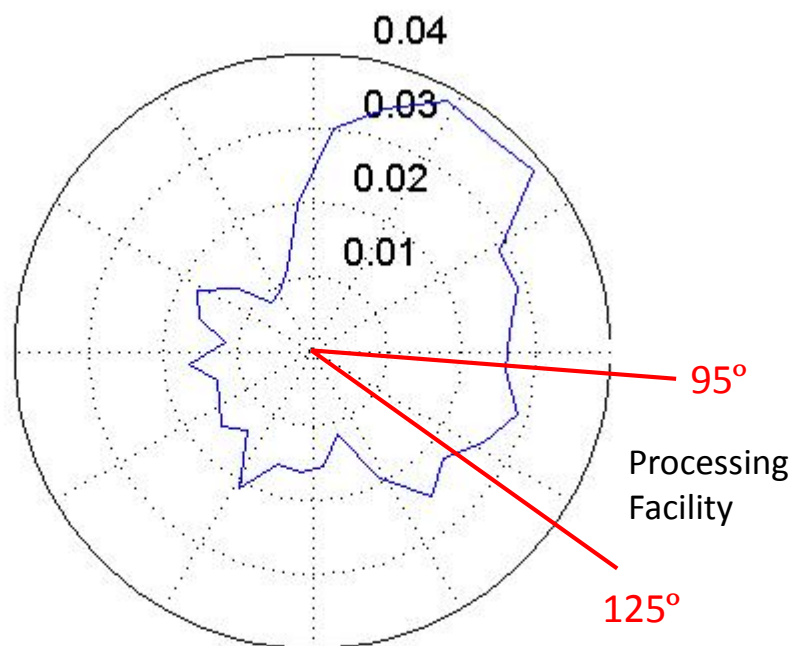


Figure II - 10: Site 6 conditional probability plots, PM<sub>10-2.5</sub> threshold 40.5 µg/m<sup>3</sup>. The center point represents the location of sampling trailer, and wind blowing between 315° to 13° is coming from the loading portion of facility operations.

### CHAPTER III: CONCLUSIONS

Particulate air quality was monitored at six residences adjacent to sand mining operations. Three of these locations were near mines with onsite processing; two were near train trans-load/transportation facilities; and one was near a processing-only facility. A portable trailer was positioned at each residence for one week to four weeks with an optical particle counter (OPC) used to measure fine ( $PM_{2.5}$ ) and coarse ( $PM_{10-2.5}$ ) particulate matter, an anemometer to measure wind speed and direction, a camera to capture images of potential sources of high PM concentrations, and sound and motion detectors to identify activities. Regression models were generated to identify determinants of elevated PM concentrations. Conditional probability plots of PM concentrations versus wind direction were prepared to relate elevated PM concentrations to specific sources.

PM concentrations were low and did not exceed the EPA NAAQS for  $PM_{10}$  or  $PM_{2.5}$ . Daily averages for each site were calculated and there was no single day that exceeded the NAAQS values for either  $PM_{10}$  or  $PM_{2.5}$ . These findings are consistent with the DNR monitors located near facilities that were included in this study. While the dust levels did not exceed NAAQS values, elevated concentrations were slightly more probable at sites when the wind was blowing from the direction of a facility. However, the increased probability observed was relatively low compared to unrelated wind directions. Variables in the regression models only explained a small fraction of the variability in PM concentration with  $R^2$  values ranging from 0.46% to 4.7% and 0.74% to 23.9% for  $PM_{10-2.5}$  and  $PM_{2.5}$ , respectively. The results of this study suggest that the sand facilities may have a small effect on ambient air quality, however this effect is not above regulatory standards for general dust.

This study highlights a novel way of identifying exposure determinates. By linking the PM concentration readings with data from a wind sensor, camera, and a sound detector, potential

sources of dust could be determined. Using data analysis techniques such as conditional probability plots, correlating wind direction with a source is simple and can help identify contributions from a specific source. With little modification to the sensors, this sampling setup could be used for many different air quality monitoring applications. Since all of the equipment is attached to a small trailer, the setup is easily moved from location to location. This setup can be used where inclement weather is a concern because all of the equipment is either housed inside the trailer or in a weather-resistant housing.

In the future, filter-based sampling methods should be used to determine if the sand facilities are causing hazardous concentrations of crystalline silica. While the results from this study did not reveal hazardous levels of general dust, there is still the potential that crystalline silica concentrations could be high. Filter-based methods should be located at similar sites to determine community exposures due to the sand facilities. Future research should also aim to set up sampling sites at varying distances from facilities to assess proximity in relation to hazardous conditions. Once filter-based sampling is performed, an accurate assessment of crystalline silica can be determined.

The concentrations observed in this study did not exceed the NAAQS for general dust, so there is a low concern for any health hazard due to general dust. However, there was a higher probability of elevated concentrations when the wind was blowing over the facilities, so there is still a possibility that hazardous levels of crystalline silica could be present. Therefore, filter-based sampling should be conducted to confirm that exposures to crystalline silica are low enough to be of little risk to the community in terms of developing silicosis. Since this study did not reveal any high concentrations of general dust related to the sand facilities, it is concluded

that in terms of general dust, sand facilities do not have a large impact on the air quality in local communities.



## APPENDIX A: FIRMWARE FOR DATA LOGGER

Code within this appendix was uploaded to the data logger and used in the field to log data at each sampling site. Takes data inputs from OPC, Wind sensor, sound detector, and camera. Logs all data onto a SD card with a time stamp that matches the logging time frame.

```
/* MySoundCamMEGA_V3_3
```

Peters Lab 2014-3-19

Picture taken when sound is above an alarm value, and motion is detected by camera

Picture stored in a folder with the date (yyyymmdd) and a filename with the time (hhmmss.jpg)

V1.1 Add capability to log sound

V2.0 Add Grimm OPC data collection

v3.2 Add Wind Sensor and motion detection capabilities

```
*/
```

```
#include <SoftwareSerial.h>
```

```
#include <Adafruit_VC0706.h>
```

```
#include <SD.h>
```

```
#include <Wire.h>
```

```
#include "RTCLib.h"
```

```
#include <SPI.h>
```

```
boolean IS_DEBUG = false; //debug Grimm OPC code with no camera or sound - 1=true for debug
```

```
boolean Is_Motion_On = true; // Turns on motion detector, False will turn off Motion detection
```

```
boolean Is_WindSensorConnected = true; // True will run code if sensor is connected, False will run code with out wind sensor
```

```
int LogInterval = 20; // seconds between logging data
```

```
int SensorReadInterval = 1; //seconds between sensor reads
```

```
uint32_t NextLogTime = 1;
```

```
uint32_t NextSensorRead = 1;
```

```
long ZZsoundTotal = 0;
```

```
int ZZsoundCount = 0;
```

```
int PM10 = 0;
```

```
int PM25 = 0;
```

```
int PM1 = 0;
```

```
long totPM10 = 0;
```

```
long totPM25 = 0;
```

```
long totPM1 = 0;
```

```
int GrimmCount = 0;
```

```
int gi = 0;
```

```
char line[85];
```

```
char RestOfLine[85];
```

```
char WindInfo[18];
```

```
char Windspeed[8];
```

```
char Winddirection[3];
```

```
char windaddress[1];
```

```

int InstWindSpeed = 0; //instrument reads m/s www.w; multiply by 10 - store value in integer
int InstWindDir = 0; //reads direction in degrees saves it as ddd stor value in integer
long totWindSpeed = 0; //Total of speed readings used to avg over time period
long totWindDir = 0; //Total of direction readings used to avg over time period
int WindCount; //counter for wind readings

const int LCD_Pin = 8;
int potAlarmPin = A2;
int ZZsoundPin = A0;

SoftwareSerial lcd = SoftwareSerial(255, LCD_Pin);
RTC_DS1307 RTC; // define the Real Time Clock object
DateTime now;

// the digital pins that connect to the LEDs
#define redLEDPin 4 //indicates flush
#define greenLEDPin 5 //indicates reading data
// the logging file
File logfile;

int AlarmValue = 0;
int ZZsoundValue = 0;

const int numReadings = 10;
int readings[numReadings]; // the readings from the analog input
int index = 0; // the index of the current reading
long total = 0; // the running total
int average = 0; // the average

#define chipSelect 10

#if ARDUINO >= 100
// On Uno: camera TX connected to pin 2, camera RX to pin 3:
//SoftwareSerial cameraconnection = SoftwareSerial(2, 3);
// On Mega: camera TX connected to pin 69 (A15), camera RX to pin 3:
//SoftwareSerial cameraconnection = SoftwareSerial(69, 3);
#else
//NewSoftSerial cameraconnection = NewSoftSerial(2, 3);
#endif
Adafruit_VC0706 cam = Adafruit_VC0706(&Serial2);

void setup() { //-----SETUP
  lcd.begin(9600);

```

```

lcd.write(0xFE); lcd.write(0x50); lcd.write(255); delay(10); // set the contrast, 255 max
lcd.write(0xFE); lcd.write(0x99); lcd.write(200); delay(10); // set the brightness, 255 max
lcd.write(0xFE); lcd.write(0x4B); lcd.write(0xFE); lcd.write(0x54); delay(10); // turn off
cursors
lcd.write(0xFE); lcd.write(0x52); delay(10); // Turns off autoscroll
lcd.write(0xFE); lcd.write(0x58); delay(10); // clear screen
lcd.write(0xFE); lcd.write(0x48); delay(10); // go 'home'
lcd.print("SoundCam v3.1");
delay(500);
lcd.println(" - Peters Lab");

// use debugging LEDs
pinMode(redLEDpin, OUTPUT);
pinMode(greenLEDpin, OUTPUT);

//from smoothing routine
// initialize all the readings to 0:
for (int thisReading = 0; thisReading < numReadings; thisReading++)
  readings[thisReading] = 0;

if(chipSelect != 10) pinMode(10, OUTPUT); // SS on Uno, etc.

Serial.begin(9600);
Serial1.begin(9600);
Serial3.begin(9600);
while(!Serial){;}
Serial.println("VC0706 Camera test");

// see if the card is present and can be initialized:
if (!SD.begin(10, 11, 12, 13)) {
  Serial.println("Card failed, or not present");
  // don't do anything more:
  return;
}

// connect to RTC
Wire.begin();
if (!RTC.begin()) {
  Serial.println("RTC failed");
}

now = RTC.now();
char foldername[9];

```

```

sprintf(foldername, "%02d%02d%02d", now.year(), now.month(), now.day());
Serial.print("Date = "); Serial.println(foldername);

char filename[7];
sprintf(filename, "%02d%02d%02d", now.hour(), now.minute(), now.second());
Serial.print("Time = "); Serial.println(filename);

// create a new file
char loggerfilename[] = "LOGGER00.CSV";
for (uint8_t i = 0; i < 100; i++) {
  loggerfilename[6] = i/10 + '0';
  loggerfilename[7] = i%10 + '0';
  if (!SD.exists(loggerfilename)) {
    // only open a new file if it doesn't exist
    logfile = SD.open(loggerfilename, FILE_WRITE);
    break; // leave the loop!
  }
}

if (!logfile) {
  error("couldnt create file");
}

Serial.print("Logging to: ");
Serial.println(loggerfilename);
String Header =
"DateTime,Sound%5V,PM10_ug_m3,PM25_ug_m3,PM1_ug_m3,WindSpeed,WindDirection";
logfile.println(Header);
Serial.println(Header);

delay(2000);

now = RTC.now();
NextLogTime = now.unixtime() + LogInterval ;
NextSensorRead = now.unixtime() + SensorReadInterval;

#if !IS_DEBUG //if IS_DEBUG is false will run the cam code
// Try to locate the camera
if (cam.begin()) {
  Serial.println("Camera Found:");
} else {
  Serial.println("No camera found?");
  return;
}
// Print out the camera version information (optional)
char *reply = cam.getVersion();

```

```

if (reply == 0) {
  Serial.print("Failed to get version");
} else {
  Serial.println("-----");
  Serial.print(reply);
  Serial.println("-----");
}

// Set the picture size - you can choose one of 640x480, 320x240 or 160x120
// Remember that bigger pictures take longer to transmit!

//cam.setImageSize(VC0706_640x480);    // biggest
cam.setImageSize(VC0706_320x240);    // medium
//cam.setImageSize(VC0706_160x120);    // small

// You can read the size back from the camera (optional, but maybe useful?)
uint8_t imgsize = cam.getImageSize();
Serial.print("Image size: ");
if (imgsize == VC0706_640x480) Serial.println("640x480");
if (imgsize == VC0706_320x240) Serial.println("320x240");
if (imgsize == VC0706_160x120) Serial.println("160x120");

// Motion detection system can alert you when the camera 'sees' motion!
//cam.setMotionDetect(true);          // turn it on
cam.setMotionDetect(Is_Motion_On);    // if Is_Motion_on is true then motion detectio will
be on

// You can also verify whether motion detection is active!
Serial.print("Motion detection is ");
if (cam.getMotionDetect())
  Serial.println("ON");
else
  Serial.println("OFF");
#endif
}

void loop() {/-------LOOP
//is it time to log? if yes, then average, log, and clear totals; otherwise look for data from Dylos
and collect other sensor data if it is time
now = RTC.now();
if (now.unixtime() >= NextLogTime){

```

```

//Average, log, clear totals, and set next log time
NextLogTime = now.unixtime() + LogInterval ;
WriteData();
ClearSensorRegisters();
} else {
//Collect data
// listen for new serial coming in from Grimm OPC:
char someChar = Serial1.read();
if( someChar != -1){
  memset(RestOfLine, 0, sizeof(RestOfLine));
  Serial1.readBytesUntil('\n',RestOfLine,85);
  line[0] = someChar;
  int i = 0;
  while (i <= sizeof(RestOfLine)) {
    line[i+1] = RestOfLine[i];
    i++;
  }

  Serial.println(line);
  ProcessLine();
}

//if it is time to read other sensors then do it
if (now.unixtime() >= NextSensorRead){
  //Read sensors
  if (Is_WindSensorConnected){ // if the sensor is connected then IS_windsensorconnected
should be set to true
    Serial3.write("MA!");
    //reads the sensor info until all info is recived
    Serial3.readBytesUntil('\r',WindInfo,18);
    sscanf(WindInfo,"%s %s %s", windaddress, &Windspeed, &Winddirection);
    InstWindSpeed = atof(Windspeed) * 10;
    totWindSpeed += InstWindSpeed;
    InstWindDir = atoi(Winddirection);
    totWindDir += InstWindDir;
    WindCount++;
  //    Serial.print(WindCount); Serial.print(" "); Serial.print(Windspeed); Serial.print(" ");
  Serial.println(Winddirection); //debug
  //    Serial.print(WindInfo); Serial.print(" "); Serial.print(InstWindSpeed); Serial.print(" ");
  Serial.println(InstWindDir); //debug

  }
  ZZsoundTotal = ZZsoundTotal + total / numReadings;
  ZZsoundCount = ZZsoundCount + 1;
}

```

```

// Serial.print(ZZsoundCount); Serial.print(" "); Serial.print(total / numReadings );
Serial.print(" "); Serial.println(ZZsoundTotal); //debug
NextSensorRead = NextSensorRead + SensorReadInterval;
}
}

#if !IS_DEBUG //if IS_DEBUG is false will run the cam code
// subtract the last reading:
total= total - readings[index];
// read from the sensor:
readings[index] = analogRead(ZZsoundPin);
// Serial.println(readings[index]); //debug

// add the reading to the total:
total= total + readings[index];
// advance to the next position in the array:
index = index + 1;

// if we're at the end of the array...
if (index >= numReadings) index = 0;
// calculate the average:
average = total / numReadings;

// send it to the computer as ASCII digits
// Serial.println(average/ 1023. * 100);
delay(1); // delay in between reads for stability

AlarmValue = analogRead(potAlarmPin);
lcd.write(0xFE); lcd.write(0x48); delay(10); // go 'home

lcd.print("Alarm="); lcd.print(AlarmValue / 1023. * 100, 0); lcd.println("%");
lcd.print("Sound="); lcd.print(average / 1023. * 100, 0); lcd.println("%");
delay(10);
#endif

#if !IS_DEBUG //if IS_DEBUG is false will run the cam code
if (average > AlarmValue && cam.motionDetected()) {
  cam.setMotionDetect(false);
  Serial.println("LOUD > SoundTrigger!");
  if (! cam.takePicture()) Serial.println("Failed to snap!"); else Serial.println("Picture taken!");

  now = RTC.now();
  char foldername[9];
  sprintf(foldername, "%02d%02d%02d", now.year(), now.month(), now.day());
  char pathfilename[21];

```



```

    sprintf(pathfilename, "%02d%02d%02d/%02d%02d%02d", now.year(), now.month(),
now.day(), now.hour(), now.minute(), now.second());
    strcat(pathfilename, ".JPG");
    Serial.print("pathfilename = ");
    Serial.println(pathfilename);

    SD.mkdir(foldername);
    File imgFile = SD.open(pathfilename, FILE_WRITE);

    uint16_t jpglen = cam.frameLength();
    Serial.print(jpglen, DEC);
    Serial.println(" byte image");

    Serial.print("Writing image to "); Serial.print(pathfilename);

    while (jpglen > 0) {
        // read 32 bytes at a time;
        uint8_t *buffer;
        uint8_t bytesToRead = min(32, jpglen); // change 32 to 64 for a speedup but may not work
with all setups!
        buffer = cam.readPicture(bytesToRead);
        imgFile.write(buffer, bytesToRead);

        //Serial.print("Read "); Serial.print(bytesToRead, DEC); Serial.println(" bytes");
        jpglen -= bytesToRead;
    }
    imgFile.close();
    Serial.println("...Done!");
    cam.resumeVideo();
    //resets motion detector

    cam.setMotionDetect(Is_Motion_On);    // turn it off (default)

    ClearSoundRollingArray();
}
#endif

}

void WriteData (void) {

    // fetch the time
    now = RTC.now();
    // log time

    char myDateTime2[21];

```

```
    sprintf(myDateTime2, "%02d/%02d/%02d %02d:%02d:%02d", now.month(), now.day(),
now.year(), now.hour(), now.minute(), now.second());
```

```
    logfile.print(myDateTime2);
    Serial.print(myDateTime2);
```

```
    float ZZsoundAvg = ZZsoundTotal/ZZsoundCount / 1023. * 100;
    logfile.print(", "); logfile.print(ZZsoundAvg);
    Serial.print(", "); Serial.print(ZZsoundAvg);
```

```
    float PMavg = totPM10 / 10. / GrimmCount;
    logfile.print(", "); logfile.print(PMavg);
    Serial.print(", "); Serial.print(PMavg);
```

```
    PMavg = totPM25 / 10. / GrimmCount;
    logfile.print(", "); logfile.print(PMavg);
    Serial.print(", "); Serial.print(PMavg);
```

```
    PMavg = totPM1 / 10. / GrimmCount;
    logfile.print(", "); logfile.print(PMavg);
    Serial.print(", "); Serial.print(PMavg);
```

```
    float avg = totWindSpeed / 10.0 / WindCount;
    logfile.print(", "); logfile.print(avg);
    Serial.print(", "); Serial.print(avg);
```

```
    avg = totWindDir / WindCount;
    logfile.print(", "); logfile.print(avg);
    Serial.print(", "); Serial.print(avg);
```

```
    logfile.println();
    Serial.println();
```

```
    digitalWrite(greenLEDpin, LOW); //end reading
```

```
    // blink LED to show we are syncing data to the card & updating FAT!
    digitalWrite(redLEDpin, HIGH);
    logfile.flush();
    digitalWrite(redLEDpin, LOW);
```

```
}
```

```
void ClearSoundRollingArray()
{
    // initialize all the readings to 0:
```

```

for (int thisReading = 0; thisReading < numReadings; thisReading++)
  readings[thisReading] = 0;
total = 0;
}

void ClearSensorRegisters()
{
  ZZsoundTotal = 0;
  ZZsoundCount = 0;
  totPM10 = 0;
  totPM25 = 0;
  totPM1 = 0;
  GrimmCount = 0;

  InstWindSpeed = 0;
  InstWindDir = 0;
  totWindSpeed = 0;
  totWindDir = 0;
  WindCount = 0;

}

void error(char *str)
{
  Serial.print("error: ");
  Serial.println(str);
  // red LED indicates error
  digitalWrite(redLEDpin, HIGH);
  while(1);
}

void ProcessLine(void){
  if (line[0] == 78){
    sscanf(line,"%*4s %d %d %d",&PM10,&PM25,&PM1);
    totPM10 = totPM10 + PM10;
    totPM25 = totPM25 + PM25;
    totPM1 = totPM1 + PM1;
    GrimmCount = GrimmCount++;

//    Serial.print("Last Values: ");
//    Serial.print(PM10);
//    Serial.print(' ');
//    Serial.print(PM25);
//    Serial.print(' ');

```

```
// Serial.println(PM1);  
//  
// Serial.print("Totals: ");  
// Serial.print(totPM10);  
// Serial.print(' ');  
// Serial.print(totPM25);  
// Serial.print(' ');  
// Serial.println(totPM1);  
}  
else  
{  
// Serial.println("Recieved line other than N");  
}  
}
```

## APPENDIX B: MATLAB CODE

The MATLAB codes in this appendix were used to generate site specific figures and tables. The first code was used to read in the CSV files created from the data logger into MATLAB. The second code was used to separate site specific datasets from the log files, and code determinate variables (wind speed, wind direction, and sound level) for regression analysis. The Conditional Probability Code used Conditional Probability Function, Polar Plot Code, and Wind Rose Code to generate the plot and wind rose using site specific PM and wind direction data.

## Code Used to Read Import Data into MATLAB

```

%Code to read in site data
clc
clear

%USER INPUT
%Input Directory
inDir = 'M:\General Research Directory\102Peters\Research\Projects\2013-Frack\Frack
Ryans\Sampling Data';
%inDir = '\Volumes/102Peters-1/Research/Projects/2013-Frack/Frack Ryans/Sampling Data';

dirList = getAllFiles(inDir);

onlyCSVName = dirList(~cellfun(@isempty,(regexp(dirList,\.CSV$))));
DateTime = [];
Sound5V = [];
PM10 = [];
PM25 = [];
PM1 = [];
WindSpeed = [];
WindDirection = [];
siteName = [];
for i = 1: size(onlyCSVName)

    newDataCheck = importdata(char(onlyCSVName(i)), ',');
    %onlyCSVName(i)
    if(~isempty(newDataCheck) )
        aa = (size(newDataCheck.data));

        if(aa(1,2) <8)
            fid = fopen(char(onlyCSVName(i)));
            newData = textscan(fid,'%s %f %f %f %f %f %d', 'delimiter',';', 'headerLines', 1);
            k = strfind(onlyCSVName(i), '\');
            strtemp = char(onlyCSVName(i));
            strSite = strtemp(k{1,1}(length(k{1:1})-1)+1:k{1,1}(length(k{1:1}))-1);
            site = newData{:,1};
            site(:) = {strSite};
            siteName = vertcat(siteName,site);
            DateTime = vertcat(DateTime,datenum(newData{:,1}));
            Sound5V = vertcat(Sound5V,newData{:,2});
            PM10 = vertcat(PM10,newData{:,3});
            PM25 = vertcat(PM25,newData{:,4});
            PM1 = vertcat(PM1,newData{:,5});
            WindSpeed = vertcat(WindSpeed,newData{:,6});
            WindDirection = vertcat(WindDirection,newData{:,7});
        end
    end
end

```

```
        fclose(fid);  
    end  
end  
end
```

## Code Used to Separated Sites and Categorize Determinates

```

%Plot data
clc
clear Date1 Date2 Degree1 Degree2 Degree3 Degree4 Plot date1num date2num WTavg WDAvg
WindDirectionnew WDIInc a AvgPM10 AvgPM25 AvgTime10 AvgTime25 SizeofPM10
SizeofPM25 v1 v2 t1 t2 starttime endtime1 endtime2 b c avgPM10 avgPM25 avgTime25
avgTime10
%ENTER QUERY
%Date Range

Date1 = '07/31/2014 16:44:00';
Date2 = '08/08/2014 14:44:00';

Date3 = '01/01/2000 00:00:00';
Date4 = '01/02/2000 00:05:00';

Degree1 = 275;
Degree2 = 335;
Degree3 = 0;
Degree4 = 10;
Degree5 = 169;
% Degree6 = 169;

% 1 min has 3 cells 10 min avg WDIInc =30
WDIInc = 30;

TopTailpm10 = 22.92; %The PM 10 cut off value
TopTailpm25 = 23.13; %The PM 2.5 cut off value

Speed = 3; %m/s

Sound = 2; % Percent sound level value

Plot1 = 1; % 1: Plot and 0:Dont Plot; Normal Distribution Line plots
Plot2 = 0; % 1: Plot and 0:Dont Plot; Normal Distribution Wind box plots
Plot3 = 0; % 1: Plot and 0:Dont Plot; Normal Distribuiton Sound box plots
Plot4 = 0; % 1: Plot and 0:Dont Plot; Log graphs vs Normal Graphs
Plot5 = 1; % 1: Plot and 0:Dont Plot; Log box vs Normal box
Plot6 = 0; % 1: Plot and 0:Dont Plot; Log box vs Normal sound box plots
Plot7 = 0; % 1: Plot and 0:Dont PLOT; Scatter plots for Concentration v Wind Direction
Plot8 = 1; % 1: Plot and 0:Dont Plot; Normal Distribution Line plots 98th percentile
Plot9 = 0; % 1: Plot and 0:Dont Plot; Normal Distribution Wind box plots 98th percentile
Plot10 = 0; % 1: Plot and 0:Dont Plot; Normal Distribuiton Sound box plots 98th percentile
Plot11 = 0; % 1: Plot and 0:Dont Plot; Log graphs vs Normal Graphs 98th percentile
Plot12 = 1; % 1: Plot and 0:Dont Plot; Log box vs Normal box 98th percentile

```



```
Plot13 = 0; % 1: Plot and 0:Dont Plot; Log box vs Normal sound box plots 98th percentile
Plot14 = 1; % 1: Plot and 0:Dont PLOT; Scatter plots for Concentration v Wind Direction 98th
percentile
```

```
Plot15 = 0;
```

```
%do you want to save the figure
```

```
%End of user input
```

```
date1num = datenum(Date1);
```

```
date2num = datenum(Date2);
```

```
a = find(DateTime >= date1num & DateTime <= date2num);
```

```
DateTimeNew = DateTime(a);
```

```
Sound5VNew = Sound5V(a);
```

```
PM10New = PM10(a);
```

```
PM25New = PM25(a);
```

```
PM10New = PM10New - PM25New;
```

```
PM1New = PM1(a);
```

```
WindSpeednew = WindSpeed(a);
```

```
WindDirectionnew = WindDirection(a);
```

```
siteNamenew = siteName(a);
```

```
RotateWD = 180 + WindDirectionnew();
```

```
WVsize = length(WindDirectionnew);
```

```
for i=1:WVsize
```

```
    if(RotateWD(i) > 360)
```

```
        RotateWD(i) = RotateWD(i) - 360;
```

```
    end
```

```
end
```

```
WindDirectionnew = RotateWD;
```

```
SpeedVariable=WindDirectionnew;
```

```
SoundVariable=WindDirectionnew;
```

```
tempWindVariable =WindDirectionnew;
```

```
WDavg = [];
```

```
j=1;
```

```
for i=1:WDInc:WVsize-WDInc
```

```
    WTavg(j) = nanmean(DateTimeNew(i:i+WDInc));
```

```

WSavg(j) = sqrt(mean(-
times(WindSpeednew(i:i+WDInc),sin(deg2rad(double(WindDirectionnew(i:i+WDInc))))))^2 +
mean(-
times(WindSpeednew(i:i+WDInc),cos(deg2rad(double(WindDirectionnew(i:i+WDInc))))))^2);

if(rad2deg(atan2(-
mean(times(WindSpeednew(i:i+WDInc),cos(deg2rad(double(WindDirectionnew(i:i+WDInc))))))
),-
mean(times(WindSpeednew(i:i+WDInc),sin(deg2rad(double(WindDirectionnew(i:i+WDInc))))))
))) <180)
    WDavg(j) = rad2deg(atan2(-
mean(times(WindSpeednew(i:i+WDInc),cos(deg2rad(double(WindDirectionnew(i:i+WDInc))))))
),-
mean(times(WindSpeednew(i:i+WDInc),sin(deg2rad(double(WindDirectionnew(i:i+WDInc))))))
))) + 180 ;
else
    WDavg(j) = rad2deg(atan2(-
mean(times(WindSpeednew(i:i+WDInc),cos(deg2rad(double(WindDirectionnew(i:i+WDInc))))))
),-
mean(times(WindSpeednew(i:i+WDInc),sin(deg2rad(double(WindDirectionnew(i:i+WDInc))))))
))) - 180 ;
end
%i=i+WDInc; You are increasing i with the loop, dont create a counter
%for a variable defined for a loop
j=j+1;
end

```

```
WindVariable = WDavg;
```

```

WDavgT=transpose(WDavg);
tempppm25 = PM25New(~isnan(PM10New));           %Get non NaN observation data for
site
tempdate = DateTimeNew(~isnan(PM10New));
tempppm10 = PM10New(~isnan(PM10New));
tempwindDir = WindDirectionnew(~isnan(PM10New));
tempSound5View = Sound5VNew(~isnan(PM10New));

```

```

reqDir1 = find(WDavgT >= Degree1 & WDavgT < Degree2);
reqDir2 = find(WDavgT >= Degree2 & WDavgT < Degree3);
reqDir3 = find(WDavgT >= Degree3 & WDavgT <= Degree4);
reqDir4 = find(WDavgT >= Degree4 & WDavgT <= Degree5);
%nonreqDir = find(WDavgT < Degree1 & WDavgT > Degree2);

```

```

WindVariable(:) = 1;
WindVariable(reqDir1) = 2;

```

```
WindVariable(reqDir2) = 3;
WindVariable(reqDir3) = 3;
WindVariable(reqDir4) = 4;
```

```
%all data
```

```
tempreqDir1 = find(WindDirectionnew >= Degree1 & WindDirectionnew < Degree2);
tempreqDir2 = find(WindDirectionnew >= Degree2 & WindDirectionnew < Degree3);
tempreqDir3 = find(WindDirectionnew >= Degree3 & WindDirectionnew < Degree4);
tempreqDir4 = find(WindDirectionnew >= Degree4 & WindDirectionnew <= Degree5);
%tempnonreqDir = find(WindDirectionnew < Degree1 & WindDirectionnew > Degree2);
```

```
tempWindVariable(:) = 1;
tempWindVariable(tempreqDir1) = 2;
tempWindVariable(tempreqDir2) = 3;
tempWindVariable(tempreqDir3) = 3;
tempWindVariable(tempreqDir4) = 4;
```

```
%*****
```

```
reqSpeed = find(WindSpeednew > Speed);
SpeedVariable(:) = 1;
SpeedVariable(reqSpeed) = 2;
```

```
reqSound = find(Sound5VNew > Sound);
SoundVariable(:) = 1;
SoundVariable(reqSound) = 2;
```

```
tempWindSpeed = WindSpeednew(~isnan(PM10New));
tempWindDirectionnew = WindDirectionnew(~isnan(PM10New));
tempWindVarAll = tempWindVariable(~isnan(PM10New));
```

```
tempSpeedVariable = SpeedVariable(~isnan(PM10New));
tempSoundVariable = SoundVariable(~isnan(PM10New));
tempsiteNamenew = siteNamenew(~isnan(PM10New));
```

```
temppm10log = log(temppm10);
temppm25log = log(temppm25);
```

```
PM10nonneg = find(temppm10>0);
PM25nonneg = find(temppm25>0);
```

```
TopPm10 = find(temppm10 >= TopTailpm10);
TopPm25 = find(temppm25 >= TopTailpm25);
```

```

log98pm10 = log(temppm10(TopPm10));
log98pm25 = log(temppm25(TopPm25));

TimeAdj = datenum(Date4)-datenum(Date3);
SizeofPM10 = size(PM10nonneg);
SizeofPM25 = size(PM25nonneg);

v1 = 1;
t1 = 1;
v2 = 1;
t2 = 1;
starttime = tempdate(1);
endtime1 = tempdate(SizeofPM10);
endtime2 = tempdate(SizeofPM25);

for b = starttime:TimeAdj:endtime1
    x1 = find(tempdate >=b & tempdate < b+TimeAdj);

    avgPM10(v1) = nanmean(temppm10(x1));
    avgTime10(t1) = nanmean(tempdate(x1));

    v1 = v1+1;
    t1 = t1+1;

    clear x1
end

for c = starttime:TimeAdj:endtime2
    x2 = find(tempdate >=c & tempdate < c+TimeAdj);

    avgPM25(v2) = nanmean(temppm25(x2));
    avgTime25(t2) = nanmean(tempdate(x2));

    v2 = v2+1;
    t2 = t2+1;

    clear x2
end

AvgPM10 = avgPM10';
AvgTime10 = avgTime10';
AvgPM25 = avgPM25';
AvgTime25 = avgTime25';

```

## Conditional Probability Code

```

% making an example of a conditional probability function plot

% for citations on CPF, see Atmospheric Environment 38 (2004) 4667i;½4673
% Comparison between Conditional ProbabilityFunction and
% Nonparametric Regression for Fine Particle Source Directions
% Eugene Kim, Philip K. Hopke

% close all
% clear variables

rand_wind_vec = ShawWD;
rand_conc_vec = ShawPM25;
WindSpeed = ShawWS;

% now make a pollution rose of it

genutil_wind_rose(rand_wind_vec,WindSpeed,'dtype','standard','n', 16, 'di', [0.5 2.1 3.6 5.7 8.8
11.1 12]);

% and now the conditional probability
options.wind_coord = 'mapdeg';

%rand_wind_vec = genutil_angle_switcher(rand_wind_vec, 'mapdeg_to_mathdeg');

figure
threshold = 1;
[ directional_PSCF plot_struct ] = genutil_calc_directional_PSCF( rand_wind_vec,
rand_conc_vec, threshold, 32, options );
%h = genutil_cos_polarplot( [plot_struct.angle_list plot_struct.radii_list]');
h = bak_genutil_cos_polarplot( plot_struct.angle_list, ...
plot_struct.radii_list);

```

## Conditional Probability Plot Function

```
function [ directional_PSCF plot_struct ] = genutil_calc_directional_PSCF( wind_vector,
PM_vector, threshold, wind_bin_count, options );
```

```
% for citations on CPF, see Atmospheric Environment 38 (2004) 4667-4673
```

```
% Comparison between Conditional Probability Function and
```

```
% Nonparametric Regression for Fine Particle Source Directions
```

```
% Eugene Kim, Philip K. Hopke
```

```
%
```

```
% Sept 26, 2010 -modifying to accept wind directions as "math"
```

```
% representation (with wind from East = 0, Wind from N 90, wind from west
```

```
% 180) and wind direction as "map" coordinates (wind from north 0m=, wind
```

```
% from west 270, wind from east 90).
```

```
% previously, wind was expected as map coordinates in degrees
```

```
if strmatch( options.wind_coord, 'mapdeg');
```

```
    % do nothing - this is what function expects
```

```
elseif strmatch( options.wind_coord, 'mathdeg')
```

```
    % convert back to map
```

```
    wind_vector = genutil_angle_switcher(wind_vector, 'mathdeg_to_mapdeg');
```

```
else
```

```
    error('options.wind_coord not recognized. see code genutil_calc_directional_PSCF\n');
```

```
end
```

```
% first place wind direction into bins
```

```
wind_bin_offset = 360/wind_bin_count/2;
```

```
wind_bin_mid = linspace(wind_bin_offset,360-wind_bin_offset,wind_bin_count);
```

```
wind_vector = genutil_make_column(wind_vector);
```

```
PM_vector = genutil_make_column(PM_vector);
```

```
numhours = length(wind_vector);
```

```
monitor_high_hours = find( PM_vector > threshold );
```

```
monitor_wind_bin_offset_matrix = abs(repmat(wind_vector,1,wind_bin_count) -
repmat(wind_bin_mid,numhours,1));
```

```
direction_bin_number_by_hour = NaN(numhours,1);
```

```
wind_bin_directional_occurrence_count = zeros(wind_bin_count,1);
```

```
high_PM_directional_occurrence_count = zeros(wind_bin_count,1);
```

```
for i=1:numhours
```

```
    if sum(~isnan(monitor_wind_bin_offset_matrix(i,:))) >= 1
```

```
        direction_bin_number_by_hour(i,1) =
```

```
min(find(monitor_wind_bin_offset_matrix(i,:)==(min(min(monitor_wind_bin_offset_matrix(i,:))
)))));
```

```

wind_bin_directional_occurrence_count(direction_bin_number_by_hour(i,1)) = ...
    wind_bin_directional_occurrence_count(direction_bin_number_by_hour(i,1)) + 1;
if PM_vector(i) > threshold
    high_PM_directional_occurrence_count( direction_bin_number_by_hour(i,1) ) = ...
        high_PM_directional_occurrence_count( direction_bin_number_by_hour(i,1) ) + 1;
end
else
    direction_bin_number_by_hour(i,1) = NaN;
end
end
directional_PSCF =
high_PM_directional_occurrence_count./wind_bin_directional_occurrence_count;

```

*% building a list of angle and radii for a polar plot*

```

angle_list = [];
radii_list = [];
bin_edge_CCW_radians = genutil_angle_switcher( wind_bin_mid - 360/wind_bin_count/2,
'mapdeg_to_mathrad');
bin_center_radians = genutil_angle_switcher( wind_bin_mid - 0, 'mapdeg_to_mathrad');
bin_edge_CW_radians = genutil_angle_switcher( wind_bin_mid + 360/wind_bin_count/2,
'mapdeg_to_mathrad');

```

```

at_center_flag = 1;
for j=1:wind_bin_count
    if directional_PSCF(j)>0
        angle_list = vertcat( angle_list, bin_center_radians(j) );
        radii_list = vertcat( radii_list, directional_PSCF(j));
        at_center_flag = 0;
    else % this angle does have a radius of zero
        if at_center_flag == 0
            at_center_flag = 1;
            angle_list = vertcat( angle_list, bin_center_radians(j) );
            radii_list = vertcat( radii_list, 0 );
        end
    end
end
% regarding closure of the circle. 4 cases
% 1 CPF exists at first and last angle
% 2 CPF exists at first but not last
% 3 CPF exists at last but not first
% 4 CPF does not exist at first or last
if and(directional_PSCF(1)>0,directional_PSCF(end)>0) % case 1
    % do nothing
end
if directional_PSCF(end)==0 % case 2

```

```

notzerolist = find(directional_PSCF>0);
if isempty(notzerolist)
    plot_struct.angle_list = [];
    plot_struct.radii_list = [];
    plot_struct.isempty = 1;
    return;
end
j=max(notzerolist)+1;
contflag=1;
if j>wind_bin_count
    contflag=0;
end
while contflag==1
    if directional_PSCF(j)==0
        angle_list = vertcat( bin_center_radians(j), angle_list );
        radii_list = vertcat( 0, radii_list);
    else % this angle does not have a radius of zero
        contflag=0;
    end
    j=j+1;
    if j>=wind_bin_count
        contflag=0;
    end
end
end
if directional_PSCF(1)==0
    contflag=1;
    j=1;
    while contflag==1
        if directional_PSCF(j)==0
            angle_list = vertcat( bin_center_radians(j), angle_list );
            radii_list = vertcat( 0, radii_list);
        else % this angle does not have a radius of zero
            contflag=0;
        end
        j=j+1;
        if j>=wind_bin_count
            contflag=0;
        end
    end
end
end

%     angle_list = vertcat( angle_list, [ bin_edge_CCW_radians(j); bin_edge_CW_radians(j); 0
]);
%     radii_list = vertcat( radii_list, [ directional_PSCF(j); directional_PSCF(j); 0 ]);

```



```
angle_list(end+1) = angle_list(1);  
radii_list(end+1) = radii_list(1);
```

```
plot_struct.angle_list = angle_list;  
plot_struct.radii_list = radii_list;
```

```
if isempty(angle_list)  
    plot_struct.isempty = 1;  
else  
    plot_struct.isempty = 0;  
end
```

## Polar Plot Code

```

function [Xi,Yi,Zi] = genutil_cos_polarplot(Zp,varargin)
% from polarplot3d
% POLARPLOT3D Plot a 3D surface from polar coordinate data
% [Xi,Yi,Zi] = polarplot3d(Zp,varargin)
% Input
% Zp      two dimensional matrix of input magnitudes or intensities
%         each column of Zp contains information along a single meridian
%         each row  of Zp contains information at  a single radius
%         the direction sense of the rows and columns is determined by
%         the relative order of the angular and radial vectors
%         by default Zp is increasing in radius down each column and
%         increasing in angle (counter-clockwise) along each row
%         the default plot is a full disc surface plot with unit radius
%
% varargin 'property','value' pairs that modify plot characteristics
%          property names must be specified as quoted strings
%          property names and their values are not case sensitive
%          for each property the default value is given below
%
% 'AngularRange' scalar or 2 element vector, radians  (default = [0 2*pi])
% 'RadialRange'  scalar or 2 element vector          (default = [0 1])
%               if a scalar is given for either range it is used as
%               the maximum value and zero is used for the minimum
% 'ColorData'   a matrix of color values, size must be equal to size(Zp)
%               the default coloring is according to Zp magnitude
% 'MeshScale'   mesh element scale factor           (default = 1)
%               values > 1 increase mesh element size (coarser mesh)
%               values < 1 decrease mesh element size (finer mesh)
% 'TickSpacing' spacing of polar tick marks in degrees (default = 10)
%               every other tick mark is labeled
% 'PolarGrid'   polar grid density vector (2 elements) (default = [10 36])
%               number of grid lines in radial and azimuthal directions
% 'ContourLines' scalar (number of contours) or a vector (contour locations)
%               the default is auto selection by the contour function
% 'PlotType'    'surfn' surface plot,              no mesh (default)
%               'surfcn' surface plot with contours, no mesh
%               'surfc' surface plot with contours
%               'surf' surface plot
%               'mesh' mesh plot
%               'meshc' mesh plot with contours
%               'meshl' mesh plot with no interpolation
%               full data matrix plotted, 'MeshScale' is ignored
% 'contour' 2D contour plot
%           use 'ContourLines' to set the number of contours

```

```

%           'wire'  wireframe polar grid plot only, no surface plot
%                   a wireframe and polar axis overlay can be added to
%                   an existing plot (the current plot is not cleared)
%           'off'  no plot is produced, interpolation only
% 'AxisLocation' 'surf'  polar axis along edge of surface  (default)
%           'min'  polar axis at minimum Zp for largest radius
%           'max'  polar axis at maximum Zp for largest radius
%           'mean' polar axis at mean  Zp for largest radius
%           'top'  polar axis at top  of plot box
%           'bottom' polar axis at bottom  of plot box
%           value  polar axis is drawn at specified height
%           'off'  no polar axis
% 'InterpMethod' 'cubic'  bicubic      interpolation on Zp (default)
%           'linear'  bilinear      interpolation on Zp
%           'spline'  spline        interpolation on Zp
%           'nearest' nearest neighbor interpolation on Zp
% 'PlotProps'    a cell array of 'property','value' pairs
%           plotprops are passed to mesh, surf and contour
%           the default value is an empty cell array
%
% Output
% Xi,Yi,Zi  Cartesian locations corresponding to polar coordinates (T,R,Zp)
%           T and R are created from Trange and Rrange using meshgrid and
%           converted to Cartesian coordinates with pol2cart
%           Xi,Yi,Zi are square matrices with size equal to the maximum
%           dimension of Zp after interpolation
%           matrix sizes are reduced or enlarged by mscale
%           if 'meshl' is specified, size(Xi)=size(Yi)=size(Zi)=size(Zp)
%
% Notes      Zp is the only required input argument
%           if no input arguments are given an example plot is produced
%           and this help text is displayed in the command window
%
% Example
% 1) a transformation of data generated by the peaks function is plotted
%    in 3d polar coordinates between 30 and 270 degrees and from radius
%    80 to 400
% 2) a surface colored according to height above the xy plane is shown
%    without Cartesian grid lines
% 3) a 4 by 24 polar grid is drawn on top of the surface
% 4) a polar axis is drawn along the perimeter of the surface
% 5) tick marks are drawn at 8 degree intervals with labels every 16 degrees
%
% P = peaks(101);                % generate interesting data
% P = (P+rot90(P)-rot90(3*fliplr(P)));
% P(62:end,:) = [];

```

```

%
% figure;                % draw 3d polar plot
% polarplot3d(P,'PlotType','surfn','PolarGrid',[4 24],'TickSpacing',8,...
%             'AngularRange',[30 270]*pi/180,'RadialRange',[80 400]);
%
%                         % set plot attributes
% set(gca,'DataAspectRatio',[10 10 1],'View',[-64,26],...
%        'Xlim',[-450 450],'Xtick',[-400 -200 0 200 400],...
%        'Ylim',[-450 450],'Ytick',[-400 -200 0 200 400]);
% title('polarplot3d example');
%
% Ken Garrard, North Carolina State University, 2006-2007
% version 1   Original function based on POLAR3D by J De Freitas
%     2   Changed argument method to 'Property',value pairs
%     2.1 Added 'ColorData' property

% argument string values for PlotType, AxisLocation and InterpMethod properties
plst = {'mesh','meshc','meshl','wire',...
        'surf','surfc','surfn','surfcn','contour','off'};
alst = {'off','const','min','max','mean','surf','top','bottom'};
mlst = {'cubic','linear','spline','nearest'};

% if function was called without arguments
% draw example plot in a new figure and display help text
if nargin < 1
    P = peaks(101);                % generate interesting data
    P = (P+rot90(P)-rot90(3*fliplr(P)));
    P(62:end,:) = [];

    figure;                        % draw 3d polar plot
    polarplot3d(P,'PlotType','surfn','PolarGrid',[4 24],'TickSpacing',8,...
                'AngularRange',[30 270]*pi/180,'RadialRange',[80 400]);

    % set plot attributes
    set(gca,'DataAspectRatio',[10 10 1],'View',[-64,26],...
          'Xlim',[-450 450],'Xtick',[-400 -200 0 200 400],...
          'Ylim',[-450 450],'Ytick',[-400 -200 0 200 400]);
    title('polarplot3d example');

    % display help text
    error(['No input arguments given\n'...
          'Please consult the help text and the example plot\n'...
          '-----\n%s'],help(mfilename));
end

%-- parse and validate input arguments

```

```

% setup property structure with default values
p.angularrange = [0 2*pi]; % angular range
p.radialrange = [0 1]; % radial range
p.plottype = 'surfn'; % surface plot, no rectangular grid
p.meshscale = 1; % no mesh scaling
p.polargrid = [10 36]; % number of azimuthal and radial grid lines
p.tickspacing = 10; % ten degree tick mark spacing
p.axislocation = ""; % handle as special case after parsing varargs
p.interpmethod = 'cubic'; % bicubic interpolation
p.colordata = []; % default coloring according to Zp values
p.contourlines = ""; % default contour specification
p.axislabels = 'on';
p.plotprops = {}; % no additional plot properties

% parse property value pairs, replacing defaults with those specified by caller
try
    p = parse_pv_pairs(p,varargin);
catch
    error('Error parsing varargin list\n??? %s',lasterr);
end

% check plot type specification
if ~ischar(p.plottype) || isempty(strmatch(lower(p.plottype),plst,'exact'))
    error('Invalid "PlotType" property value');
end
p.plottype = lower(p.plottype);

% choose default polar axis location
if isequal(p.axislocation,"")
    if ~isempty(strmatch(p.plottype,{'meshc','surf','surfn'},'exact'))
        p.axislocation = 'bottom'; % plot box bottom for contour plots
    else p.axislocation = 'surf'; % along perimeter of surface otherwise
    end
end

% user specified polar axis location as a numeric value
if isnumeric(p.axislocation)
    [r,c] = size(p.axislocation);
    if (((r ~= 1) || (c ~= 1)) || ~isreal(p.axislocation))
        error("'AxisLocation' property value must be scalar, positive and real");
    end
    polax = p.axislocation;
    p.axislocation = 'const';
end

% check polar axis location specification

```

```

if ~ischar(p.axislocation) || isempty(strmatch(lower(p.axislocation),alst,'exact'))
    error('Invalid "AxisLocation" property value');
end
p.axislocation = lower(p.axislocation);

% check angular and radial range vectors
p.angularrange = p.angularrange(:);
if isscalar(p.angularrange), p.angularrange = [0; p.angularrange]; end
if length(p.angularrange) ~= 2 || ~isreal(p.angularrange)
    error(['"AngularRange" property value must be a scalar'...
        ' or a two element numeric vector']);
end

p.rrange = p.radialrange(:);
if isscalar(p.radialrange), p.radialrange = [0; p.radialrange]; end
if length(p.radialrange) ~= 2 || ~isreal(p.radialrange)
    error(['"RadialRange" property value must be a scalar'...
        ' or a two element numeric vector']);
end

% angular and radial range vectors define data order
% reflect Zp left-right and/or up-down depending on angular and radial ranges
if p.angularrange(1) > p.angularrange(2), Zp = fliplr(Zp); end
if p.radialrange(1) > p.radialrange(2), Zp = flipud(Zp); end

[Tmin,Tmax] = deal(min(p.angularrange),max(p.angularrange)); % Tmin < Tmax
[Rmin,Rmax] = deal(min(p.radialrange ),max(p.radialrange )); % Rmin < Rmax

% angular range cannot be more than one full circumference
if abs(Tmax - Tmin) > 2*pi
    error('Angular range cannot be greater than 2*pi');
end

% extract radial and azimuthal grid density from parameter structure
p.polargrid = p.polargrid(:);
if length(p.polargrid) ~= 2 || ~isreal(p.polargrid)
    error('"PolarGrid" property value must be a two element numeric vector');
end
[radgrid,azmgrid] = deal(p.polargrid(1),p.polargrid(2));

% check azimuthal and radial grid density
if ~isnumeric(radgrid) || radgrid < 0
    error('Non-numeric or non-positive radial grid parameter');
end
if ~isnumeric(azmgrid) || azmgrid < 0
    error('Non-numeric or non-positive azimuthal grid parameter');
end

```

```

end

% check mesh scale factor property value
[r,c] = size(p.meshscale);
if (((r ~= 1) || (c ~= 1)) || ~isreal(p.meshscale)) || p.meshscale <= 0
    error("'MeshScale' property value must be scalar, positive and real");
end

% check tick spacing property value
[r,c] = size(p.tickspacing);
if (((r ~= 1) || (c ~= 1)) || ~isreal(p.tickspacing)) || p.tickspacing <= 0
    error("'TickSpacing' property value must be scalar, positive and real");
end

% check contour lines property value
if ~isnumeric(p.contourlines) && ~isequal(p.contourlines, '');
    error("'ContourLines' property value must be numeric");
end
p.contourlines = p.contourlines(:);

% check interpolation method
p.interpmethod = lower(p.interpmethod);
if ~ischar(p.interpmethod) || isempty(strmatch(p.interpmethod,mlst,'exact'))
    error('Invalid "InterpMethod" property value');
end

% check input data size
[r,c] = size(Zp);
if (r < 5) || (c < 5)
    error('Zp matrix size must be greater than 4 x 4');
end

% check if mesh scale factor is compatible with input data dimension
if round(max(r,c)/p.meshscale) < 4
    error('Mesh scale factor is too large, not enough data remaining to plot');
end

% choose default color matrix
if isempty(p.colordata), p.colordata = Zp; end    % surface height coloring

% check color matrix
if ~isnumeric(p.colordata) || ~isequal(size(p.colordata),[r,c])
    error('Color matrix must be numeric and the same size as Zp');
end

% no polar axis or grid is generated if no plot was requested

```

```

% or if the plot type is a 2D contour plot
if ~isempty(strmatch(p.plottype,{'off','contour'},'exact'))
    p.axislocation = 'off';
    azmgrid = 0;
    radgrid = 0;
end

%-- create polar grid and interpolate data

% create radius and angle vectors and polar grid for input data matrix
rho = linspace(Rmin,Rmax,r);           % radius vector
angl = linspace(Tmin,Tmax,c);          % angle vector
[xx,yy] = meshgrid(angl,rho);          % mesh matrices

% check for 'meshl' plot
if isequal(p.plottype,'meshl')          % no interpolation
    Xi = rho * cos(angl);                % matrix of x's
    Yi = rho * sin(angl);                % matrix of y's
    Zi = Zp;                             % z's == input data

% interpolate Zp to a scaled polar grid
else
    q = fix(max(r,c)/p.meshscale);       % new mesh size
    rho = linspace(Rmin,Rmax,q);         % radius vector
    angl = linspace(Tmin,Tmax,q);        % angle vector
    [theta,rad] = meshgrid(angl,rho);     % create polar grid
    T = interp2(xx,yy,Zp,theta,rad,p.interpmethod); % interpolate to grid
    [Xi,Yi,Zi] = pol2cart(theta,rad,T);   % convert to Cartesian
end

% interpolate color data to same grid as height data
if isequal(p.plottype,'meshl')          % no interpolation needed
    Ci = p.colordata;                    % for 'meshl' plots
else Ci = interp2(xx,yy,p.colordata,theta,rad,p.interpmethod);
end

%-- plot the Cartesian surface

switch p.plottype
    case 'wire', grid on;
    case 'meshc', meshc(Xi,Yi,Zi,Ci);
    case 'mesh', mesh(Xi,Yi,Zi,Ci,p.plotprops{:});
    case 'meshl', mesh(Xi,Yi,Zi,Ci,p.plotprops{:});
    case 'surf', surf(Xi,Yi,Zi,Ci,p.plotprops{:});
    case 'surfc', surfc(Xi,Yi,Zi,Ci,p.plotprops{:});
    case 'surfn', surf(Xi,Yi,Zi,Ci,'LineStyle','none',p.plotprops{:});

```



```

case 'surfc', surfc(Xi,Yi,Zi,Ci,'LineStyle','none',p.plotprops{:});
case 'contour', axis equal; polar([Tmin Tmax],[Rmin Rmax]); hold on;
    contour(Xi,Yi,Zi,p.contourlines); colorbar; hold off;
end

%-- plot the polar axis

% axis and tick font attributes
fontargs = {'FontName','Arial','FontSize',10,'FontWeight','bold'};

if ~isequal(p.axislocation,'off')

    % create polar axis data just outside the largest radius
    xa = Rmax * 1.005 .* cos(angl);
    ya = Rmax * 1.005 .* sin(angl);

    % create polar axis tic marks at p.tickspacing intervals
    ts = 180/p.tickspacing;
    ta = pi/ts * (round(Tmin*ts/pi):1:round(Tmax*ts/pi));
    tr = Rmax * [1.005; 1.03; 1.1];
    xt = tr * cos(ta);
    yt = tr * sin(ta);

    % set polax to z location of polar axis
    switch p.axislocation
    case 'min', polax = min (Zi(end,:));
    case 'max', polax = max (Zi(end,:));
    case 'mean', polax = mean(Zi(end,:));
    case 'top', zlim = get(gca,'zlim'); polax = zlim(2);
    case 'bottom', zlim = get(gca,'zlim'); polax = zlim(1);
    end

    % z values for polar axis and tick marks
    if isequal(p.axislocation,'surf'), % vary along edge of surface
        za = Zi(end,:);
        zt = interp1(angl,za,ta,'linear');
    else
        za = zeros(size(xa)) + polax; % constant location
        zt = zeros(1,length(ta)) + polax;
    end

    % label every other tick mark
    nl = round(length(ta)/2);

    % beginning and end of a full polar axis are identical, label once
    if abs(Tmin-Tmax) == 2*pi, nl = nl-1; end

```

```

% plot the polar axis
hold on;
line(xa,ya,za,'Color','k','LineWidth',1);
line(xt(1:2,:),yt(1:2,:),[zt;zt],'Color','k'); % add tick marks

if strcmp(p.axislabels,'on','EXACT')
    % draw tick labels
    for k = 2 * (1:nl) - 1
        text(xt(3,k),yt(3,k),zt(k),num2str(ta(k)*180/pi),...
            'HorizontalAlignment','Center','fontargs{:}');
    end
end
hold off;
end

%-- draw polar grid lines

if azmgrid > 0 || radgrid > 0

    % interpolate data to a fine mesh to produce smooth grid lines
    N = 360; % new grid size
    m = abs(fix(N/max(1,azmgrid))); % angular grid spacing
    r = abs(fix(N/max(1,radgrid+1))); % radial grid spacing
    rho = linspace(Rmin,Rmax,N+1); % radius vector
    angl = linspace(Tmin,Tmax,N+1); % angle vector
    [theta,rad] = meshgrid(angl,rho); % create polar grid
    T = interp2(xx,yy,Zp,theta,rad,p.interpmethod); % interpolate to grid
    [xi,yi,zi] = pol2cart(theta,rad,T); % convert to Cartesian
    hold on; % plot in same figure

    % don't draw polar grid lines at minimum radius unless the plot
    % region is an annulus or only meridian grid lines are requested
    k = r+1;
    if Rmin > 0 || radgrid == 0, k = 1; end

    % draw radial grid lines in azimuthal direction (meridians)
    if azmgrid > 0
        xr = xi(k:end,1:m:end);
        yr = yi(k:end,1:m:end);
        zr = zi(k:end,1:m:end);
        plot3(xr,yr,zr,'Color','k','LineWidth',1); % plot grid lines
    end

    % draw azimuthal grid lines in radial direction (concentric arcs)
    if radgrid > 0

```

```
    xm = xi(k:r:end-1,:);  
    ym = yi(k:r:end-1,:);  
    zm = zi(k:r:end-1,:);  
    plot3(xm',ym',zm','Color','k','LineWidth',1); % plot grid lines  
end  
hold off;  
end  
  
%-- set axis font  
if ~isequal(p.plottype,'off'), set(gca,fontargs{:}); end
```

## Wind Rose Code

```

function varargout = wind_rose(D,F,varargin)

% NOTE - FLIPPED THE DIRECTION SO THAT IN METEO
% MODE THE ANGLES POINT TOWARD THE WIND DIRECTION
%
% THE DIRECTIONS SHOULD BE THE DIRECTION THE WIND IS BLOWING FROM

USER_FONTSIZE = 16;

% WIND ROSE Wind rose of direction and intensity
%
% Syntax:
% HANDLES = WIND_ROSE(D,I,VARARGIN)
%
% Inputs:
% D Directions
% I Intensities
% VARARGIN:
% -dtype, type of input directions D, standard or meteo,
%   if meteo, the conversion dnew=mod(-90-D,360) is done;
%   if not meteo, standard is used (default)
% -n, number of D subdivisions
% -di, intensities subdivisions, default is automatic
% -ci, percentage circles to draw, default is automatic
% -labtitle, main title
% -lablegend, legend title
% -cmap, colormap [jet]
% -colors, to use instead of colormap, for each di
% -quad, Quadrant to show percentages [1]
% -ri, empty internal radius, relative to size of higher
%   percentage [1/30]
% -legtype, legend type: 1, continuous, 2, separated boxes [2]
% -bcolor, full rectangle border color ['none']
% -lcolor, line colors for axes and circles ['k']
% -percbg, percentage labels bg ['w']
% -ax, to place wind rose on pervious axes, the input for ax
%   must be [theax x y width], where theax is the previous
%   axes, x and y are the location and width is the wind
%   rose width relative to theax width (default=1/5)
% -iflip, flip the intensities as they go outward radially, ie,
%   highest values are placed nearest the origin [{0} 1]
%
% Output:
% HANDLES Handles of all lines, fills, texts
%

```

```

% Examle:
% d=0:10:350;
% D=[];
% V=[];
% for i=1:length(d)
%     n=d(i)/10;
%     D=[D ones(1,n)*d(i)];
%     V=[V 1:n];
% end
%
% figure
% wind_rose(D,V)
%
% figure
% wind_rose(D,V,'iflip',1)
%
% figure
% wind_rose(D,V,'ci',[1 2 7],'dtype','meteo')
%
% % place it on a previous axes:
% ax=axes;
% plot(lon,lat)
% wind_rose(D,V,'ax',[ax x y 1/3])
%
% MMA 26-11-2007, mma@odyle.net
%
% IEO, Instituto Español de Oceanografía
% La Coruña, España
%
% 10-12-2007 - Added varargin ci and n (nAngles removed as input)
% 17-12-2007 - Added varargin ax, colors
% 22-02-2008 - Added varargin dtype
% 08-05-2008 - Bug fix (bar at dir=0 could be incorrect in some cases)
% 14-05-2008 - Added varargin iflip

```

```

%figure;
handles=[];

```

```

% varargin options:
dtype='standard';
nAngles=36;
ri=1/30;
quad=1;
legType=2;

```

```

percBg='w';
titStr="";
legStr="";
cmap=jet;
colors=[];
Ag=[]; % intensity subdvs.
ci=[]; % percentage circles
lineColors='k';
borderColor='none';
onAxes=false;
iflip=0;
lowwind_flag =0; % default

vin=varargin;
for i=1:length(vin)
    if isequal(vin{i},'dtype')
        dtype=vin{i+1};
    elseif isequal(vin{i},'lowwind')
        lowwind_flag=1;
        lowwind_speed=vin{i+1};
    elseif isequal(vin{i},'n')
        nAngles=vin{i+1};
    elseif isequal(vin{i},'ri')
        ri=vin{i+1};
    elseif isequal(vin{i},'quad')
        quad=vin{i+1};
    elseif isequal(vin{i},'legtype')
        legType=vin{i+1};
    elseif isequal(vin{i},'percbg')
        percBg=vin{i+1};
    elseif isequal(vin{i},'labtitle')
        titStr=vin{i+1};
    elseif isequal(vin{i},'lablegend')
        legStr=vin{i+1};
    elseif isequal(vin{i},'cmap')
        cmap=vin{i+1};
    elseif isequal(vin{i},'colors')
        colors=vin{i+1};
    elseif isequal(vin{i},'di')
        Ag=vin{i+1};
    elseif isequal(vin{i},'ci')
        ci=vin{i+1};
    elseif isequal(vin{i},'lcolor')
        lineColors=vin{i+1};
    elseif isequal(vin{i},'bcolor')
        borderColor=vin{i+1};

```

```

elseif isequal(vin{i}, 'ax')
    ax=vin{i+1};
    try
        onAxes=ax(1);
        onAxesX=ax(2);
        onAxesY=ax(3);
        onAxesR=ax(4);
    catch
        disp(':: cannot place wind rose on axes, bad argument for ax')
        return
    end
elseif isequal(vin{i}, 'iflip')
    iflip=vin{i+1};
end
end

% other options:
% size of the full rectangle:
rs=1.2;
rl=1.7;

% directions conversion:
if isequal(dtype, 'meteo')
    D=mod(-90-(D+180),360);
end

% angles subdivisons:
D=mod(D,360);
Ay=linspace(0,360,nAngles+1)-0.5*360/nAngles;

% calc instensity subdivisons:
if isempty(Ag)
    % gen Ag:
    f=figure('visible','off');
    plot(F); axis tight;
    yl=get(gca, 'ytick');
    close(f)
    dyl=diff(yl); dyl=dyl(1);
    if min(F)>yl(1), yl=[yl(1)-dyl yl]; end
    if max(F)>yl(end), yl=[yl yl(end)+dyl]; end
    Ag=yl;
end

if lowwind_flag == 1
    bad_times = find(F<lowwind_speed);

```

```

lowwind_count = length(bad_times);
D = D( find(F>=lowwind_speed));
F = F( find(F>=lowwind_speed));
titStr = [ titStr sprintf(' %d calm',lowwind_count) ];
end

IncHiLow=1; % include values higher and lower than the limits of Ag.
for i=1:length(Ay)-1
    if i==1
        I=find( (D>=Ay(i) & D<Ay(i+1)) | D>=Ay(end));
    else
        I=find(D>=Ay(i) & D<Ay(i+1));
    end
    b=F(I);

    for j=1:length(Ag)-1
        J=find(b>=Ag(j) & b<Ag(j+1));
        E(i,j)=length(J);
    end

    if IncHiLow
        E(i,1)=length(find(b<Ag(2)));
        E(i,end)=length(find(b>=Ag(end-1)));
    end
end
b=sum(E,2)/length(D)*100;

% check if has values higher or lower than the Ag limits
hasH=length(find(F>=Ag(end)));
hasL=length(find(F<Ag(1)));

% calc number of percentage circles to draw:
if isempty(ci)
    dcircles=[1 2 5 10 15 20 25 30 50];
    ncircles=3;
    d=abs(1./(dcircles/max(b))-ncircles);
    i=find(d==min(d));
    d=dcircles(i(1));
    if d*ncircles<max(b)
        ncircles=ncircles+1;
    end
    ci=[1:ncircles]*d;
    g=ncircles*d;
else
    ncircles=length(ci);
    g=max(max(ci),max(b));
end

```



end

```

% plot axes, percentage circles and percent. data:
wrAx=axes('units','normalized');
ri=g*ri;
handles(end+1)=fill([-rs*g rl*g rl*g -rs*g],[-rs*g -rs*g rs*g rs*g],'w',...
    'EdgeColor',borderColor);
if onAxes
    set(handles(end),'facecolor','none')
end
hold on
handles(end+1)=plot([-g-ri -ri nan ri g+ri nan 0 0 nan 0 0],...
    [0 0 nan 0 0 nan -g-ri -ri nan ri g+ri],':','color',lineColors);
t0=[0:360]*pi/180;
labs=[];
Ang=[1/4 3/4 5/4 7/4]*pi;
Valign={'top' 'top' 'bottom' 'bottom'};
Halign={'right' 'left' 'left' 'right'};
for i=1:ncircles
    x=(ci(i)+ri)*cos(t0);
    y=(ci(i)+ri)*sin(t0);

    handles(end+1)=plot(x,y,':','color',lineColors);

    labs(i)=text((ci(i)+ri)*cos(Ang(quad)),(ci(i)+ri)*sin(Ang(quad)),[num2str(ci(i)),'%'],...
        'VerticalAlignment',Valign{quad},'HorizontalAlignment',Halign{quad},...
        'BackgroundColor',percBg,'FontSize',USER_FONTSIZE);
end
handles=[handles labs];

% calc colors:
if isempty(colors)
    cor={};
    for j=1:length(Ag)-1
        cor{j}=caxcolor(Ag(j),[Ag(1) Ag(end-1)],cmap);
    end
else
    cor=colors;
end

% fill data:
n=sum(E,2);
if iflip, E=fliplr(E); end
for i=1:length(Ay)-1
    if n(i)

```

```

t=linspace(Ay(i),Ay(i+1),20)*pi/180;
r1=ri;
for j=1:length(Ag)-1
    r2=E(i,j)/n(i) *b(i) +r1;

    x=[r1*cos(t(1)) r2*cos(t) r1*cos(fliplr(t))];
    y=[r1*sin(t(1)) r2*sin(t) r1*sin(fliplr(t))];

    if iflip, jcor=length(Ag)-1-j+1;
    else, jcor=j;
    end

    if E(i,j)>0, handles(end+1)=fill(x,y,cor{jcor}); end
    r1=r2;
end
end
axis equal
axis off
uistack(labs,'top')

% N S E W labels:
bg='none';
args={'BackgroundColor',bg,'FontSize',USER_FONTSIZE};
h(1)=text(-g-ri, 0,'WEST', 'VerticalAlignment','top', 'HorizontalAlignment','left', args{:});
h(2)=text( g+ri, 0,'EAST', 'VerticalAlignment','top', 'HorizontalAlignment','right',args{:});
h(3)=text( 0,-g-ri,'SOUTH','VerticalAlignment','bottom','HorizontalAlignment','left', args{:});
h(4)=text( 0, g+ri,'NORTH','VerticalAlignment','top', 'HorizontalAlignment','left', args{:});
handles=[handles h];

set(h,'FontSize',USER_FONTSIZE);

% scale legend:
L=(g*r1-g-ri)/7;
h=(g+ri)/10;
dy=h/3;

x0=g+ri+(g*r1-g-ri)/7;
x1=x0+L;
y0=-g-ri;

if legType==1 % continuous.
for j=1:length(Ag)-1
    lab=num2str(Ag(j));
    if j==1 & hasL & ~IncHiLow
        lab="";

```

```

end
y1=y0+h;
handles(end+1)=fill([x0 x1 x1 x0],[y0 y0 y1 y1],cor{j});

handles(end+1)=text(x1+L/4,y0,lab,'VerticalAlignment','middle','fontSize',USER_FONTSIZE);
y0=y1;
end
if ~ (hasH & ~IncHiLow)

handles(end+1)=text(x1+L/4,y0,num2str(Ag(end)),'VerticalAlignment','middle','fontSize',USER_
FONTSIZE);
end
elseif legType==2 % separated boxes.
for j=1:length(Ag)-1
lab=[num2str(Ag(j)) ' - ' num2str(Ag(j+1))];
if j==1 & hasL & ~IncHiLow
lab=['<',num2str(Ag(2))];
end
if j==length(Ag)-1 & hasH & ~IncHiLow
lab=['>=',num2str(Ag(j))];
end
y1=y0+h;
handles(end+1)=fill([x0 x1 x1 x0],[y0+dy y0+dy y1 y1],cor{j});

handles(end+1)=text(x1+L/4,(y0+dy+y1)/2,lab,'VerticalAlignment','middle','fontSize',USER_FO
NTSIZE);
y0=y1;
end

end

% title and legend label:
x=mean([-g*rs,g*rl]);
y=mean([g*ri,g*rs]);
handles(end+1)=text(x,y,titStr,'HorizontalAlignment','center','fontSize',USER_FONTSIZE);

x=x0;
y=y1+dy;
handles(end+1)=text(x,y,legStr,'HorizontalAlignment','left','VerticalAlignment','bottom','fontSize'
,USER_FONTSIZE);

if onAxes
place_wr(onAxes,wrAx,onAxesX,onAxesY,onAxesR);
end

if nargout==1

```

```

    varargout{1}=handles;
end

function place_wr(ax,ax2,x,y,width)
if nargin < 5
    width=1/5;
end
uax=get(ax,'units');
pax=get(ax,'position');
set(ax,'units',uax)
axXlim=get(ax,'xlim');
axYlim=get(ax,'ylim');

x_ax2=pax(1)+pax(3)*(x-axXlim(1))/diff(axXlim);
y_ax2=pax(2)+pax(4)*(y-axYlim(1))/diff(axYlim);

pax2=get(ax2,'position');
width=pax(3)*width;
height=pax2(4)*width/pax2(3);
pax2=[x_ax2 y_ax2 width height];

if 1
    % place at centre of the wr, not the bottom left corner:
    ax2Xlim=get(ax2,'xlim');
    ax2Ylim=get(ax2,'ylim');
    dx=(0-ax2Xlim(1))/diff(ax2Xlim)*pax2(3);
    dy=(0-ax2Ylim(1))/diff(ax2Ylim)*pax2(4);
    x_ax2=x_ax2-dx;
    y_ax2=y_ax2-dy;
    pax2=[x_ax2 y_ax2 width height];
end
set(ax2,'position',pax2)

function cor = caxcolor(val,cax,cmap)
% CAXCOLOR Caxis color for value
% Find the color for a given value in a colormap.
%
% Syntax:
% COLOR = CAXCOLOR(VALUE,CAXIS,COLORMAP)
%
% Inputs:
% VALUE
% CAXIS Default is current caxis
% COLORMAP Default is current colormap

```

```

%
% Output:
%   COLOR  RGB color vector
%
% Example:
%   figure
%   pcolor(peaks)
%   color=caxcolor(0);
%   set(gcf,'color',color)
%
% MMA 28-5-2007, martinho@fis.ua.pt

% Department of Physics
% University of Aveiro, Portugal

if nargin < 3
    cmap = get(gcf,'colormap');
end
if nargin < 2
    cax = caxis;
end

n=size(cmap,1);
i= (val-cax(1))/diff(cax) * (n-1) +1;
a=i-floor(i);
i=floor(i);

i=min(i,n);
i=max(i,1);

if i==n
    cor=cmap(n,:);
elseif i==1
    cor=cmap(1,:);
else
    cor=cmap(i,:)*(1-a) + cmap(i+1,:)*a;
end

```

## APPENDIX C: SITE DESCRIPTION AND SUMMARIES OF COLLECTED DATA

This Appendix contains a general information about the sites within this study, and complete summaries of data collected at each site. Each summary contains five sections. Location and Facility which contains an image of the site, sampling time frame, and specific notes written down in the field. Descriptive Stats containing probability plots. Regression Analysis of both PM<sub>10-2.5</sub> and PM<sub>2.5</sub> concentrations above the breakpoint concentration, using categorized determinate variables. Conditional Probability Plots of wind direction compared to PM concentrations above breakpoint concentration and EPA NAAQS. Wind Rose of wind data for the complete wind data set during each sampling time frame.

**C-1: Site 1** August 8, 2014 to August 15, 2014

1. Location and facility

Distance from Center of facility: 1489 feet

Operations:

- Mining: Overburden removal/excavation, blasting, and crushing of materials
- Processing: Washing, Drying, and Storing
- Transportation: loading sand and Truck sand out of facility

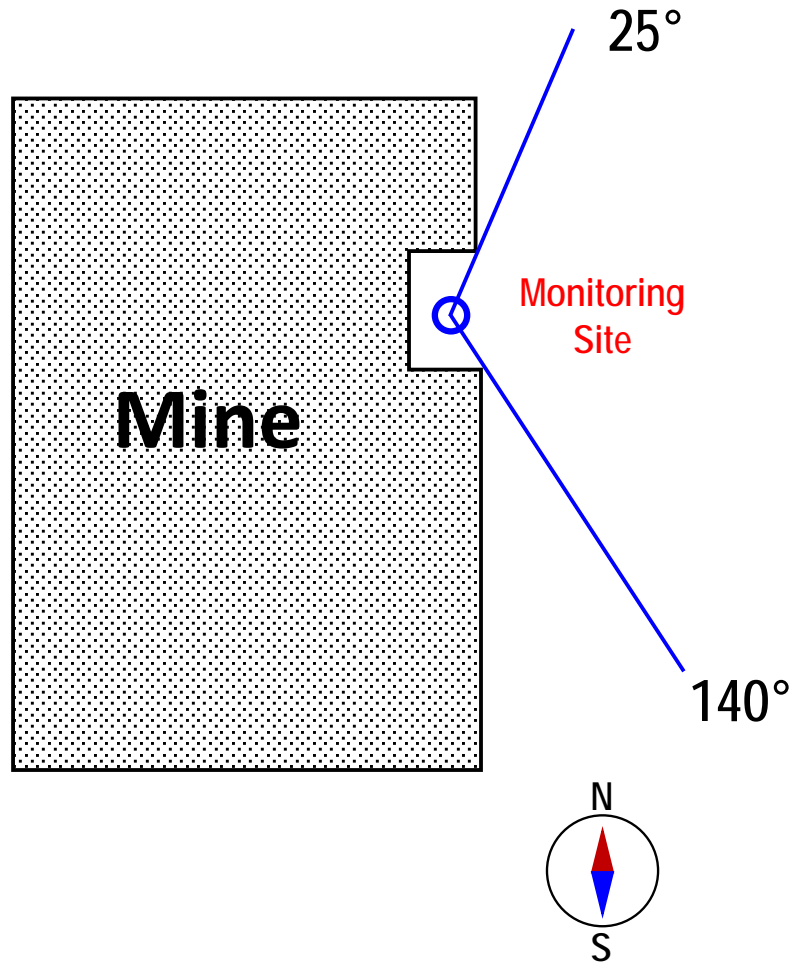


Figure C - 1: Map Image of Site 1 Relative to the Facility

Wind Directions

- Wind over mine if blowing from directions between  $140^\circ$  and  $25^\circ$
- Wind not related to mine if blowing from directions between  $26^\circ$  to  $139^\circ$

Site Observation

- Dump truck and loader mainly located due west of sampling location, looked like primary sand dump site.

## 2. Descriptive Stats

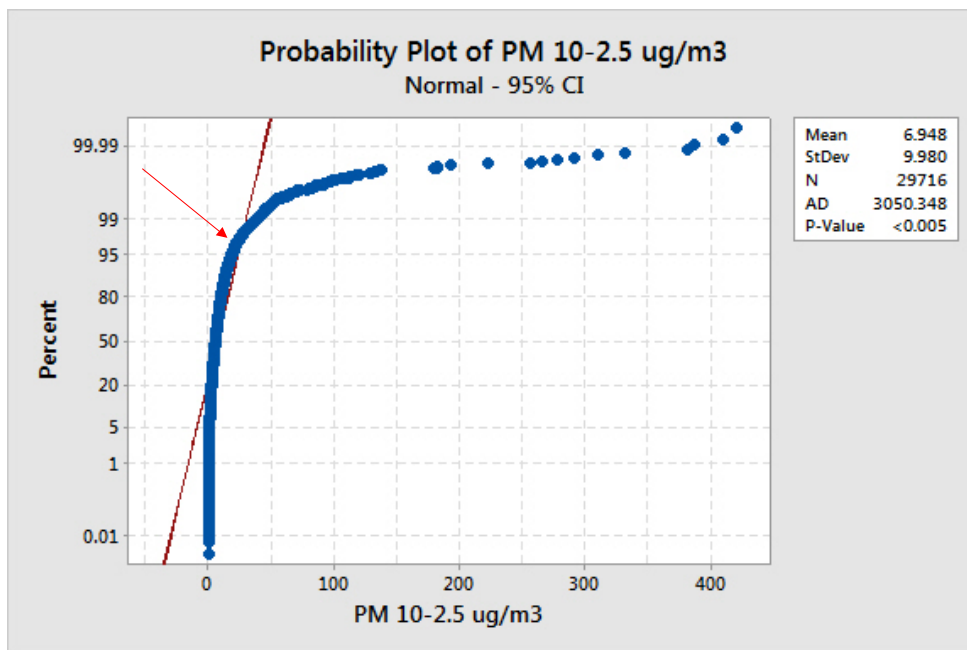


Figure C - 2: PM<sub>10-2.5</sub>  $\mu\text{g}/\text{m}^3$  Break point (indicated by arrow) = 26.7  $\mu\text{g}/\text{m}^3$  at a percentile = 97.9%

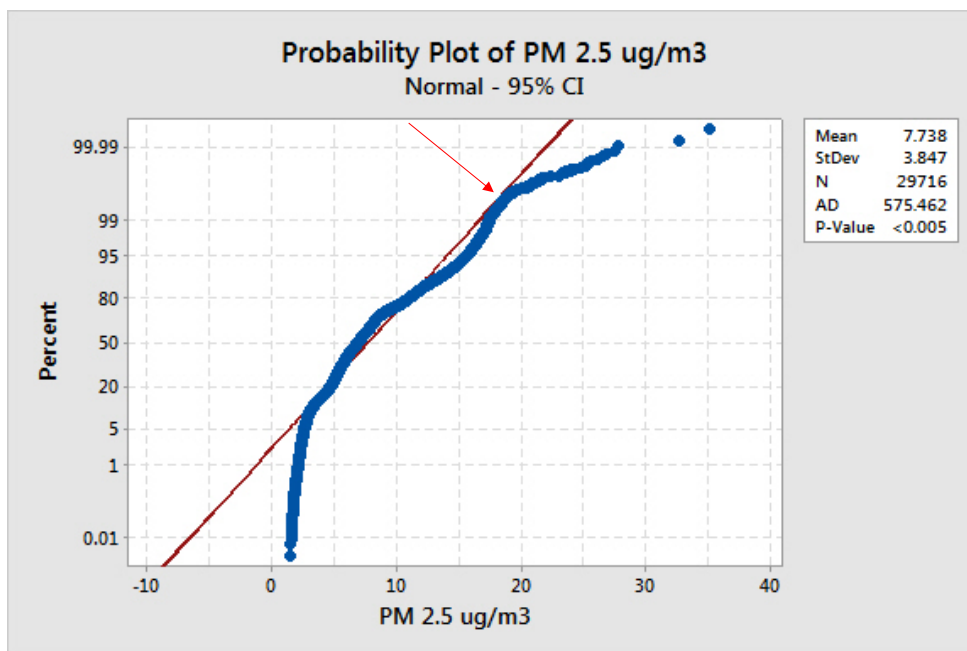


Figure C - 3: PM<sub>2.5</sub>  $\mu\text{g}/\text{m}^3$  Break point (indicated by arrow) = 18.7  $\mu\text{g}/\text{m}^3$  at a percentile = 99.72



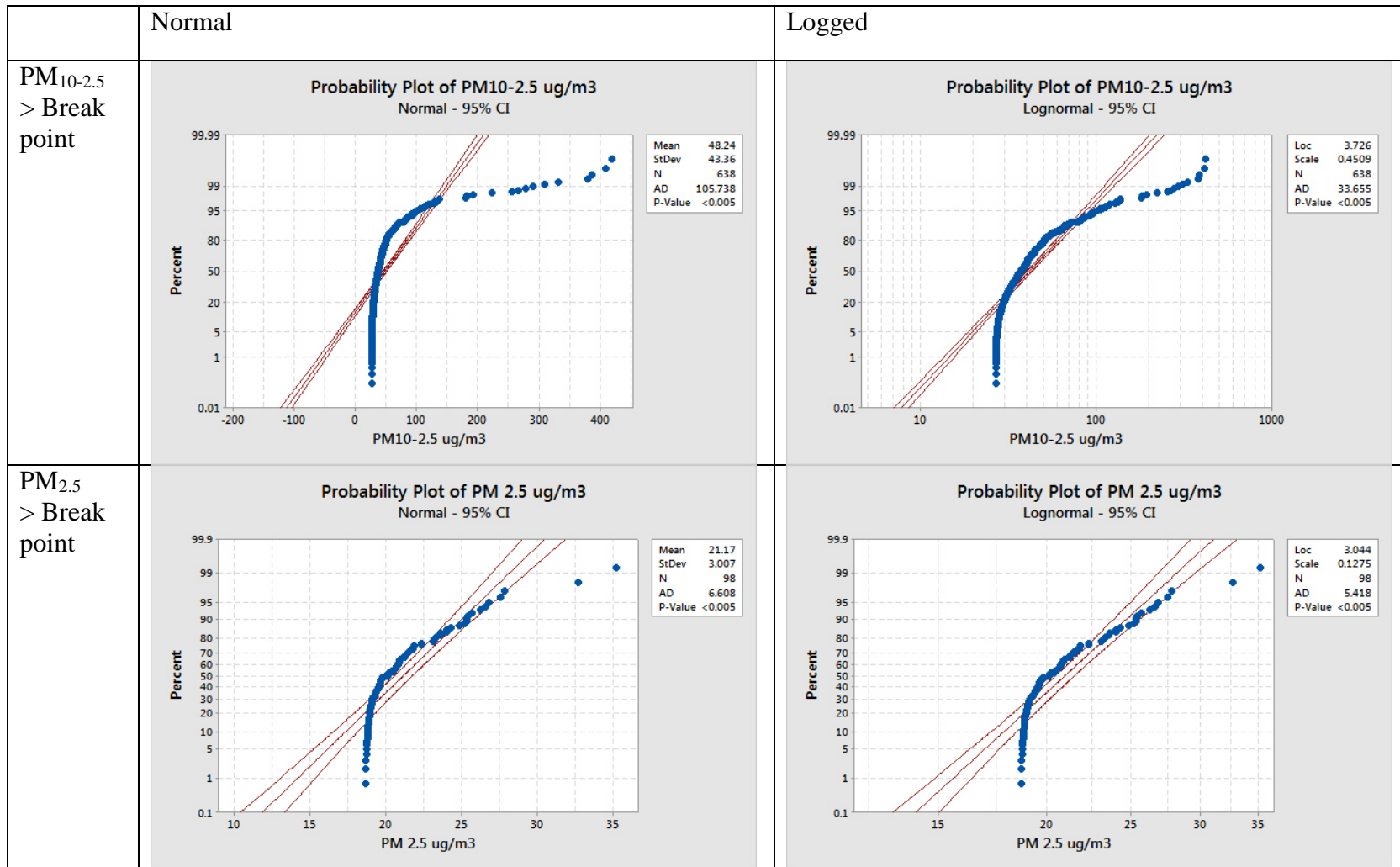


Figure C - 4: Probability Plots of PM>Breakpoint Concentration for Site 1

### 3. Regression Analysis

Table C - 1: Regression Analysis for PM>Breakpoint Concentration at Site 1

Regression Analysis for Matlab Binned Break Point Data					
A: Log PM 10-2.5					
Location	Variable	*SS	*SS/**TSS	P-Value	Coefficients
Arcadia R <sup>2</sup> = (0.53%)	Sound	0.059	0.000	0.590	Low = 0 High = -0.248
	Wind Speed	0.485	0.004	0.123	Low = 0 High = -0.148
	Wind Direction	0.034	0.000	0.682	Unrelated = 0 Mine = 0.041
	Regression Model	0.682	0.005	0.340	-
B: Log PM 2.5					
Location	Variable	SS	SS/TSS	P-Value	Coefficients
Arcadia R <sup>2</sup> = (3.49%)	Sound	-	-	-	-
	Wind Speed	0.003	0.002	0.648	Low = 0 High = -0.0296
	Wind Direction	0.051	0.032	0.079	Unrelated = 0 Mine = 0.1320
	Regression Model	0.055	0.035	0.185	-
*SS = Sum of Squares					
**TSS = Total Sum of Squares for the Regression					

#### Regression Inputs

Wind vectors were coded as either, “Over the Mine” or “Not over the facility” and used as a categorical variable. Wind Speed and sound were coded as high or low. Only values larger than the break point values were used, and the values were converted to logged values to make the data set linear.

## 4. Conditional Probability Plots

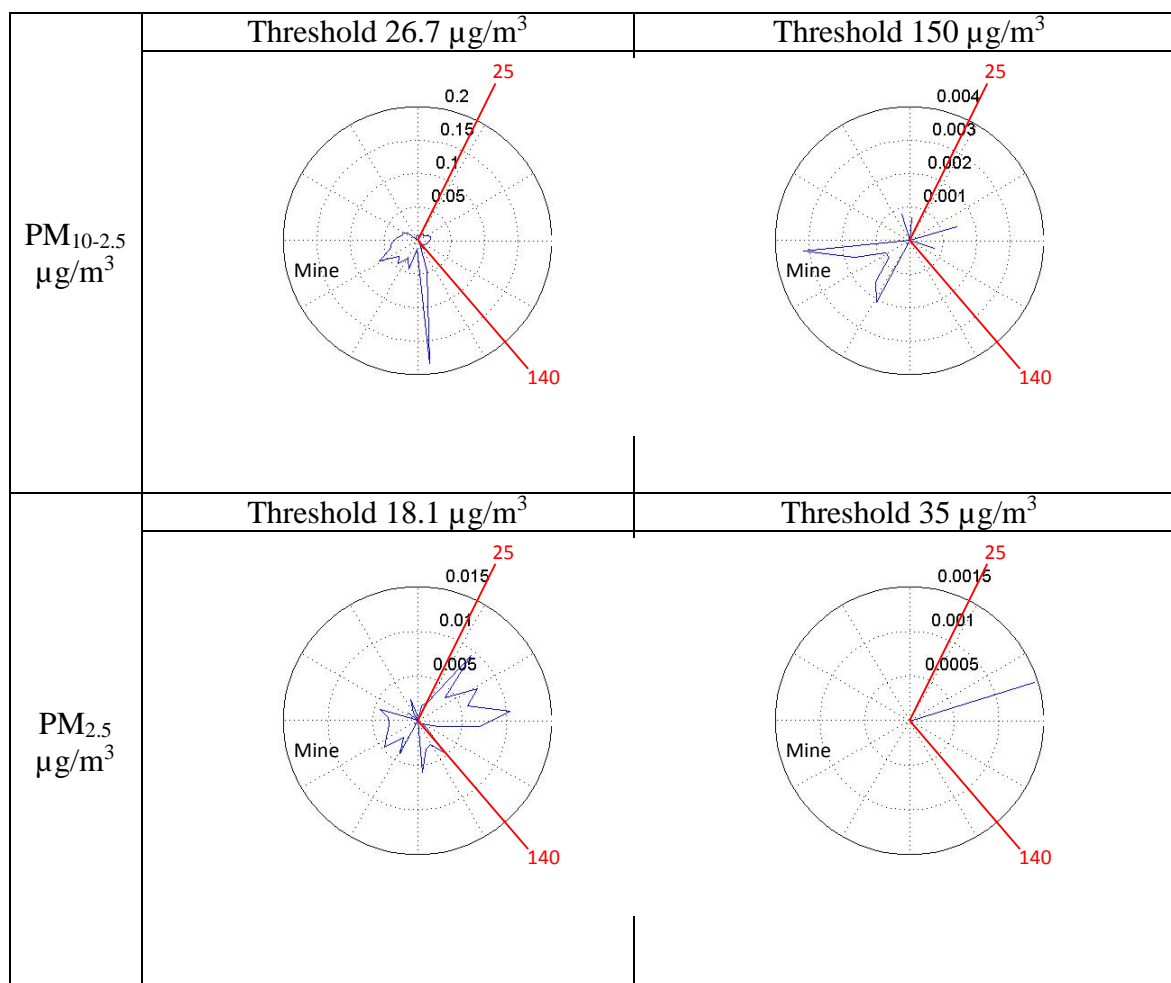


Figure C - 5: Conditional Probability Plots for Site 1

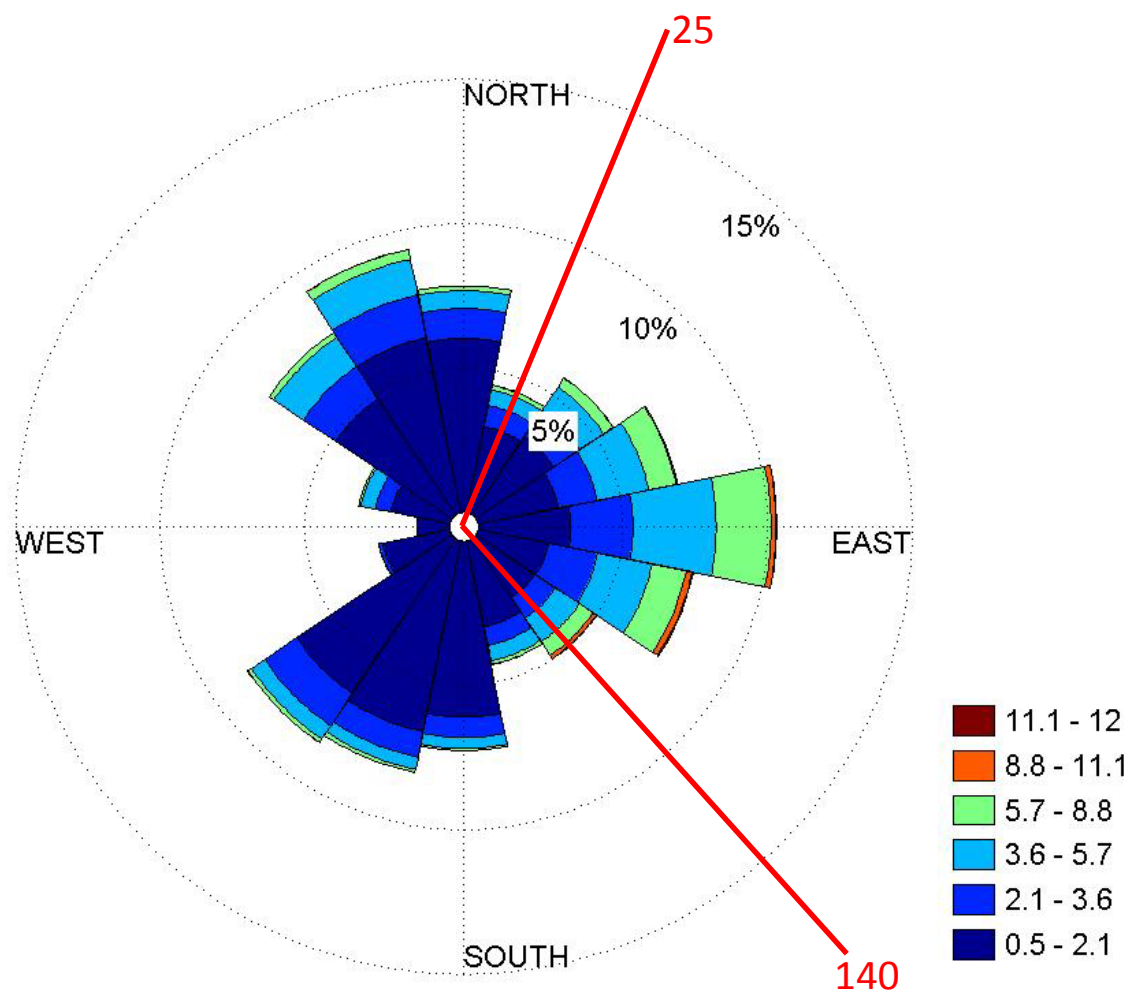


Figure C - 6: Wind Rose for Site 1

## C-2: Site 2 September 9, 2014 to October 9, 2014

### 1. Location and facility

Distance from facility: 616 feet

### Loading Operations

- Sand is trucked in on city streets
- Truck dumps sand into large pile
- Loader scoops up sand from pile and dumps into rail cars
- Most cars are uncovered from this facility

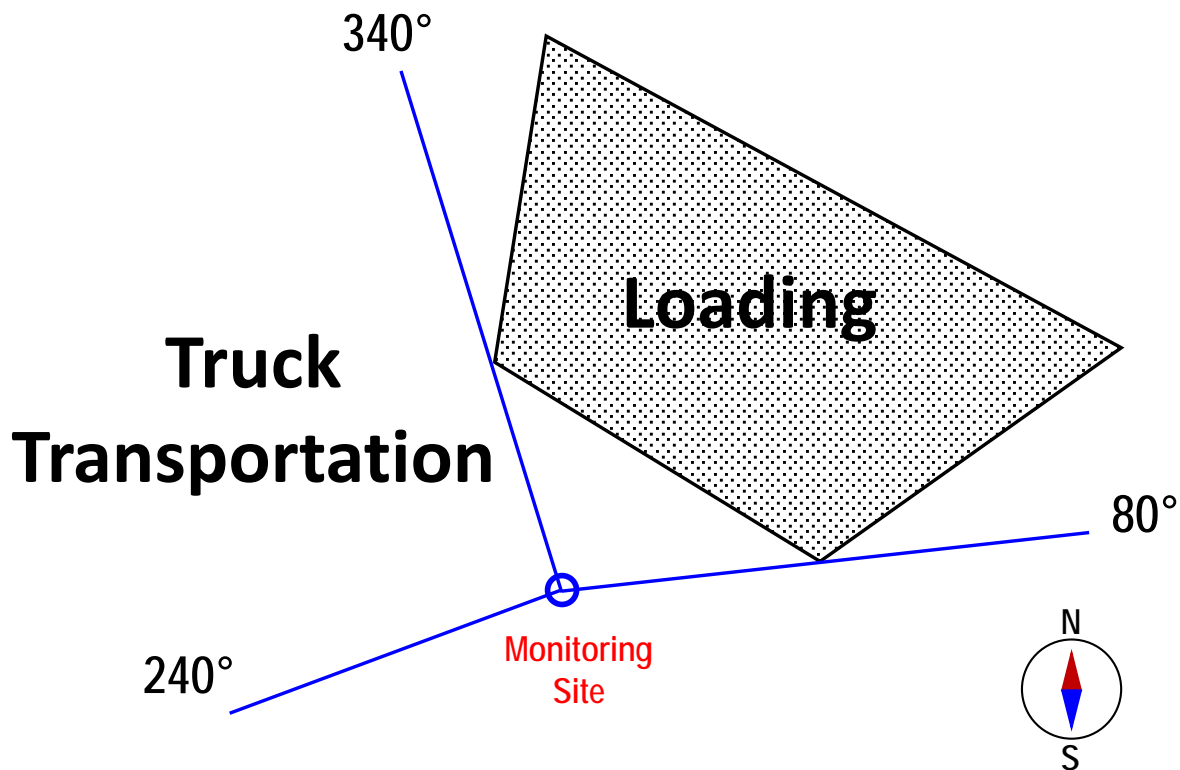


Figure C - 7: Map Image of Site 2 Relative to the Facility

### Wind Directions

- Wind over trucking route if blowing from directions between 245° to 340°
- Wind over loading facility if blowing from direction between 340° to 80°
- Wind not related to the facility if blowing from directions between 80° to 245°

### Site Observation

- Trucks dumped sand in large pile at about 350 degree mark. Wall between facility and sampling site

## 2. Descriptive Stats

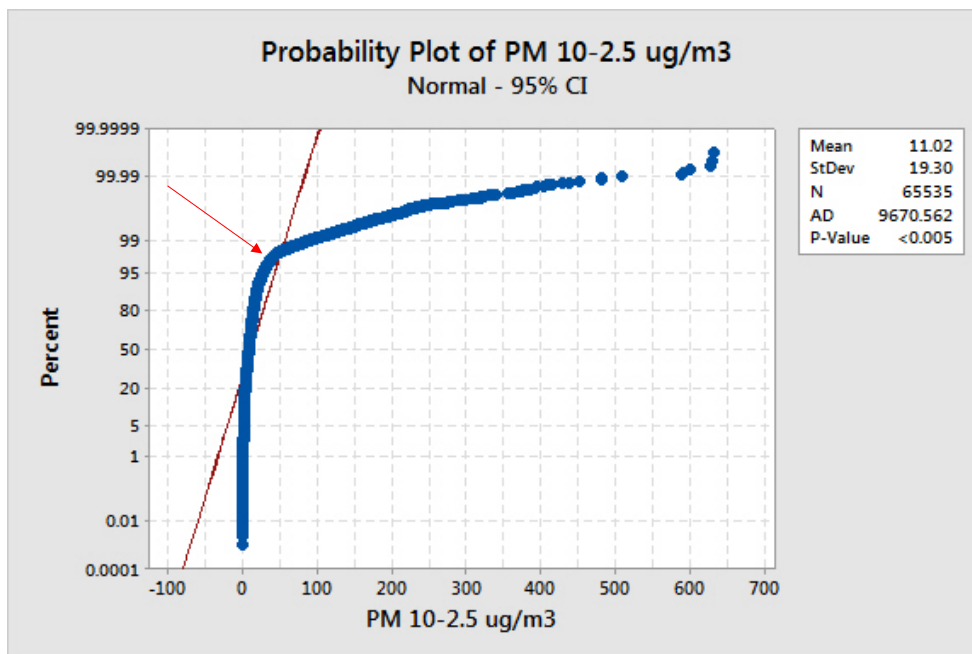


Figure C - 8: PM<sub>10-2.5</sub>  $\mu\text{g}/\text{m}^3$  Break point (indicated by arrow) = 40.8  $\mu\text{g}/\text{m}^3$  at a percentile = 97.6

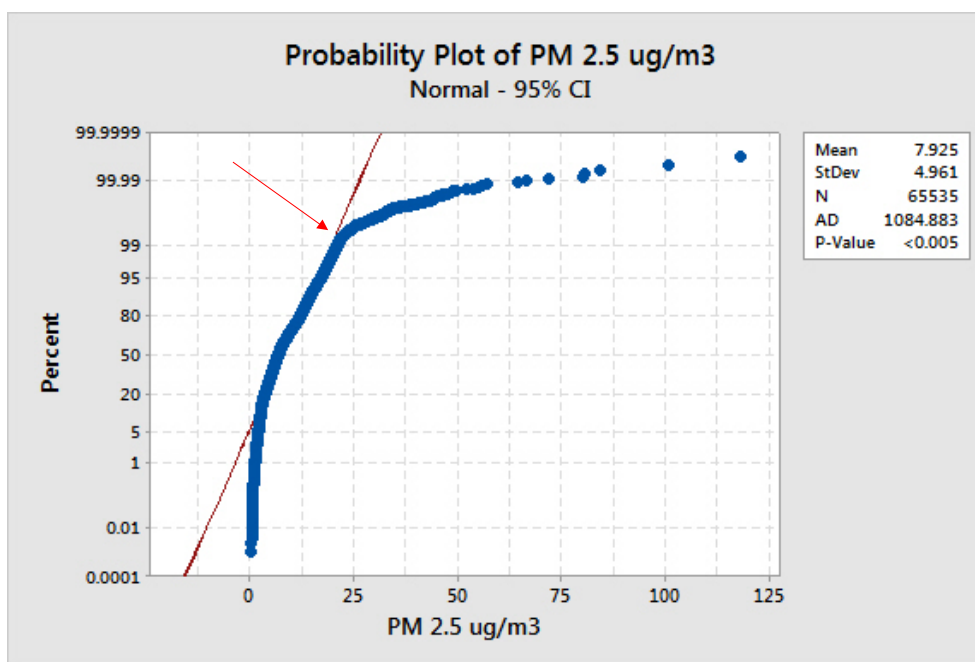


Figure C - 9: PM<sub>2.5</sub>  $\mu\text{g}/\text{m}^3$  Break point (indicated by arrow) = 22  $\mu\text{g}/\text{m}^3$  at a percentile = 99.3

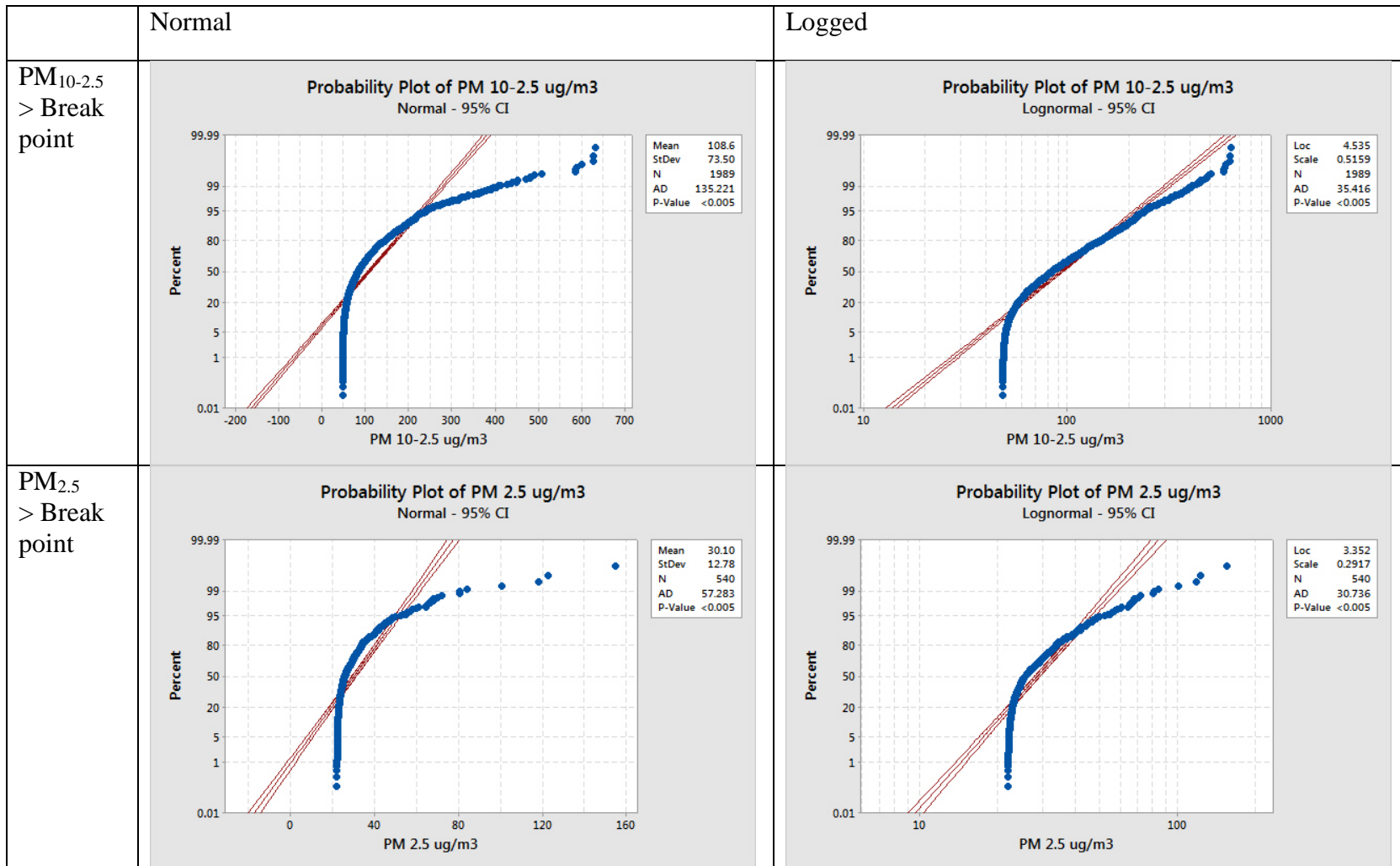


Figure C - 10: Probability Plots of PM>Breakpoint Concentration for Site 2

### 3. Regression Analysis

Table C - 2: Regression Analysis for PM>Breakpoint Concentration at Site 2

Regression Analysis for Matlab Binned Break Point Data					
A: Log PM 10-2.5					
Location	Variable	*SS	*SS/**TSS	P-Value	Coeffiecents
Bjorlo R <sup>2</sup> = (0.47%)	Sound	0.438	0.001	0.230	Low = 0 High = -0.0739
	Wind Speed	2.256	0.003	0.006	Low = 0 High = 0.0867
	Wind Direction	1.659	0.002	0.065	Unrelated = 0 Trucking = -0.058 Loading = -0.039
	Regression Model	3.493	0.005	0.021	-
B: Log PM 2.5					
Location	Variable	SS	SS/TSS	P-Value	Coeffiecents
Bjorlo R <sup>2</sup> = (10.52%)	Sound	0.2455	0.005	0.074	Low = 0 High = -0.0739
	Wind Speed	3.1549	0.069	<0.001	Low = 0 High = 0.0867
	Wind Direction	0.2236	0.005	0.234	Unrelated = 0 Trucking = -0.058 Loading = -0.039
	Regression Model	4.8237	0.105	<0.001	-
*SS = Sum of Squares					
**TSS = Total Sum of Squares for the Regression					

#### Regression Inputs

Wind vectors were coded as either, “Over the loading,” “Over trucking route,” or “Not over the facility” and used as a categorical variable. Wind Speed and sound where coded as high or low. Only values larger than the break point values were used, and the values were converted to logged values to make the data set linear.



4. Conditional Probability Plots

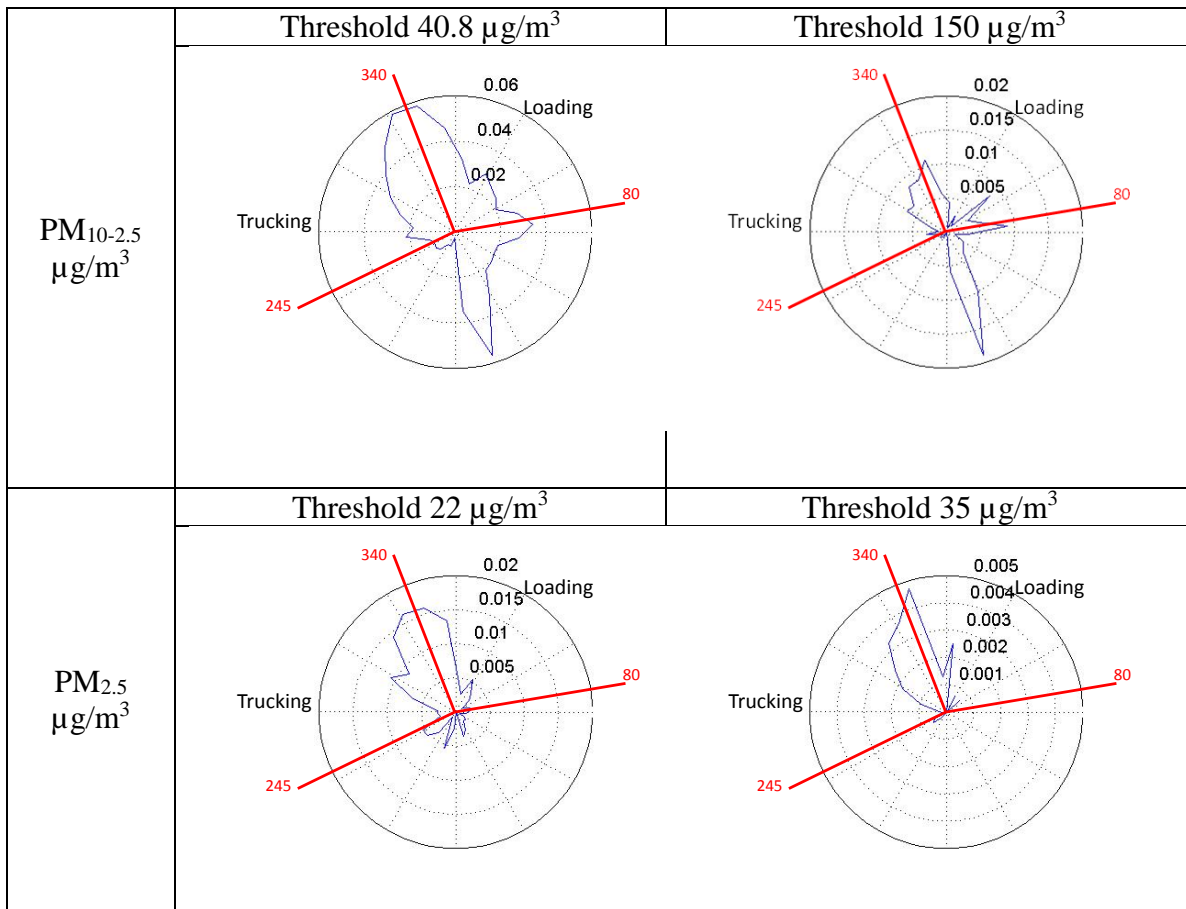


Figure C - 11: Conditional Probability Plots for Site 2

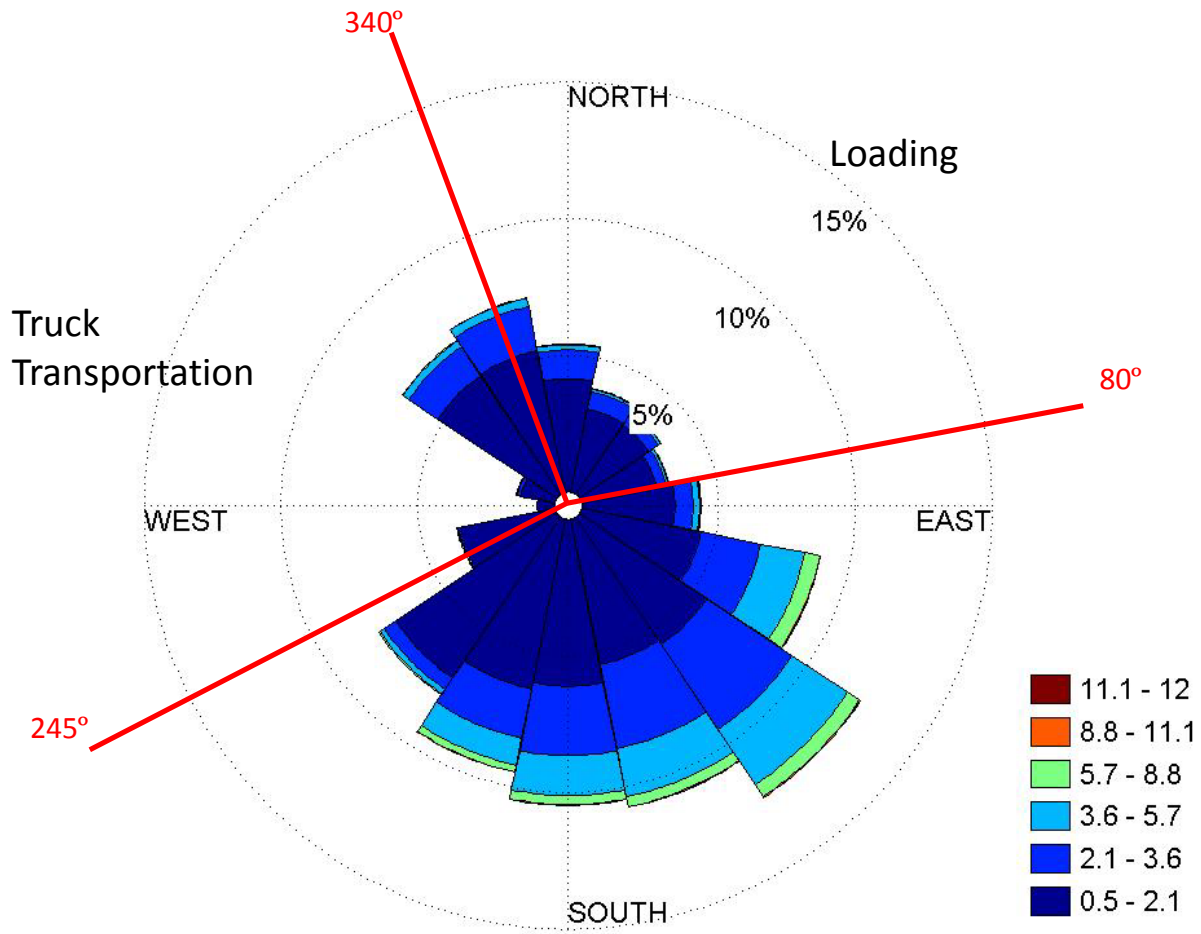


Figure C - 12: Wind Rose for Site 2

**C-3: Site 3** June 24, 2014 to July 7, 2014

## 1. Location and facility

Distance from facility: 32 feet

## Train Transportation

- Sound over a level of 2.75 % of the potentiometer was considered to be a train passing by.

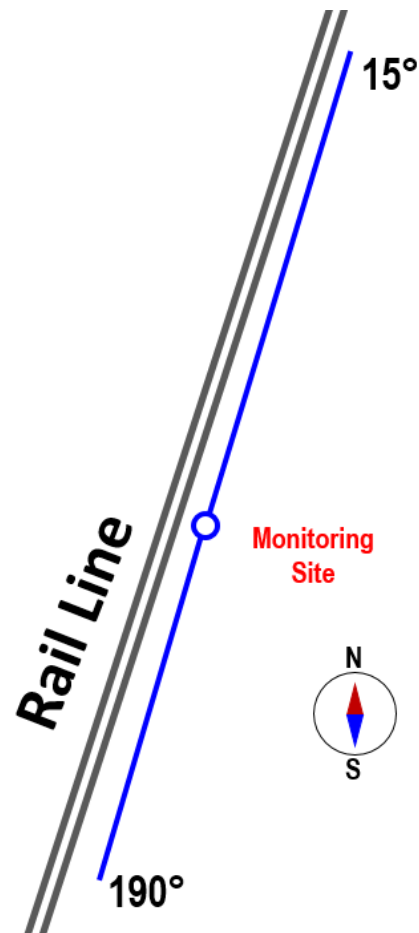


Figure C - 13: Map Image of Site 3 Relative to the Facility

## Wind Directions

- Wind over rail road if blowing from directions between  $190^\circ$  to  $15^\circ$
- Wind not related to rail road if blowing from directions between  $16^\circ$  to  $189^\circ$

## Site Observations

- Average of 50 trains day
- Highly traveled road on the opposite side of the house

## 2. Descriptive Stats

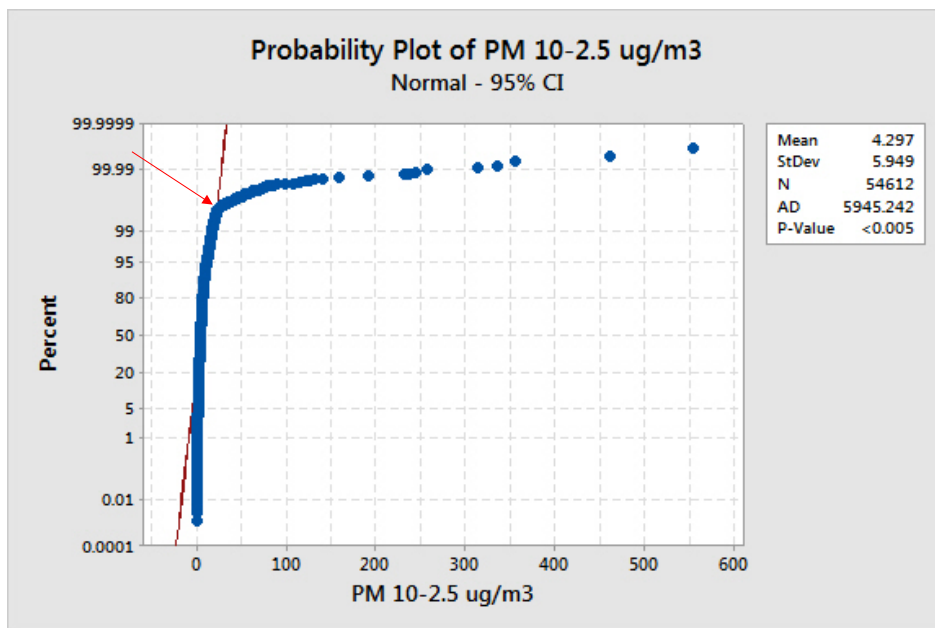


Figure C - 14: PM<sub>10-2.5</sub>  $\mu\text{g}/\text{m}^3$  Break point (indicated by arrow) = 22.5  $\mu\text{g}/\text{m}^3$  at a percentile = 99.7

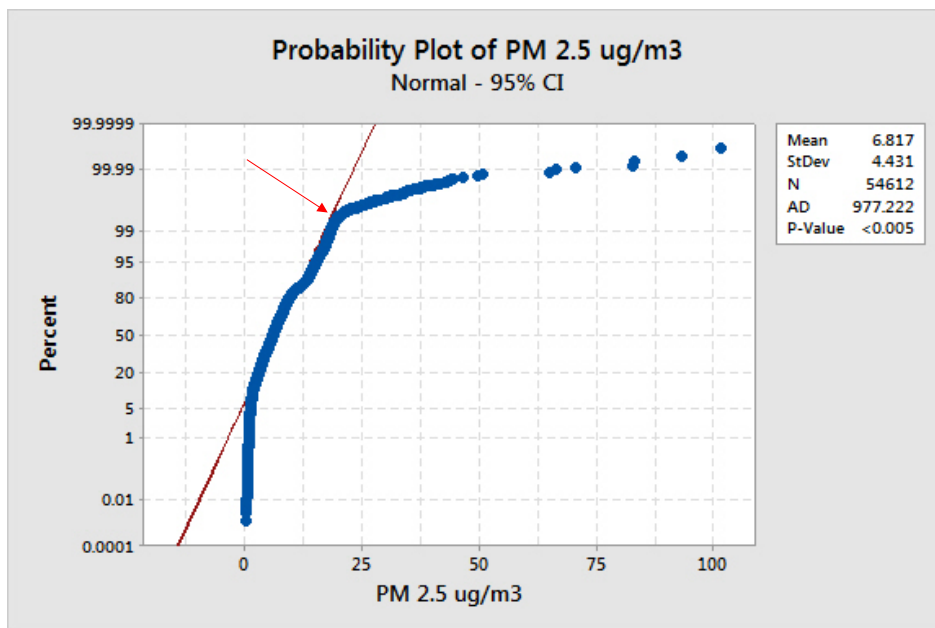


Figure C - 15: PM<sub>2.5</sub>  $\mu\text{g}/\text{m}^3$  Break point (indicated by arrow) = 19.7  $\mu\text{g}/\text{m}^3$  at a percentile = 99.53

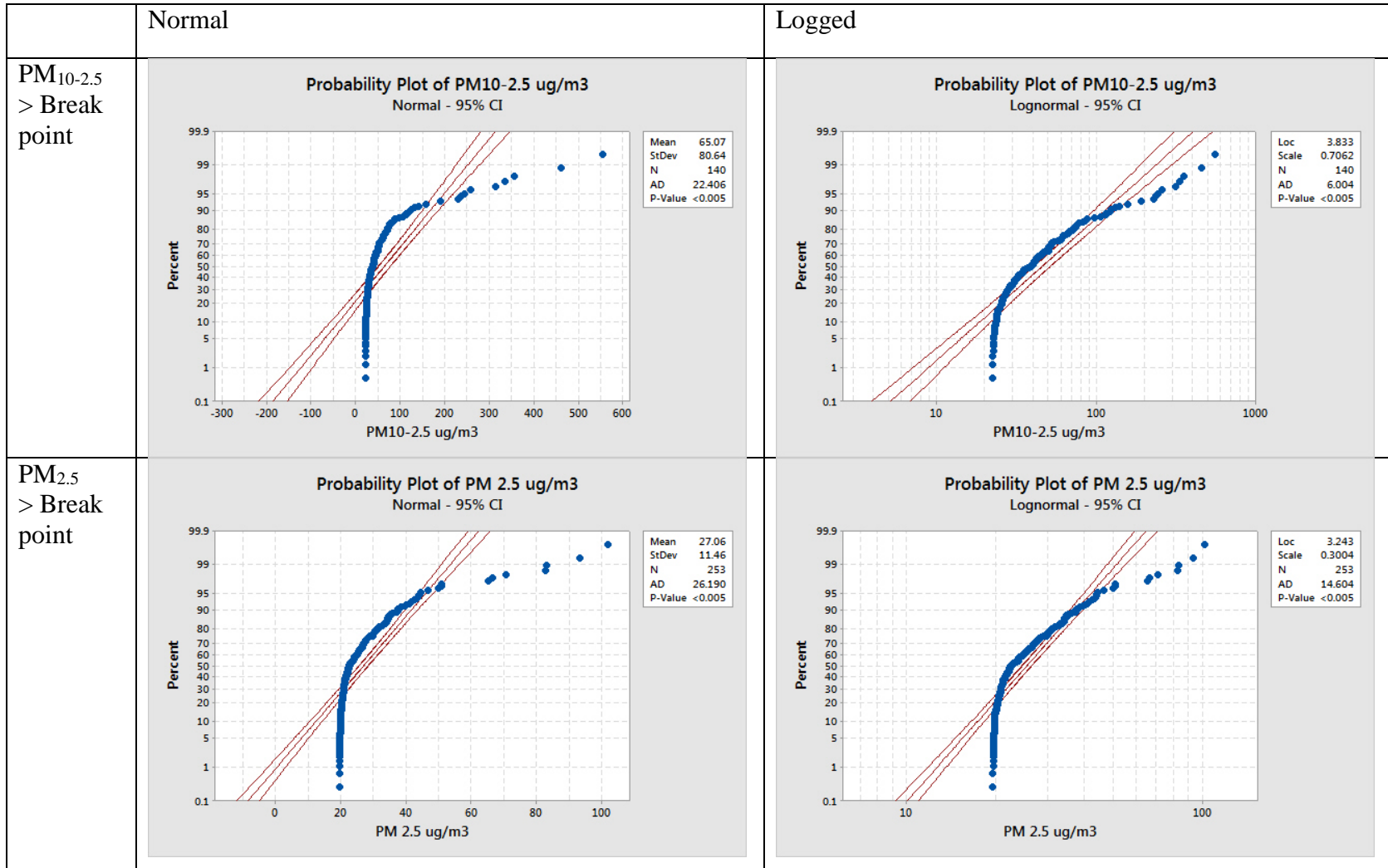


Figure C - 16: Probability Plots of PM>Breakpoint Concentration for Site 3

### 3. Regression Analysis

Table C - 3: Regression Analysis for PM>Breakpoint Concentration at Site 3

Regression Analysis for Matlab Binned Break Point Data					
A: Log PM 10-2.5					
Location	Variable	Sum of Squares	SS/Total SS	P-Value	Coefficients
Dawg House R <sup>2</sup> = (2.98%)	Sound	1.7174	0.025	0.065	No Train = 0 Train = -0.3030
	Wind Speed	0.6062	0.009	0.270	Low = 0 High = 0.139
	Wind Direction	0.0123	0.000	0.875	Unrelated = 0 Rail Line = -0.034
	Regression Model	2.0628	0.030	0.249	-
B: Log PM 2.5					
Location	Variable	Sum of Squares	SS/Total SS	P-Value	Coefficients
Dawg House R <sup>2</sup> = (0.74%)	Sound	0.0332	0.001	0.546	No Train = 0 Train = -0.0365
	Wind Speed	0.1147	0.005	0.262	Low = 0 High = 0.0430
	Wind Direction	0.0346	0.002	0.537	Unrelated = 0 Rail Line = 0.0460
	Regression Model	0.1684	0.007	0.603	-

#### Regression Inputs

Wind vectors were coded as either, “Over the rail road” or “Not over the rail road” and used as a categorical variable. Wind Speed was coded as high or low, and sound value of 2.75% and greater was considered to be a passing train. Only values larger than the break point values were used, and the values were converted to logged values to make the data set linear.

4. Conditional Probability Plots

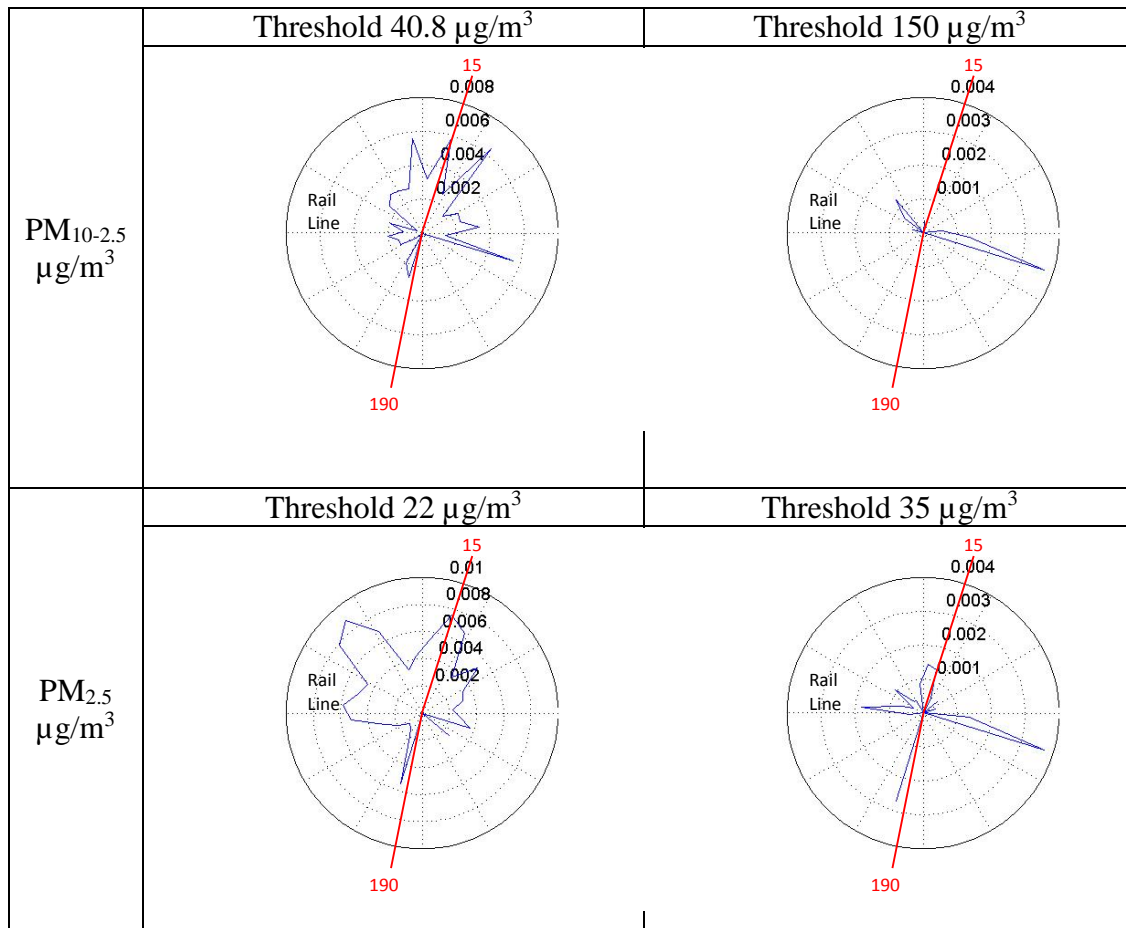


Figure C - 17: Conditional Probability Plots for Site 3

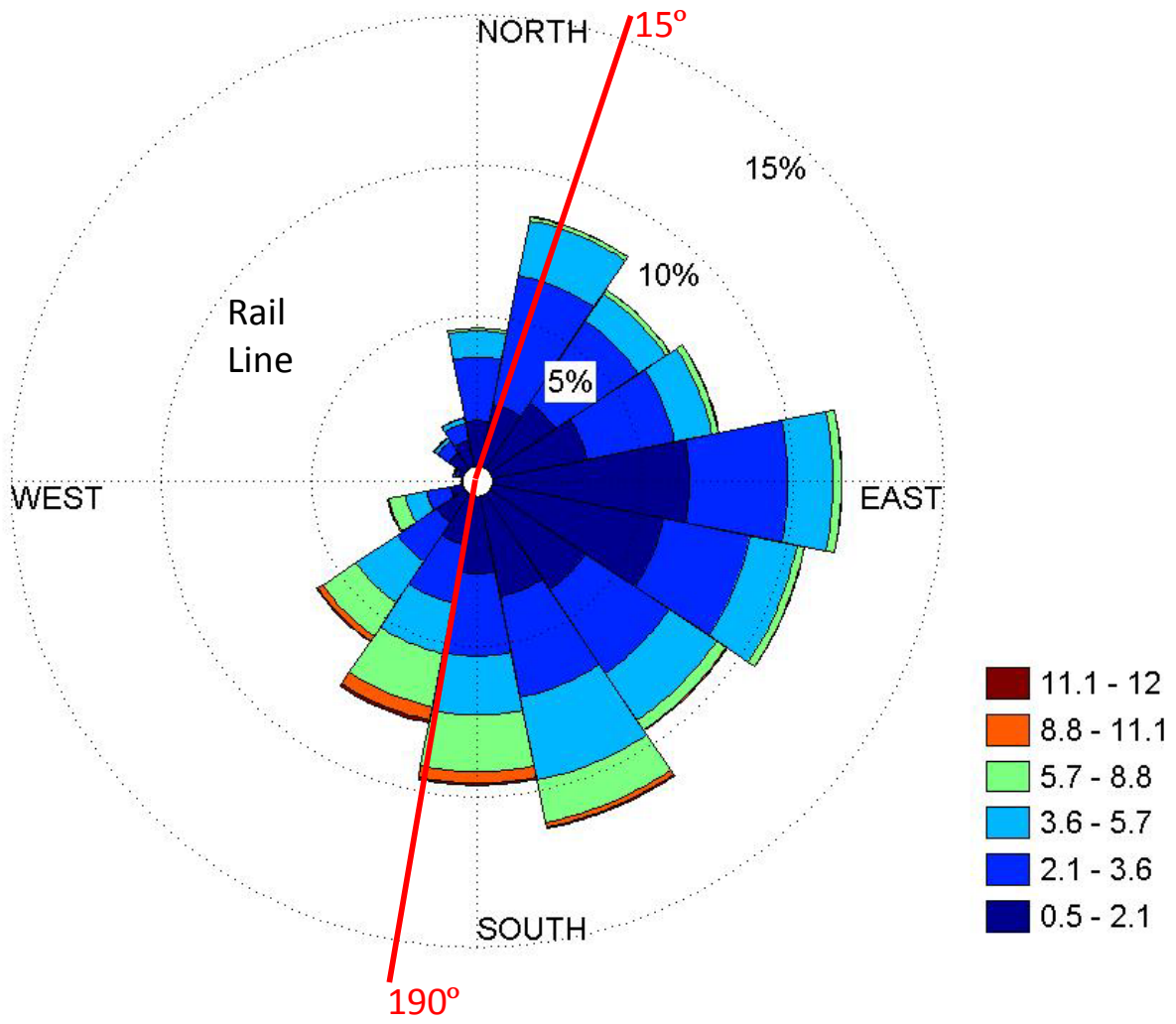


Figure C - 18: Wind Rose for Site 3



**C-4: Site 4** July 31, 2014 – August 8, 2014

## 1. Location and Facility

Distance from center of:

Mine: 1,700 ft.

Conveyor: 2,450 ft.

Processing: 4,800 ft.

Operations:

- Mining: Overburden removal/excavation, blasting, and crushing of materials
- Processing: Washing, Drying, and Storing
- Transportation: loading materials, Truck, and rail transportation

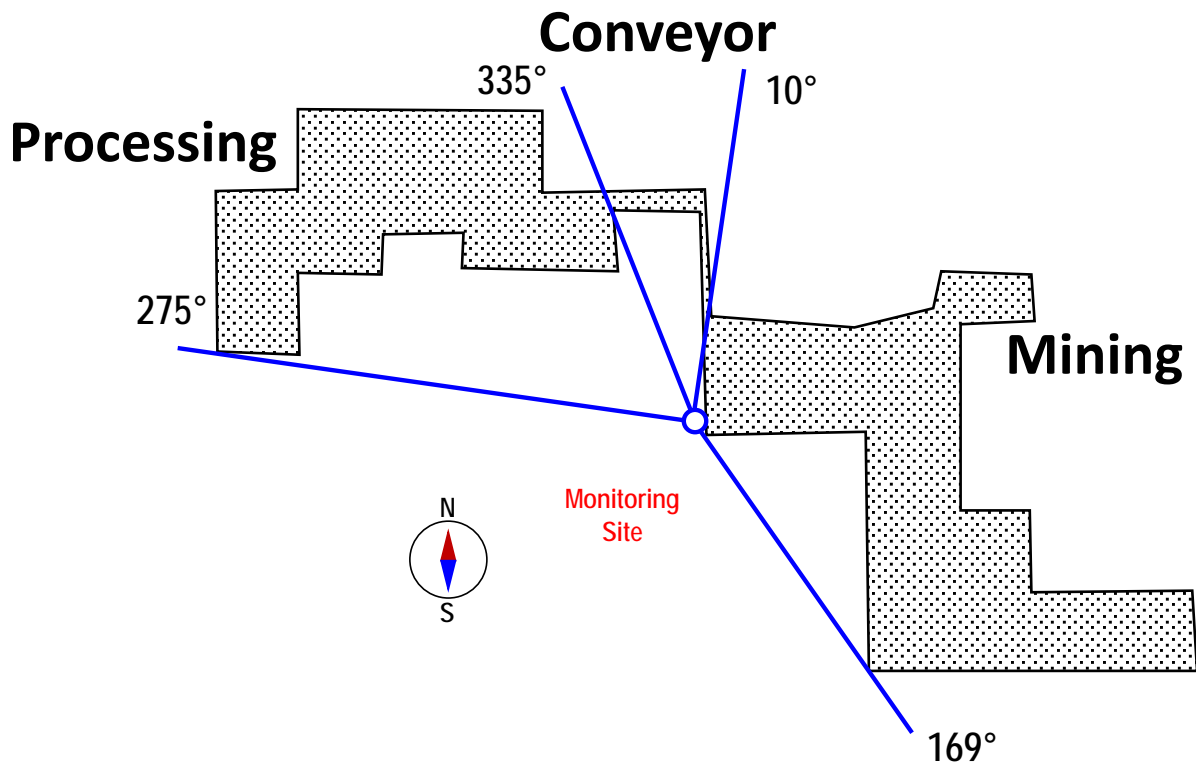


Figure C - 19: Map Image of Site 4 Relative to the Facility

## Wind Directions

- Wind over mine if blowing from directions between 10° - 169°
- Wind not related to mine if blowing from directions between 170° - 274°
- Wind over processing if blowing from directions between 275° - 334°
- Wind over conveyer if blowing from directions between 335° - 9°

## Site Observation

- Property line for the mine is really close but most of the mining during sampling time was done in the Northeast portion of the mining section.

## 2. Descriptive Stats

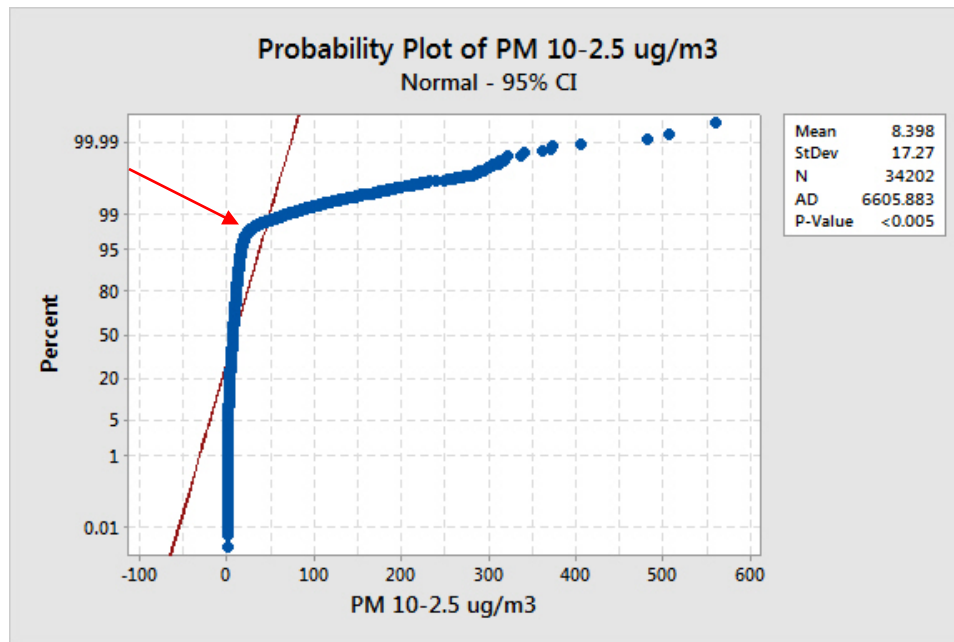


Figure C - 20: PM<sub>10-2.5</sub>  $\mu\text{g}/\text{m}^3$  Break point (indicated by arrow) = 22.9  $\mu\text{g}/\text{m}^3$  at a percentile = 97.6

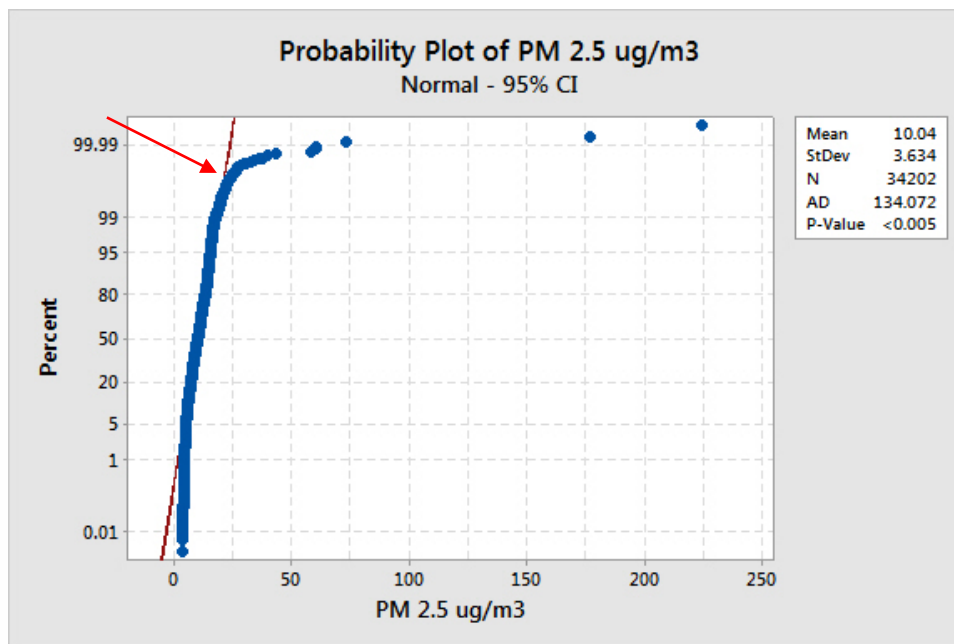


Figure C - 21: PM<sub>2.5</sub>  $\mu\text{g}/\text{m}^3$  Break point (indicated by arrow) = 23.1  $\mu\text{g}/\text{m}^3$  at a percentile = 99.8

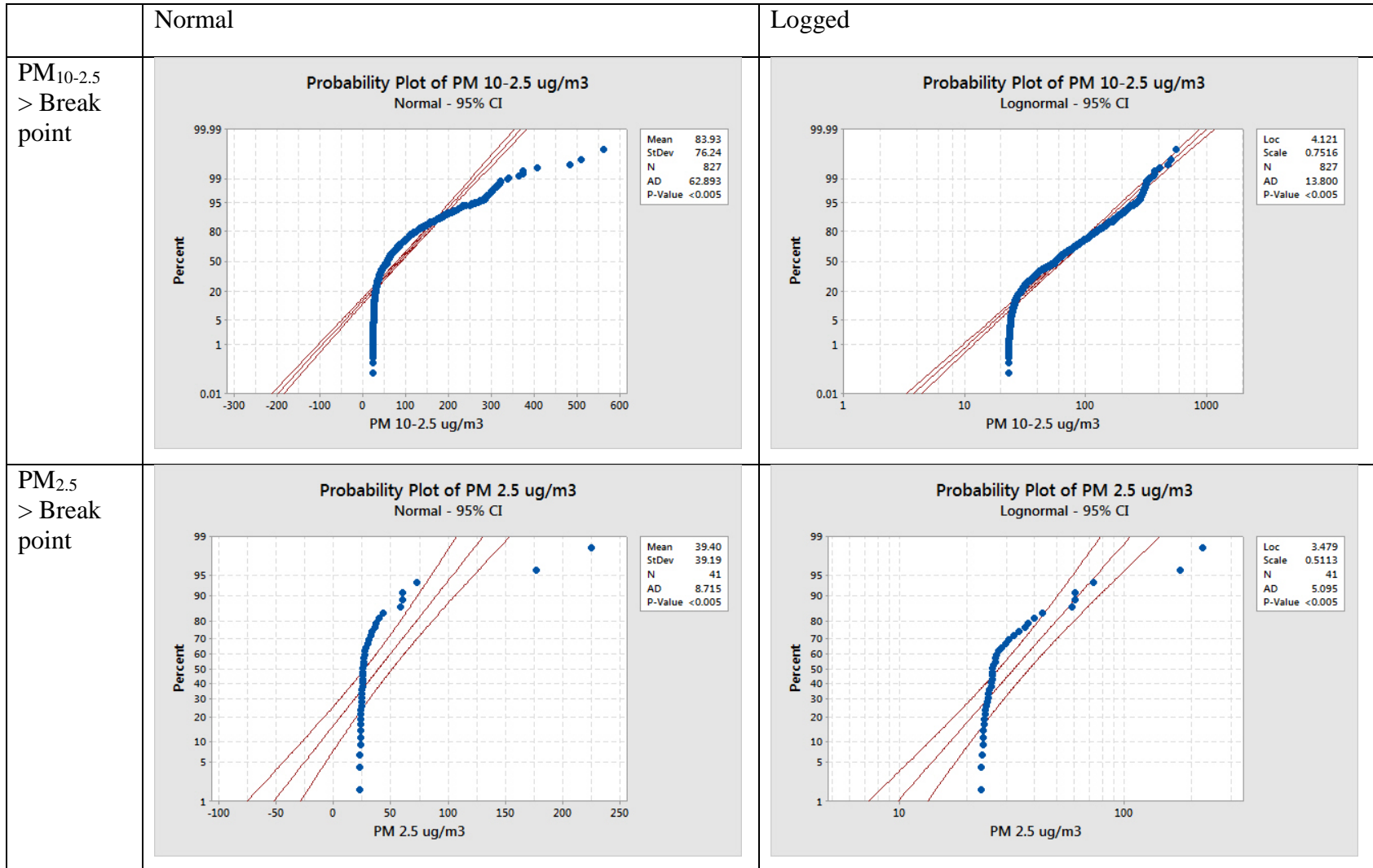


Figure C - 22: Probability Plots of PM>Breakpoint Concentration for Site 4

### 3. Regression Analysis

Table C - 4: Regression Analysis for PM>Breakpoint Concentration at Site 4

Regression Analysis for Matlab Binned Break Point Data					
A: Log PM 10-2.5					
Location	Variable	SS	SS/TSS	P-Value	Coefficients
Hy-Crush R <sup>2</sup> = (4.79%)	Sound	0.391	0.001	0.396	Low = 0 High = 0.187
	Wind Speed	5.112	0.011	0.002	Low = 0 High = -0.329
	Wind Direction	11.763	0.025	<0.001	Unrelated = 0 Processing = -0.104 Conveyer = -0.429 Mine = 0.2373
	Regression Model	22.336	0.048	<0.001	-
B: Log PM 2.5					
Location	Variable	SS	SS/TSS	P-Value	Coefficients
Hy-Crush R <sup>2</sup> = (32.2%)	Sound	1.7784	0.17007603	0.005	Low = 0 High = 0.505
	Wind Speed	0.7608	0.07275857	0.061	Low = 0 High = 0.418
	Wind Direction	0.2277	0.02177593	0.772	Unrelated = 0 Processing = 0.096 Conveyer = 0.043 Mine = 0.190
	Regression Model	3.3672	0.3220198	0.015	-
*SS = Sum of Squares					
**TSS = Total Sum of Squares for the Regression					

#### Regression Inputs

Wind direction was coded as either, “Over the mine,” “Not over facility,” “Over conveyer,” or “Over processing,” and used as a categorical variable. Wind Speed and Sound was coded as a high or low value. Only values larger than the break point values were used, and the values were converted to logged values to make the data set linear.

## 4. Conditional Probability Plots

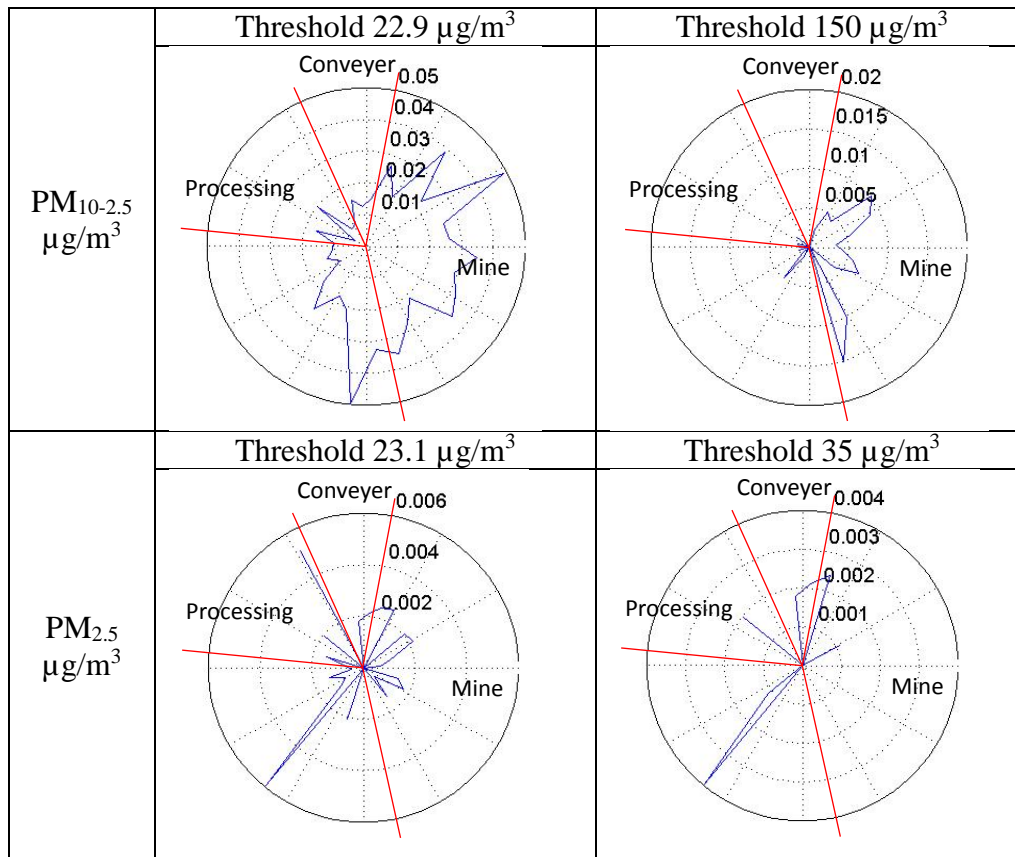


Figure C - 23: Conditional Probability Plots for Site 4

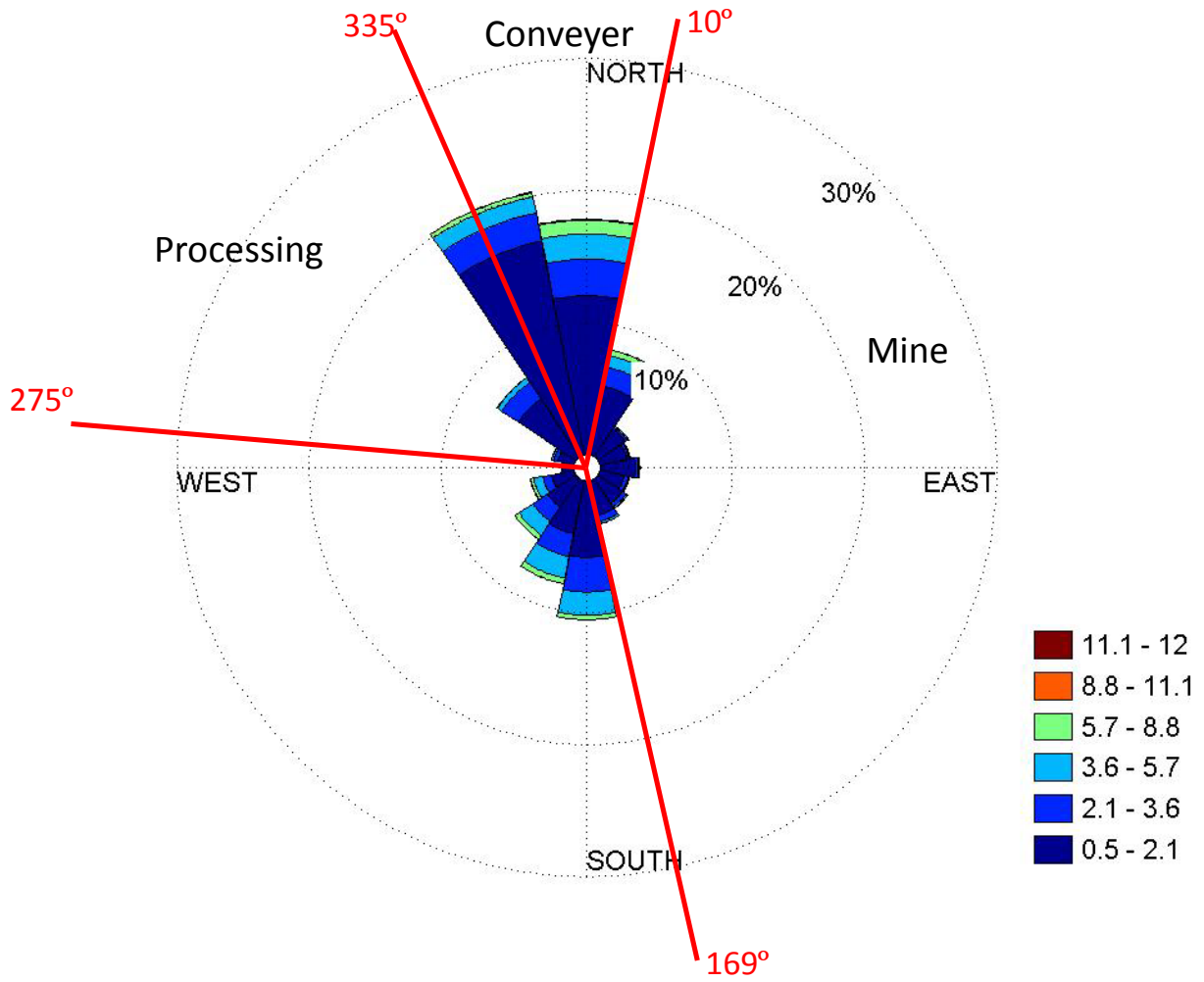


Figure C - 24: Wind Rose for Site 4

**C-5: Site 5** July 7, 2014 to July 31, 2014

## 1. Location and facility

Distance from facility: 4820 feet

## Operations:

- Mining: Overburden removal/excavation, blasting, and crushing of materials
- Processing: Washing, Drying, and Storing
- Transportation: loading materials, Truck, and rail transportation

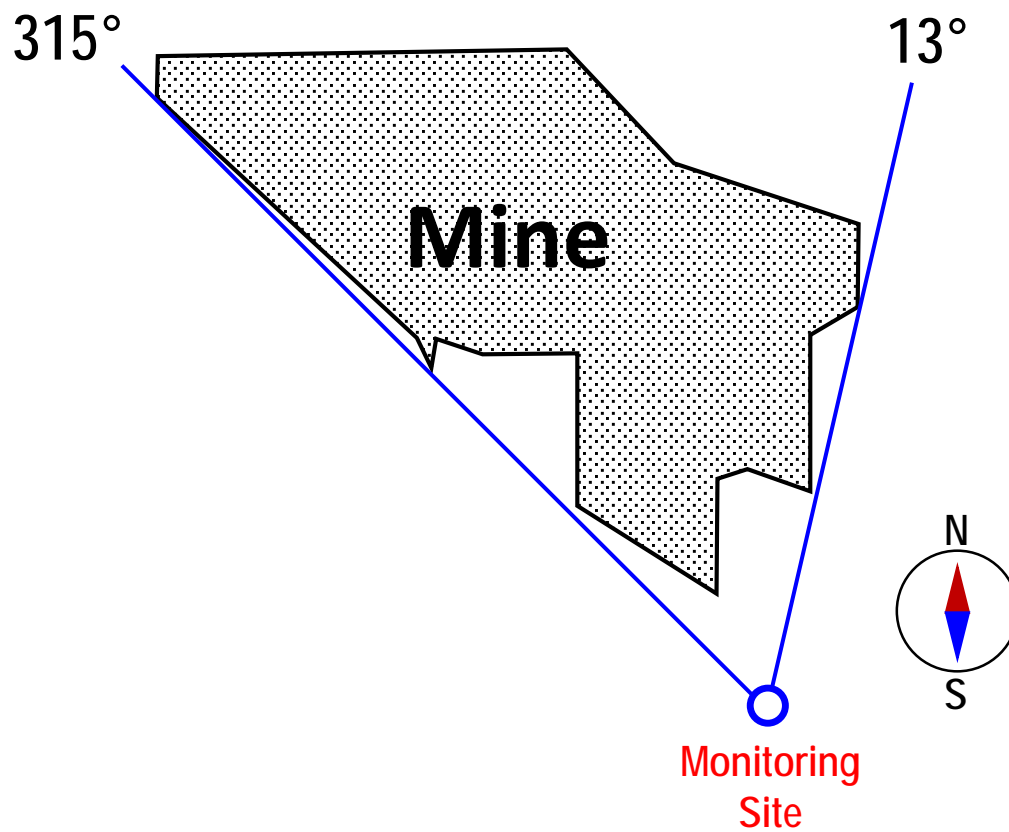


Figure C - 25: Map Image of Site 5 Relative to the Facility

## Wind Directions

- Wind over mine if blowing from directions between 315° to 13°
- Wind not related with the mine if blowing from directions between 16° to 314°

## Site Observation

- Located on a dairy farm, with farm operations South Southeast

## 2. Descriptive Stats

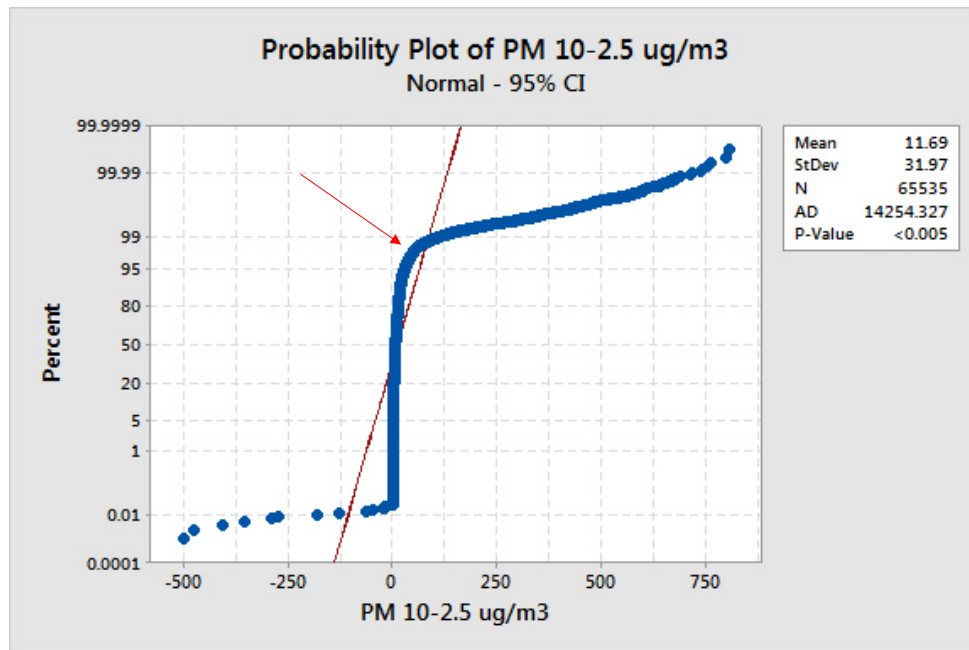


Figure C - 26: PM<sub>10-2.5</sub>  $\mu\text{g}/\text{m}^3$  Break point (indicated by arrow) = 45  $\mu\text{g}/\text{m}^3$  at a percentile = 97.4

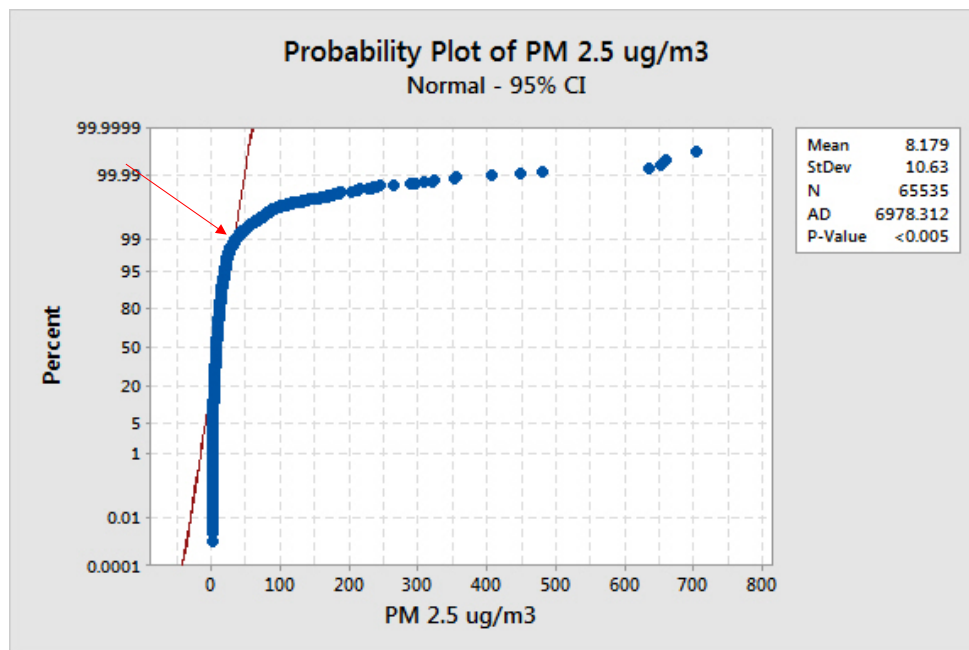


Figure C - 27: PM<sub>2.5</sub>  $\mu\text{g}/\text{m}^3$  Break point (indicated by arrow) = 35.6  $\mu\text{g}/\text{m}^3$  at a percentile = 99.1



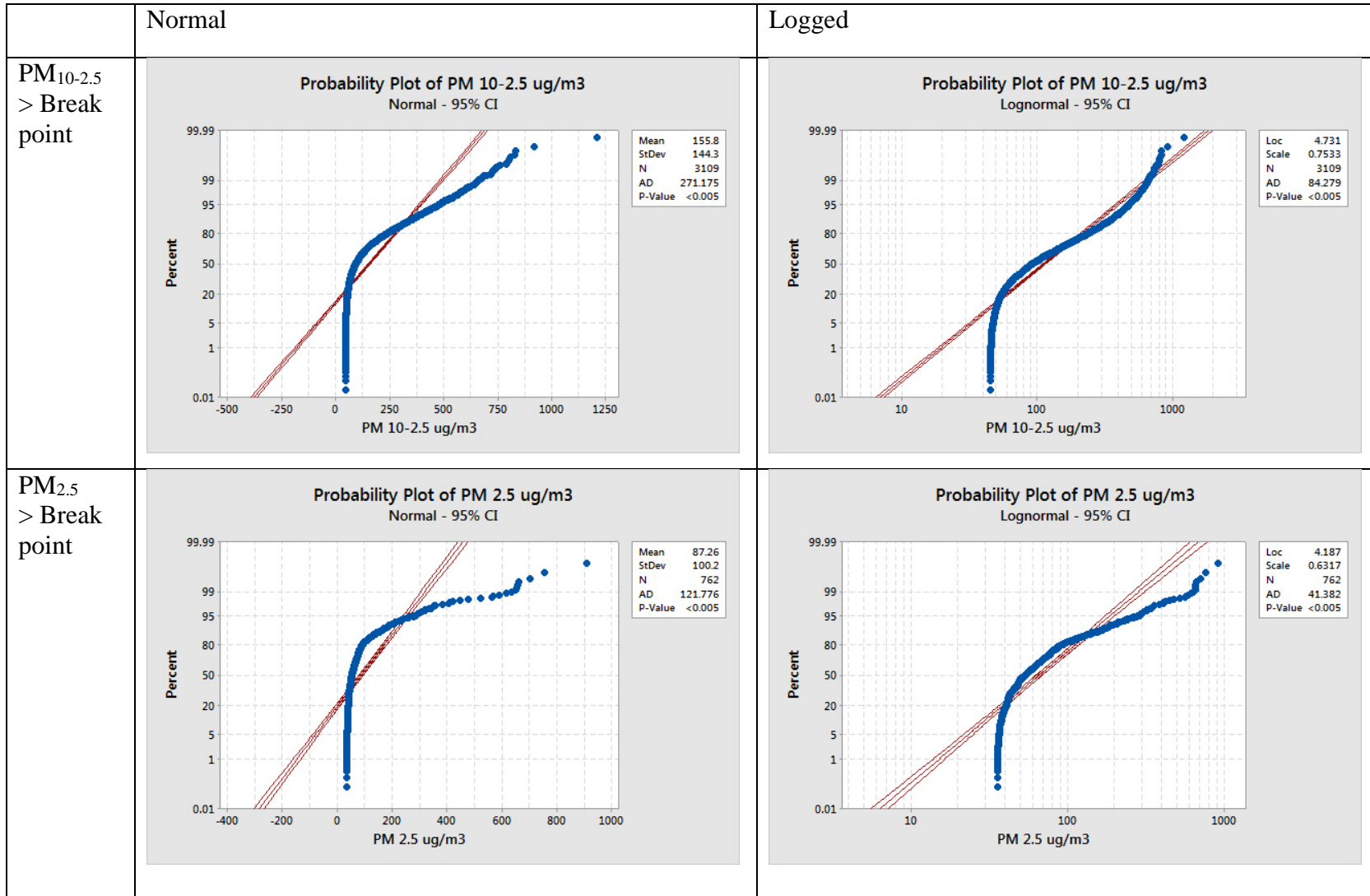


Figure C - 28: Probability Plots of PM>Breakpoint Concentration for Site 5

### 3. Regression Analysis

Table C - 5: Regression Analysis for PM>Breakpoint Concentration at Site 5

Regression Analysis for Matlab Binned Break Point Data					
A: Log PM 10-2.5					
Location	Variable	Sum of Squares	SS/Total SS	P-Value	Coefficients
Preferred R <sup>2</sup> = (2.61%)	Sound	2.47	0.001	0.035	Low = 0 High = 0.1193
	Wind Speed	43.37	0.025	<0.001	Low = 0 High = -0.3030
	Wind Direction	1.32	0.001	0.123	Unrelated = 0 Mine = -0.0912
	Regression Model	46.01	0.026	<0.001	-
B: Log PM 2.5					
Location	Variable	Sum of Squares	SS/Total SS	P-Value	Coefficients
Preferred R <sup>2</sup> = (2.7%)	Sound	0.421	0.001	0.299	Low = 0 High = 0.0784
	Wind Speed	6.514	0.021	<0.001	Low = 0 High = -0.1942
	Wind Direction	1.015	0.003	0.107	Unrelated = 0 Mine = 0.192
	Regression Model	8.193	0.027	<0.001	-

#### Regression Inputs

Wind vectors were coded as either, “Over the Mine” or “Not over the facility” and used as a categorical variable. Wind Speed and sound were coded as high or low. Only values larger than the break point values were used, and the values were converted to logged values to make the data set linear.

4. Conditional Probability Plots

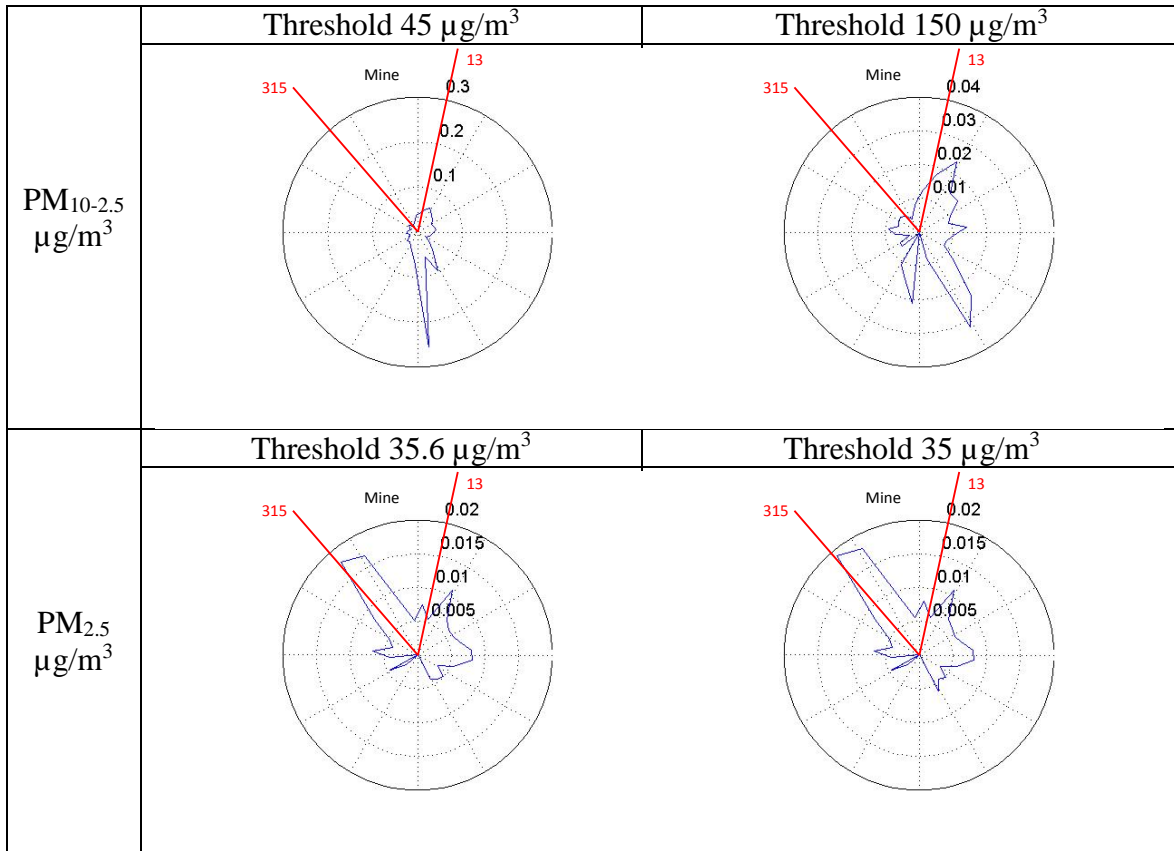


Figure C - 29: Conditional Probability Plots for Site 1

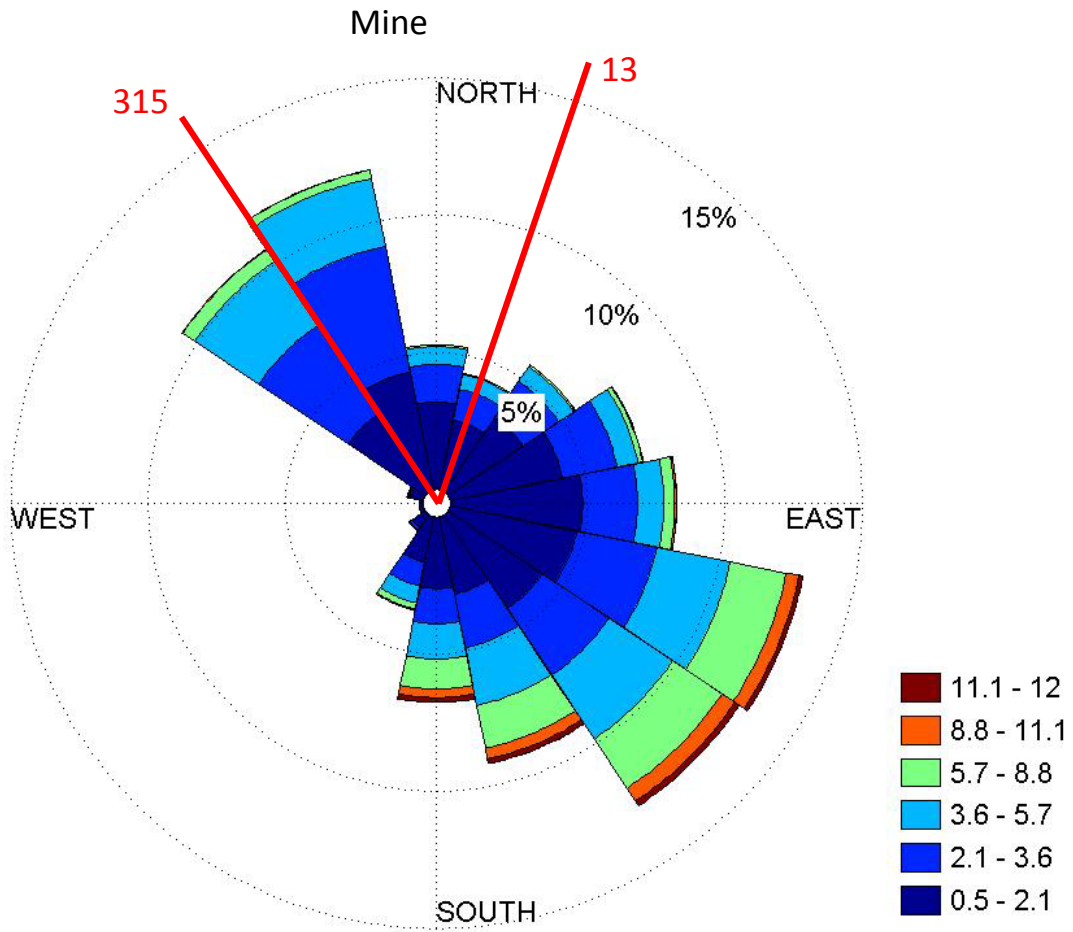


Figure C - 30: Wind Rose for Site 5

**C-6: Site 6** October 9, 2014 to November 4, 2014

## 1. Location and facility

Distance from facility: 1,260 feet

## Sand Processing Operations:

- Raw sand is trucked into facility and dumped
- Sand is then washed as it passes over a screen to separate large and small particles
- Next it is stored for drying
- It is dried and then sorted on last time before leaving the facility
- Finally it is trucked or railed out of the facility

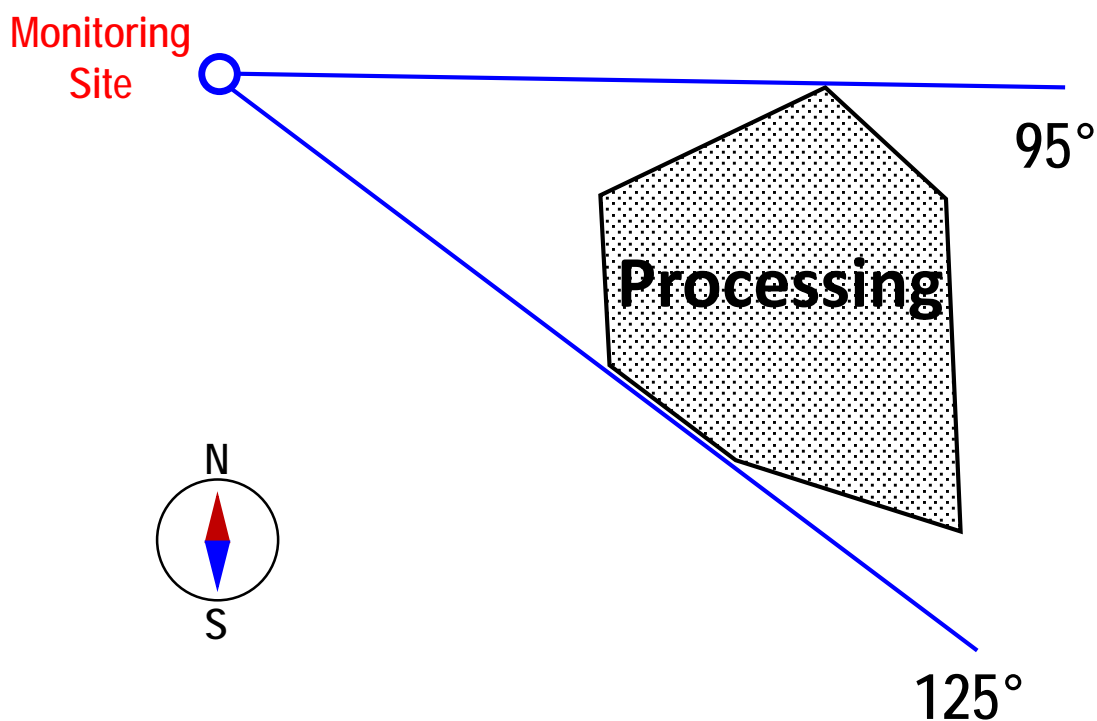


Figure C - 31: Map Image of Site 1 Relative to the Facility

## Wind Directions

- Wind over processing facility if blowing from directions between 95° to 125°
- Wind not related with the facility if blowing from directions between 126° to 94°

## Site Observation

- Secluded location with many trees between facility and sampling site

## 2. Descriptive Stats

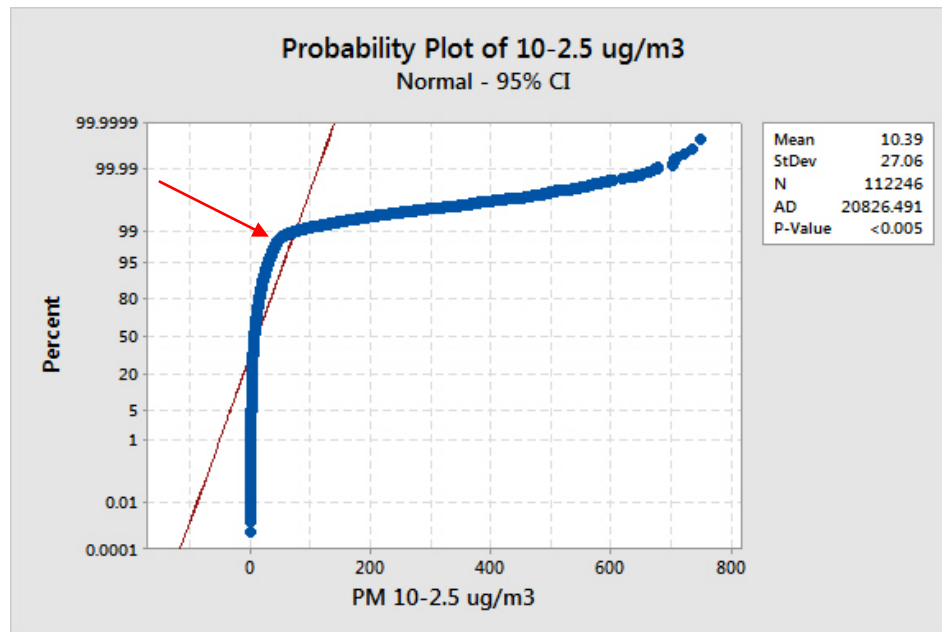


Figure C - 32: PM<sub>10-2.5</sub> µg/m<sup>3</sup> Break point (indicated by arrow) = 40.5 µg/m<sup>3</sup> at a percentile = 97.6

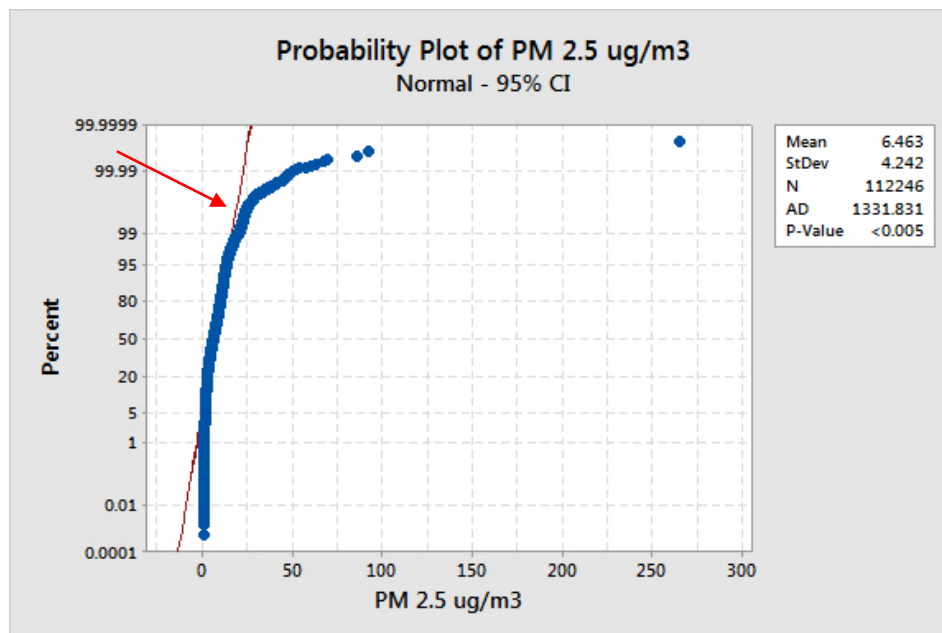


Figure C - 33: PM<sub>2.5</sub> µg/m<sup>3</sup> Break point (indicated by arrow) = 19.8 µg/m<sup>3</sup> at a percentile = 99.6

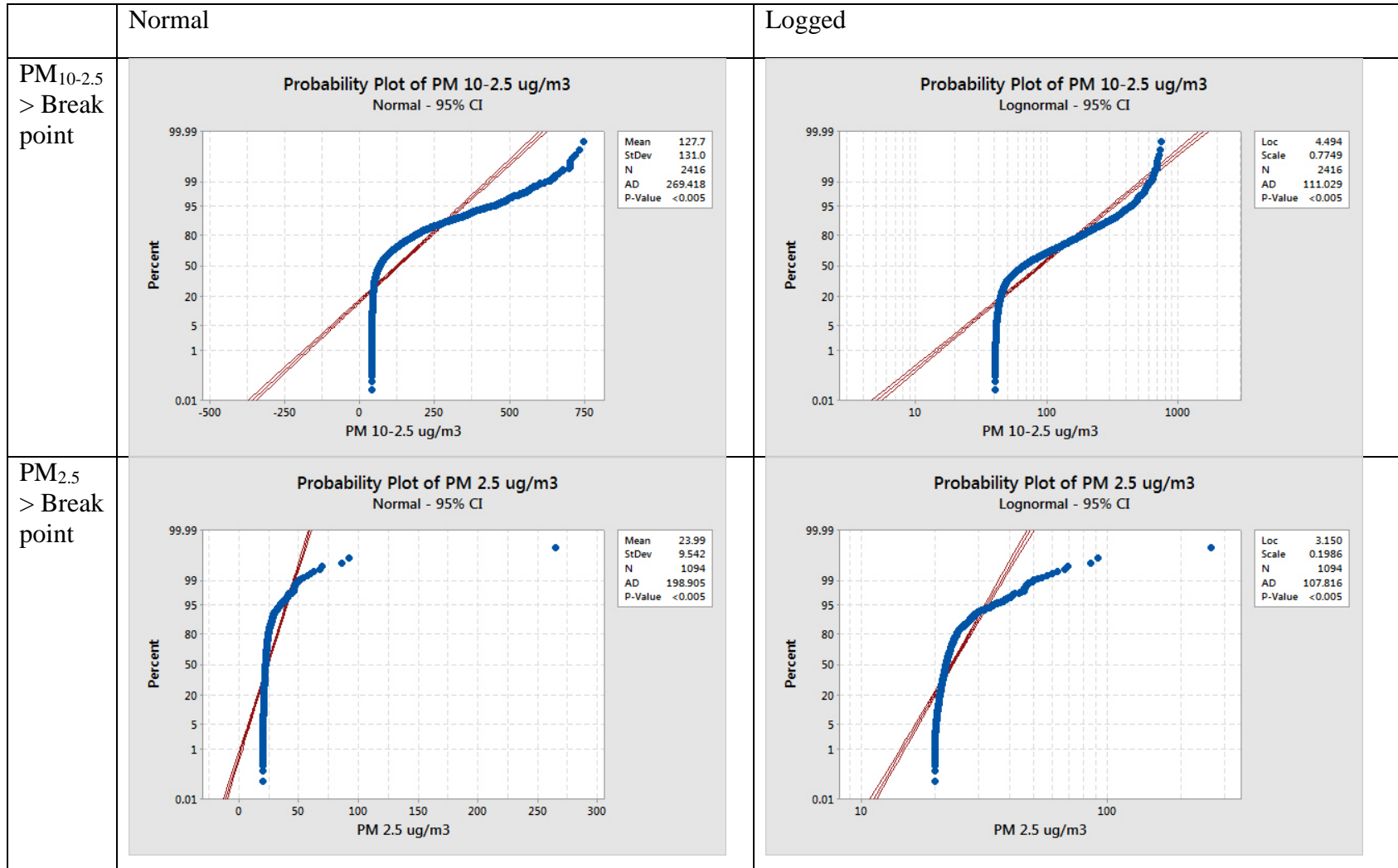


Figure C - 34: Probability Plots of PM>Breakpoint Concentration for Site 6

### 3. Regression Analysis

Table C - 6: Regression Analysis for PM<sub>10</sub> Breakpoint Concentration at Site 6

Regression Analysis for Matlab Binned Break Point Data					
A: Log PM 10-2.5					
Location	Variable	*SS	*SS/**TSS	P-Value	Coefficients
Shaw House R <sup>2</sup> = (3.11%)	Sound	3.4	0.002	0.016	Low = 0
	Wind Speed	33.91	0.023	<0.001	Low = 0 High = -0.5749
	Wind Direction	3.48	0.002	0.015	Unrelated = 0 Mine = -0.0976
	Regression Model	45.15	0.031	<0.001	-
B: Log PM 2.5					
Shaw House R <sup>2</sup> = (12.35%)	Sound	5.2831	1.22E-01	<0.001	Low = 0
	Wind Speed	1.0086	2.34E-02	<0.001	Low = 0 High = -0.3194
	Wind Direction	0.0082	1.90E-04	0.627	Unrelated = 0 Mine = -0.0087
	Regression Model	5.3312	1.23E-01	<0.001	-
*SS = Sum of Squares					
**TSS = Total Sum of Squares for the Regression					

#### Regression Inputs

Wind vectors were coded as either, “Over the Mine” or “Not Over the Mine,” and used as a categorical variable. Only values larger than the break point values were used, and the values were converted to logged values to make the data set linear.



## 4. Conditional Probability Plots

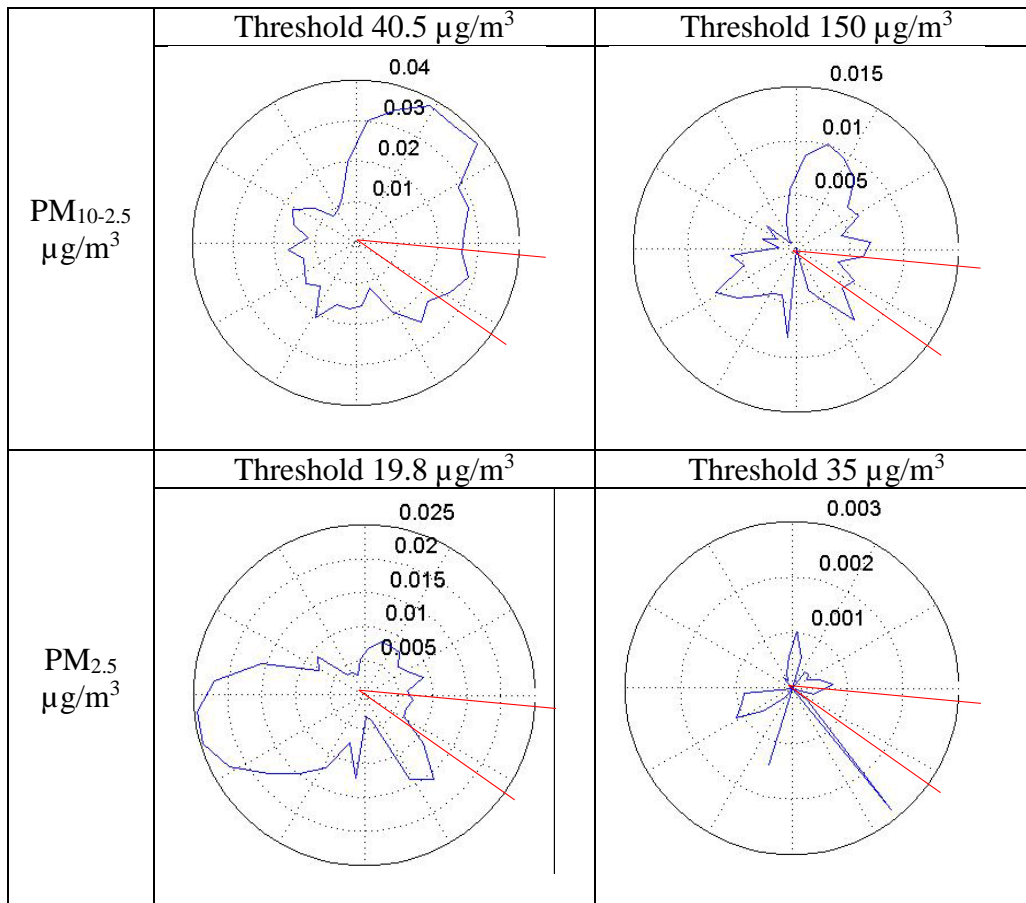


Figure C - 35: Conditional Probability Plots for Site 6

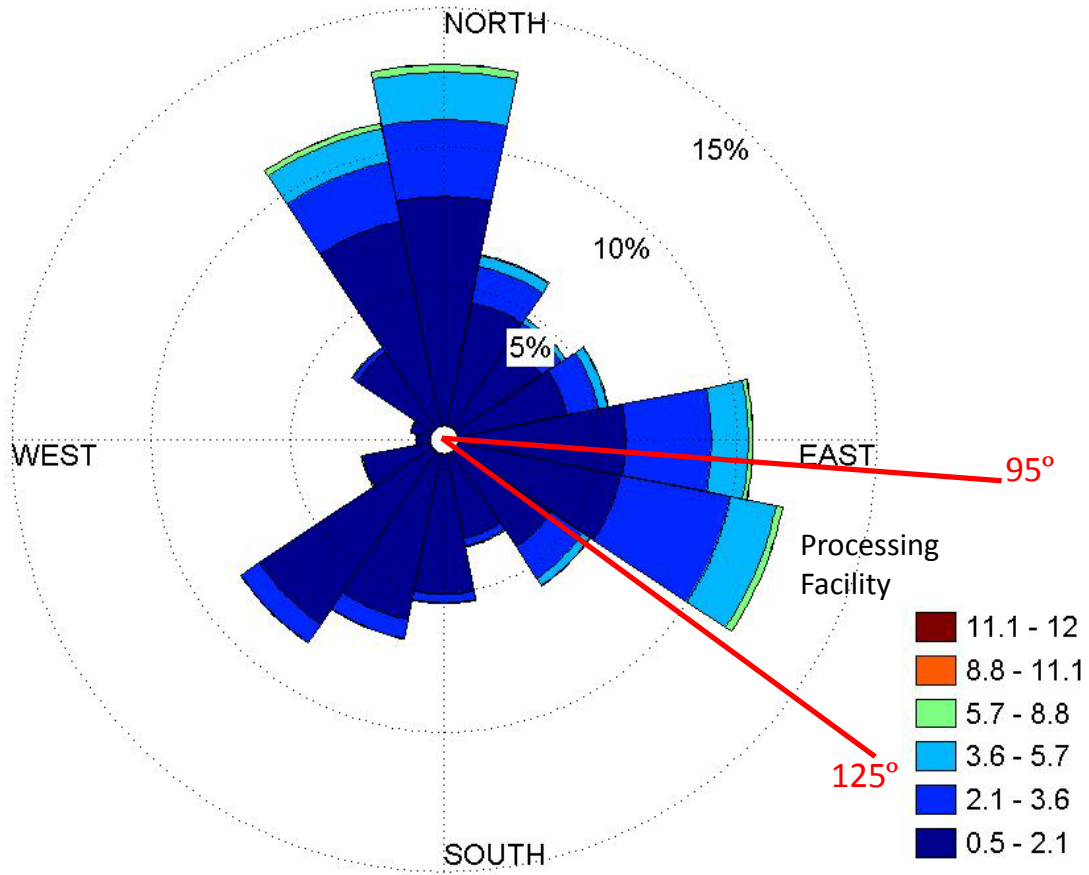


Figure C - 36: Wind Rose for Site 6

## REFERENCES

- ACGIH. (2014). *TLVs and BEIs*. Cincinnati Ohio: Signature Publications.
- Bridge, G. (2004). CONTESTED TERRAIN: Mining and the Environment. *Annual Review of Environment and Resources*, 29(1), 205-259. doi: 10.1146/annurev.energy.28.011503.163434
- CDC. (2004). Silicosis: Learn the Facts. In NIOSH (Ed.), (Vol. 2004-108).
- CDC. (2005). *Silicosis Mortality Prevention, and Control-United States, 1968-2002*. American Medical Association.
- Davidson, C. I., Phalen, R. F., & Solomon, P. A. (2005). Airborne Particulate Matter and Human Health: A Review. *Aerosol Science and Technology*, 39(8), 737-749. doi: 10.1080/02786820500191348
- Deller, S. C., & Schreiber, A. (2012). Frac Sand Mining and community economic development. *Staff Paper Series*.
- DNR, W. (2011). *Report to the Natural Resources Board: Silica Study*. (AM-407).
- DNR, W. (2012a). *Particulate Matter Emissions and Pollution Requirements*. (AM-406). Retrieved from <http://dnr.wi.gov/files/pdf/pubs/am/am406.pdf>.
- DNR, W. (2012b). *Silica Sand Mining in Wisconsin*.
- DNR, W. (2012c). *Template Best Management Practices of Fugitive Dust Control Plans for Ledge Rock Quarry and Industrial Sand Mining Industries*. Wisconsin DNR webpage: Retrieved from [http://dnr.wi.gov/cias/guidance/guidanceexternal/guidanceitem.aspx?item\\_seq\\_no=2091](http://dnr.wi.gov/cias/guidance/guidanceexternal/guidanceitem.aspx?item_seq_no=2091).
- Dolley, T. P. (2014). *Sand and Gravel (Industrial)*. Mineral Commodity Summaries.
- Ehrlich, C., Noll, G., Wusterhausen, E., Kalkoff, W. D., Remus, R., & Lehmann, C. (2013). Respirable Crystalline Silica (RCS) emissions from industrial plants – Results from measurement programmes in Germany. *Atmospheric Environment*, 68, 278-285. doi: 10.1016/j.atmosenv.2012.10.069
- Ellickson, K., & Hedman, J. (2014a). *Shokopee Sand Ambient Air Monitoring*.
- Ellickson, K., & Hedman, J. (2014b). *Tiller-North Branch Ambient Air Monitoring*.
- EPA. (2012, Dec 14, 2012). National Ambient Air Quality Standards. Retrieved Feb 18, 2015, 2015, from <http://www.epa.gov/air/criteria.html>

- EPA. (2013). Particulate Matter. Retrieved March 3, 2015, 2015, from <http://www.epa.gov/airsceience/air-particulatematter.htm>
- EQB. (2013). *Report on Silica Sand*. Environmental Quality Board (EQB).
- Esswein, E. J., Breitenstein, M., Snawder, J., Kiefer, M., & Sieber, W. K. (2013). Occupational exposures to respirable crystalline silica during hydraulic fracturing. *J Occup Environ Hyg*, *10*(7), 347-356. doi: 10.1080/15459624.2013.788352
- Fubini, B., Bolis, V., Cavenago, A., & Volante, M. (1995). HealthPhysicochemical properties of crystalline silica dusts and their possible implication in variousbiological responses. *Scandinavian journal of Work, Environment & Health*, *21*(2), 9-14.
- Garcia, A., Jones, E., Echt, A. S., & Hall, R. M. (2014). An evaluation of an aftermarket local exhaust ventilation device for suppressing respirable dust and respirable crystalline silica dust from powered saws. *J Occup Environ Hyg*, *11*(11), D200-207. doi: 10.1080/15459624.2014.955182
- Harrison, R. M., & Yin, J. (2000). Particulate matter in the atmosphere: which particle properties are important for its effects on health? *Sci Total Environ*, *249*(1-3).
- Hellmann, J. R., Scheetz, B. E., Luscher, W. G., Hartwich, D. G., & Koseski, R. P. (2014). Proppants for Shale Gas and Oild Recovery. *American Ceramic Society Bulletin*, *93*(1), 28-35.
- IARC. (1999). *IARC Monographs on the Evaluation of Carcinogenic*. International Agency for Research on Cancer.
- Kennedy, T. (2012). Local Officials Dealing Themselves a Piece of Frac Sand Boom. *StarTribune*. Retrieved from StarTribune website: <http://www.startribune.com/local/184771921.html>
- Kim, E., & Hopke, P. K. (2004). Comparison between Conditional Probability Function and Nonparametric Regression for Fine Particle Source Directions. *Atmospheric Environment*, *38*(28), 4667-4673. doi: 10.1016/j.atmosenv.2004.05.035
- Kirkhorn, S. R., & Garry, V. F. (2000). Agricultural Lung Diseases. *Environmental Health Perspectives*, *108*(4), 705-712.
- Klepeis, N. E., Hughes, S. C., Edwards, R. D., Allen, T., Johnson, M., Chowdhury, Z., . . . Hovell, M. F. (2013). Promoting smoke-free homes: a novel behavioral intervention using real-time audio-visual feedback on airborne particle levels. *PLoS One*, *8*(8), e73251. doi: 10.1371/journal.pone.0073251

- Linch, K. D., Miller, W. E., Althouse, R. B., Groce, D. W., & Hale, J. M. (1998). Surveillance of Respirable Crystalline Silica Dust Using OSHA Compliance Data (1979-1995). *American Journal of Industrial Medicine*, 34(6), 11. doi: 10.1002/(SICI)1097-0274(199812)34:6<547::AID-AJIM2>3.0.CO;2-B
- Locations of Industrial Sand Mines and Processing Plants in Wisconsin. (2014, January 16, 2015). Retrieved February 2, 2015
- Minerals, B. o. I. (1992). *Crystalline Silica Primer*.
- Mossman, B. T., & Churg, A. (1998). Mechanisms in the Pathogenesis of Asbestosis and Silicosis. *American Journal of Respiratory and Critical Care Medicine*, 157(5), 1666-1680.
- Muhle, H., Takenaka, S., Mohr, U., Dasenbrock, C., & Mermelstein, R. (1989). Lung Tumor Inuction Upon Long-Term Low-Level Inhalation of Crystalline Silica. *American Journal of Industrial Medicine*, 15(3), 3. doi: 10.1002/ajim.4700150309
- NIOSH. (1978). *Occupational Health Guideline for Crystalline Silica*. CDC: CDC.
- NIOSH. (2008). *Work-Related Lung Disease Surveillance Report 2007*. DHHS (NIOSH).
- NR 415 Control of Particulate Emissions, NR 415 C.F.R. § NR 415.04 (2003).
- OEHHA. (2005). *CHRONIC TOXICITY SUMMARY SILICA (CRYSTALLINE, RESPIRABLE)*. CA.gov: Office of Environmental Health Hazard Assessment (OEHHA).
- Osborn, S. G., Vengosh, A., Warner, N. R., & Jackson, R. B. (2011). Methane contamination of drinking water accompanying gas-well drilling and hydraulic fracturing. *Proc Natl Acad Sci U S A*, 108(20), 8172-8176. doi: 10.1073/pnas.1100682108
- OSHA. (2006). *Air Contaminants. 29 CFR 1910.1000*. Occupational Safety and Health Administration (OSHA).
- OSHA. (2010). *Occupational Exposure to Respirable Crystalline Silica -- Review of Health Effects Literature and Preliminary Quantitative Risk Assessment*.
- OSHA. (2013). *Annotated Table Z-3 Mineral Dust*. Retrieved from <https://www.osha.gov/dsg/annotated-pels/tablez-3.html>.
- Parks, C. G., Conrad, K., & Cooper, G. S. (1999). Occupational Exposure to Crystalline Silica and Autoimmune Disease. *Environmental Health Perspectives*, 107(5), 793-802.

- Pearson, T. W. (2013). Frac Sand Mining in Wisconsin: Understanding Emerging Conflicts and Community Organizing. *Culture, Agriculture, Food and Environment*, 35(1), 30-40. doi: 10.1111/cuag.12003
- Radnoff, D., Todor, M. S., & Beach, J. (2014). Occupational exposure to crystalline silica at Alberta work sites. *J Occup Environ Hyg*, 11(9), 557-570. doi: 10.1080/15459624.2014.887205
- Richards, J. R., Brozell, T. T., Rea, C., Boraston, G., & Hayden, J. (2009). PM4Crystalline Silica Emission Factors and Ambient Concentrations at Aggregate-Producing Sources in California. *Journal of the Air & Waste Management Association*, 59(11), 1287-1295. doi: 10.3155/1047-3289.59.11.1287
- SCOEL. (2003). *Recommendations from the Scientific Committee on Occupational Exposure Limits for Silica, Crystalline (respirable dust)*
- Seely, R. (2011). Northern Wisconsin Sand Mining Boom Includes New Jobs, New Problems. *Wisconsin State Journal*. Retrieved from Wisconsin State Journal website: [http://host.madison.com/wsj/news/local/environment/northern-wisconsin-sand-mining-boom-includes-new-jobs-new-problems/article\\_d37f0f2c-22c1-11e1-8f78-001871e3ce6c.html](http://host.madison.com/wsj/news/local/environment/northern-wisconsin-sand-mining-boom-includes-new-jobs-new-problems/article_d37f0f2c-22c1-11e1-8f78-001871e3ce6c.html)
- Shiraki, R., & Holmen, B. A. (2002). Airborne Respirable Silica Near a Sand and Gravel Facility in Central California: XRD and Elemental Analysis To Distinguish Source and Background Quartz. *Environmental Science and Technology*, 36(23), 4956-4961.
- Smathers, J. (2011). Sand Mining Surges in Wisconsin. Retrieved February 2, 2015
- Steinle, S., Reis, S., Sabel, C. E., Semple, S., Twigg, M. M., Braban, C. F., . . . Wu, H. (2015). Personal exposure monitoring of PM2.5 in indoor and outdoor microenvironments. *Sci Total Environ*, 508, 383-394. doi: 10.1016/j.scitotenv.2014.12.003
- Survey, W. G. N. H. (2013a). Frac Sand: How is it Mined. Retrieved January 15, 2015, 2015, from <http://wgnhs.uwex.edu/wisconsin-geology/frac-sand-mining/frac-sand-mining-process/>
- Survey, W. G. N. H. (2013b). Frac Sand: How is it Mined? Retrieved February 2, 2015, from <http://wgnhs.uwex.edu/wisconsin-geology/frac-sand-mining/frac-sand-mining-process/>
- Valavanidis, A., Fiotakis, K., & Vlachogianni, T. (2008). Airborne Particulate Matter and Human Health: Toxicological Assessment and Importance of Size and

Composition of Particles for Oxidative Damage and Carcinogenic Mechanisms.  
*Journal of Environmental Science and Health*, 26(4).

Watson, J. G., Chow, J. C., & Mathai, C. V. (2012). Receptor Models in Air Resources Management: A Summary of the APCA International Specialty Conference. *Japca*, 39(4), 419-426. doi: 10.1080/08940630.1989.10466539

Yu, K. N., Cheung, Y. P., Cheung, T., & Henry, R. C. (2004). Identifying the impact of large urban airports on local air quality by nonparametric regression. *Atmospheric Environment*, 38(27), 4501-4507. doi: 10.1016/j.atmosenv.2004.05.034